

Lehrstuhl für Organische Chemie und Biochemie
der Technischen Universität München

**The Anatomy of the Host-Guest Binding
Energetics of Bicyclic Guanidinium-Oxoanion
Ion-Pairs.**

Manal Haj-Zaroubi

Vollständiger Abdruck der von der Fakultät für Chemie der Technischen Universität
München zur Erlangung des akademischen Grades eines

Doktors der Naturwissenschaften

genehmigten Dissertation.

Vorsitzender: Univ.-Prof. Dr. P. Schieberle

Prüfer der Dissertation: 1. Univ.-Prof. Dr. F. P. Schmidtchen
2. Univ.-Prof. Dr. W. Hiller

Die Dissertation wurde am 5.07.02 bei der Technischen Universität München
eingereicht und durch die Fakultät für Chemie am 25.07.02 angenommen.

Acknowledgements

This thesis was carried out during the period of January, 1999 – May, 2002 in the Department of Organic Chemistry and Biochemistry at the Technical University, Munich.

This work could not have been done without the continuous advice and support of Prof. Dr. F. P. Schmidtchen, who guided me throughout the research with a lot of patience, understanding and encouragement. His insight into organic and supramolecular chemistry has set me on the right track and helped me avoid a lot of obstacles and pitfalls that appeared in the course of the work. For all of this I express my deepest gratitude.

I thank Dr. Anette Schier and Dr. Norbert W. Mitzel for obtaining the X-ray crystal structures for some of the compounds produced during this work.

I am grateful to Prof. Vladimir Král for many discussions and numerous useful suggestions.

I wish to acknowledge my colleagues Dr. Michael Berger, Dr. Thordis Hinnekeuser, Marzena Lewinska, Dr. Elena Nicoletti, Andreas Pfletschinger and Dr. Nasser Yehia for their help over the past 3.5 years.

I would like to thank my parents, to whom I dedicate this work, for their love, constant encouragement and belief in my ability to 'make it'.

Finally, I express my affectionate gratitude to Saleem, my husband, for his love, constant motivation, intensive support, and patience that enabled me go through this experience. Without him this journey would have been much more difficult.

Table of Contents

1.	Introduction	1
1.1	Supramolecular Chemistry	1
1.2	Noncovalent interactions	2
1.2.1	Coulomb interactions	3
1.2.2	Hydrogen bonding	6
1.2.3	Cation- π interaction	8
1.2.4	π - π interaction	9
1.2.5	Hydrophobic effects	10
1.3	Design principles of supramolecular host	10
1.4	A correlation between structure and energetics	12
1.5	Isothermal Titration Calorimetry (ITC)	16
1.6	Hosts for cationic guest molecules	19
1.7	Hosts for anions in particular oxoanions like phosphate and carboxylate	20
2.	Aim of this work	31
3.	Synthesis	
3.1	Synthesis of bicyclic guanidine host 48 and 70	
3.1.1	The synthetic strategies for host 48	34
3.1.2	The synthesis of hosts 70 and 71	42
3.2	Synthesis of the phosphate and phosphinate guests	
3.2.1	Synthetic strategy for phosphates 78 and 83	43
3.2.2	Synthetic strategy for phosphinate 92	46

4.	Results and discussion	
4.1	Complexation of different guanidinium cation hosts with carboxylate 129	57
4.2	Different conformations of the tetraphenylguanidinium cation with different counter-anions	70
4.3	Complexation of different guanidinium cation hosts with phosphate 78	73
5.	Experimental Part	
5.1	General methods and materials	83
5.2	Synthetic procedures	84
6.	Summary	111
7.	References	115

Abbreviations

Ac	acetate
DMF	dimethylformamide
DMSO	dimethylsulfoxide
EDIPA	ethyldiisopropylamine
ESI	electrospray-ionization
EtOH	ethanol
FAB	fast-atom-bombardment
h	hour
HPLC	high performance liquid chromatography
ITC	isothermal titration calorimetry
lit	literature
MeOH	methanol
mp	melting point
MW	molecular weight
O.N.	over night
RP	reversed phase
RT	room temperature
R_v	retention volume
TBA	tetrabutylammonium
TEA	triethylamine
TEAI	tetraethylammonium iodide
TFA	trifluoroacetic acid
THF	tetrahydrofuran
TMS	tetramethylsilan

1. Introduction

1.1 Supramolecular Chemistry

Supramolecular chemistry is one of the most popular and fastest growing areas of experimental chemistry. It is highly interdisciplinary in nature and, as a result, attracts not just chemists but biochemists, biologists, environmental scientists, and others [1].

Chemistry at the microscopic level is dominated by the chemistry of the covalent bond. Supramolecular chemistry extends beyond the realm of individual molecules to focus on intermolecular non-covalent interactions between two or more entities to create an organized association or structure. Jean-Marie-Lehn, who won the Nobel prize for his work in the area in 1987, has defined supramolecular chemistry as the “the chemistry of molecular assemblies and of the intermolecular bond” or “the chemistry beyond the molecule” [2].

Non-covalent interactions between molecules are the basis of the processes that occur in biology, such as substrate binding to an enzyme or a receptor, the assembling of protein complexes, intermolecular reading of the genetic code, signal induction by neurotransmitters, cellular recognition, and so on [1-3].

The weak noncovalent interactions ubiquitous in the living systems have provoked scientists to mimic these bonds by the design of artificial receptor (host) molecules capable of binding substrate (guest) species strongly and selectively, forming supramolecular entities or host-guest complexes of well defined structures and functions [2].

Commonly, the host is a large molecule or aggregate such as an enzyme or synthetic cyclic compound. The guest may be a monoatomic cation, a simple inorganic anion, or a more sophisticated molecule such as a hormone, pheromone or neurotransmitter. The relationship with the resulting host-guest complex has been defined by Donald Cram (1986) as “complexes that are composed of two or more molecules or ions held together in unique structural relationships by intermolecular forces”. Forces such as, ion-pairing (electrostatic interactions), hydrogen bonds, hydrophobic interactions, π -acid to π -base interaction, metal-to-ligand binding, van der Waals attractive forces and solvent structure [1].

A host-guest relationship involves a complementary stereoelectronic arrangement of binding sites in host and guest. In addition to these sites, the host (receptor) may

bear reactive sites that can transform the bound guest (substrate), which would make the host a molecular reagent or catalyst. Furthermore, the host may act as a molecular carrier if it is fitted with lipophilic groups that allow it to dissolve in a membrane. Thus, the functional properties of a supermolecule cover molecular recognition, catalysis, and transport etc.

Host-guest chemistry goes back more than a century and its roots are based upon three historical concepts [1,2]:

1. The fact that selective binding must involve attraction or mutual affinity between host and guest. This is, in effect, a generalization of Alfred Werner's 1893 theory of coordination chemistry, in which metal ions coordinate ligands into a sphere.

2. The recognition by Emil Fisher [9] (1894) that binding must be selective, as part of the study of receptor-substrate binding by enzymes. He described this by a 'lock and key' image of steric fit in which the guest has a geometric size or shape complementarity to the receptor or host. This concept laid the basis for molecular recognition.

3. It was Paul Ehrlich in 1906 who recognized that molecules don't act if they don't bind, in this way he introduced the concept of a biological receptor.

In the course of the development of the field of supramolecular chemistry, enormous progress has been made on quantifying the details of receptors with affinity to guests that fit inside them. The lock-and-key notion went through successive waves of revision provoked by the introduction of the concepts chelation, preorganization and complementarity, solvation and the alteration in the very definition of 'molecular shape'.

1.2 Nature of supramolecular interaction (noncovalent interactions)

One of the noncovalent interactions, van der Waals interactions, were first recognized by J. D. van der Waals in the nineteenth century [4]. The role of the noncovalent interaction in nature was fully recognized only in the past two decades. Noncovalent interactions lead to the formation of molecular clusters while covalent interactions lead to the formation of classical molecules. The formation of a noncovalent cluster does affect the properties of the subsystems, thereby inducing changes that are important for the detection of cluster formation. The stronger the interaction is, the larger are the changes in the properties of the subsystem. For

example, the marked changes that occur in H-bonded systems, result in large variations of the stretch frequencies upon complex formation.

A covalent bond is formed when partially occupied orbitals of interacting atoms overlap and form a new molecular orbital of lower energy, which is occupied by a pair of electrons shared by these atoms. This bond is generally shorter than 2 Å and highly directional. Noncovalent interactions are induced by the electrical properties of the subsystem and are normally effective over short distances, shorter than few angstroms, but can occasionally form bonds at distances as large as tens of angstroms. The stabilizing energy of noncovalent complexes generally consists of various energy terms such as electrostatic (or coulombic), induction, dispersion, repulsion and charge-transfer [1,3,4]. The repulsive contribution, which is called exchange-repulsion, prevents the subsystems from drawing too close together. The term induction, refers to the general ability of charged molecules to polarize neighboring species. The dispersion interaction term, results from the interactions between fluctuating multipoles. In charge-transfer (CT) interactions the electron translocates from the donor to the acceptor. The term “van der Waals forces” is frequently used to describe dispersion and exchange-repulsion contributions. All of these interactions involve host and guest as well as their surroundings (*e.g.* solvation).

1.2.1 Coulomb interactions

Coulomb interaction is one type of the most important noncovalent interactions (ion-pairing, ion-dipole, dipole-dipole *etc.*) in synthetic host-guest complexes as well as in many biological systems [1,3]. The driving force for these interactions is naturally electrostatic (coulombic). In general, the coulomb interaction between two point charges is described by the coulomb potential energy [5],

$$V = \frac{q_1 q_2}{4\pi\epsilon r} \quad (1)$$

where q_1 and q_2 are the electric charge of two point masses at a distance r in a medium of permittivity ϵ . It is common to express the permittivity as a multiple of the vacuum permittivity ϵ_0 , and to write $\epsilon = \epsilon_r \epsilon_0$, where ϵ_r is the relative permittivity (or dielectric constant) of the medium. Note that in general $\epsilon_r \geq 1$, where it assumes the value of unity in vacuum. The coulomb potential energy is equal to the work that must be done to bring up a charge q_1 from infinity to a distance r from a charge q_2 . The

coulomb energy is inversely proportional to the interionic distance. The electrical force, F , exerted by a charge q_1 on a second charge q_2 has magnitude

$$F = \frac{q_1 q_2}{4\pi\epsilon r^2} \quad (2)$$

the force itself is a vector directed along the line joining the two charges.

In organic ions the charge is heavily delocalized therefore the point charges formulae 1 and 2 do not hold anymore, a fact that complicates the theoretical analysis of ion-pairing. Fortunately, it is possible to describe interactions approximately by referring to the whole group where the ions are considered as spherical point like ions that follow the Debye-Hückel theory [3,5].

According to this theory, oppositely charged ions attract one another. As a result, anions are more likely to be found near cations in solution, and vice versa. Overall the solution is electrically neutral, but near any given ion there is an excess of counter ions. Averaged over time, counter ions are more likely to be found near any given ion. This time-averaged, spherical haze around the central ion, in which counter ions outnumber ions of the same charge as the central ion, has a net charge equal in magnitude but opposite in sign to that on the central ion, and is called its ionic atmosphere. The energy, and therefore the chemical potential, of any given central ion is lowered as a result of its electrostatic interaction with its ionic atmosphere. This lowering of energy appears as a difference between the molar Gibbs energy G_m and the ideal value G_m^{ideal} of the solute, and hence can be identified by $RT \ln \gamma_{\pm}$, where γ is the activity coefficient.

The well-known Debye-Hückel equation for the activity coefficient of an ion i with a charge number z_i in water has the form,

$$\log \gamma_i = -Az_i^2 I^{1/2} / \left(1 + 0.33a_i I^{1/2}\right) \quad (3)$$

where a_i (Å) is the distance of the closest approach between ions and $A = 0.509$ is a constant for an aqueous solution at 25°C. I , is the dimensionless ionic strength of the solution, related to the charge number of the ion and its molality. In very diluted electrolyte solutions ($I < 0.01$ M) the term $0.33a_i I^{1/2}$ in the denominator may be neglected and equation (3) can be simplified to an equation linear with respect to $I^{1/2}$,

$$\log \gamma_i = -Az_i^2 I^{1/2} \quad (4)$$

known as the limiting Debye-Hückel law. The Debye-Hückel theory applies to the case of hard-sphere charges in a uniform medium and small electric potentials.

For spherical ions A and B with point charges Bjerrum has, on the basis of the Debye-Hückel theory, described the association constant, K , as a function of the charges z_A , z_B , the dielectric constant ϵ , and a factor $Q(b)$ which depends on ϵ , z and on the distance of closest approach a between A and B [3]:

$$K = (4\pi N/1000) \left(z_A z_B e^2 / \epsilon kT \right)^3 Q(b) \quad (5)$$

where $b = z_A z_B e^2 / \epsilon kTa$, $z_A z_B$ is taken by its absolute value. The distance a equals the sum of ionic radii of A and B and the parameter b is related to the so-called critical distance $q = ab/2 = z_A z_B e^2 / 2\epsilon kT$, defined as the distance at which the mutual electric energy of ions A and B equals $2kT$. Bjerrum theory considers that the ion-pairing occurs if the centers of ions A and B approach each other at a distance shorter than or equal to q , which becomes very large in solvents of lower dielectric constants. Large ions with $a > q$ according to this theory don't associate at all.

For contact ion pairs the Fuoss equation [87] gives

$$K = (4\pi Na^3/3000) \exp\left(z_A z_B e^2 / \epsilon kTa \right) \quad (6)$$

or (at 298 K)

$$K = 0.00252a^3 \exp\left(560 z_A z_B e^2 / \epsilon a \right) \quad (7)$$

This equation is applicable also for solvent-separated pairs and for loose solvated complexes provided the solvent molecule size is included in evaluation of a . The experimental results do not allow a clear distinction between Bjerrum and Fuoss equations, however, the latter is often preferred because of its simpler mathematical form and conceptual basis.

For strongly interacting ions, when association free energies are $\gg kT$, even a simple equation ,

$$K = \exp\left(560 z_A z_B e^2 / \epsilon kTa \right) \quad (8)$$

derived from consideration of ion-pairing in terms of the Born cycle gives satisfactory results. The theoretical expressions for enthalpic and entropic contributions to association free energy can be obtained by differentiation of $\ln K$ by T (van't Hoff equation, see later). Thus, from the Fuoss equation it follows that

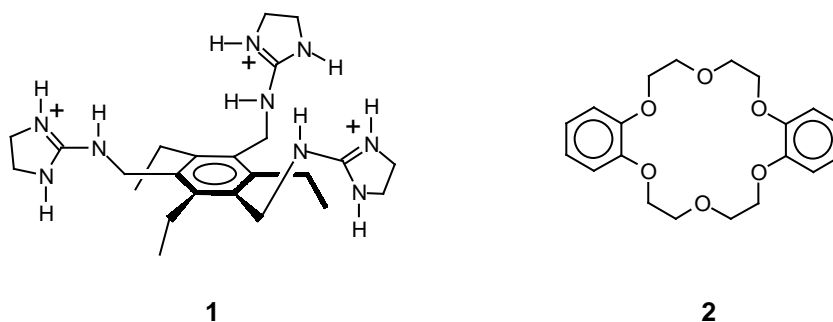
$$\Delta H = -\left(z_A z_B e^2 / \epsilon kTa \right) RT^2 \left(\frac{d \ln \epsilon}{dT + 1/T} \right) \quad (9)$$

and

$$\Delta S = R \ln(4\pi N a^3 / 3000) - (z_A z_B e^2 / \epsilon k T a) RT \left(\frac{d \ln \epsilon}{dT} \right) \quad (10)$$

Considerable improvement has been achieved by application of new numerical methods of solution of the Poisson equation [6,7], which allows one to take into account also polarization effects and charge delocalizations. Salt effects, particularly for DNA, are well described by Manning's counter-ion condensation theory [8].

An example of ion-ion (ion-pairing) interaction is the electrostatic binding of tricarboxylates with host **1**. An example for ion-dipole interaction is an alkali metal cation e.g. K^+ with crown ether **2** in which the ether oxygen lone pairs are attracted to the cation positive charge. Between neutral polar molecules like organic carbonyl compounds the electrostatic contribution mostly derives from dipole-dipole interactions.



1.2.2 Hydrogen bonding

A hydrogen bond is a particular kind of dipole-dipole interactions [10] in which a hydrogen atom, attached to an electronegative atom (or electron withdrawing group), is also attracted to a neighboring dipole on an adjacent molecule or functional group. The hydrogen bond is a complex interaction composed of several constituents that are different in their nature [11]. The total energy of a hydrogen bond is split into contributions from electrostatics, polarization, charge transfer, dispersion, and exchange repulsion [12]. The distance and angular characteristics of these constituents are very different. In particular, it is important that of all the constituents, the electrostatic contribution reduces slowest with increasing distance. The hydrogen bond potential for any particular donor-acceptor combination is, therefore, dominated by electrostatics at long distances, even if charge transfer plays an important role at

optimal geometry [10]. Chemical variations of donor, acceptor, and the environment, can gradually change a hydrogen bond to another interaction type. The transition to pure van der Waals interaction is very common. The polarity of A–H or B (or both) in the array $A-H^{\delta-}\cdots B^{\delta+}$ can be reduced by suitable variation of A or B. In consequence, the electrostatic part of the interaction is reduced while the van der Waals component gains relative weight, and the angular characteristics gradually change from directional to isotropic with interaction energies independent of the contact angle θ .

A hydrogen bond has relatively strong and directional nature, an angular lower cutoff can be set at $>90^\circ$ or, somewhat more conservatively, at $>110^\circ$. A necessary geometric criterion for hydrogen bonding is a positive directionality preference, that is, linear $A-H\cdots B$ angles must be statistically favored over bent ones.

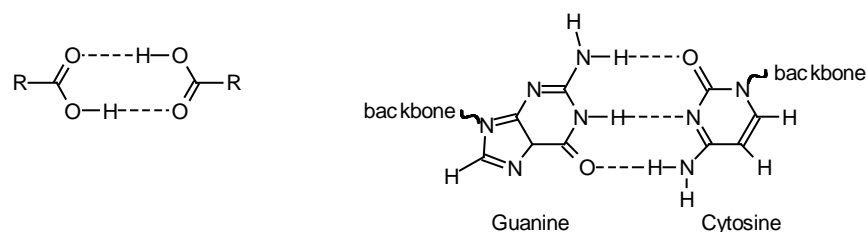


Figure 1. Carboxylic acid dimer bound by hydrogen bonding and base pairing in DNA associated by hydrogen bonding.

Examples of hydrogen bonding are [1]: the formation of carboxylic acid dimers (figure 1), the hydrogen bonding network feature of water, the creation of the elementary secondary structures in proteins, the binding of substrates to numerous enzymes, and the formation of the double helix structure of DNA. A base pairing in DNA by hydrogen bonding is shown in figure 1. The hydrogen bonds exist with a continuum of strengths, nevertheless it is useful to introduce a classification, such as “weak”, “strong”, and “moderate”. Table 1 follows the system described by Jeffrey [13], who called hydrogen bonds moderate if they resemble those between water molecules or in carbohydrates, and are associated with energies in the range 4-15 kcal mol⁻¹. Hydrogen bonds with energies above and below this range are termed strong and weak, respectively. It must be stressed that there are no “natural” borderlines between these categories. Unlike moderate and weak hydrogen bonds, strong hydrogen bonds are quasi-covalent in nature [14]. If the hydrogen bond is understood as an incipient proton-transfer reaction, a moderate hydrogen bond represents an early

stage of such a reaction, while a strong one represents an advanced stage. It is called as well the symmetric hydrogen bonds A–H–A, where an H atom is equally shared between two chemically identical atoms A, no distinction can be made between a donor and an acceptor, or a “covalent” A–H and “noncovalent” H···A bond. A key finding of spectroscopy is that very strong hydrogen bonds are formed only if the pK_a values of the partners suitably match. If the pK_a values are very different, either a moderate A–H···B or an ionic A[−]···H···B⁺ hydrogen bond is formed, both of which are not very covalent. The concept of hydrogen bonding has also been extended to the weaker C–H···O type [15,16]. Although, this type of interaction is at the weaker end of the energy scale, the presence of electronegative atoms near the carbon can enhance significantly the acidity of the C–H proton, resulting in a significant dipole.

Table 1. Strong, moderate, and weak hydrogen bonds in the gas phase following the classification of Jeffrey. The numerical data are guiding values only.

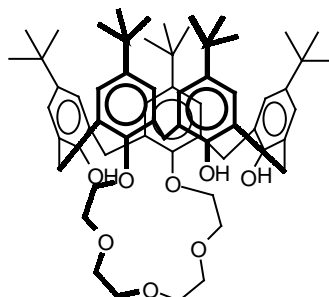
	strong	moderate	weak
A–H···B interaction	strongly covalent	mostly electrostatic	electrostatic/ dispersion
bond enthalpy (kcal mol ^{−1})	15–40	4–15	<4
bond lengths (Å): H···B	1.2–1.5	1.5–2.2	>2.2
A···E	2.2–2.5	2.5–3.2	3.2–4.0
bond angles (°)	170–180	130–180	90–150
directionality	strong	moderate	weak
examples	gas phase dimers with strong acids/bases HF complexes	acids biological molecules	C–H hydrogen bonds O–H···π hydrogen bonds

An example of the C–H···O bond, is the interaction of the methyl group of nitromethane with pyridyl crown ether [17].

1.2.3 Cation-π interaction

Cation-π interaction is normally an interaction between a cation and a π-face of an aromatic structure [1,3], such as K⁺ ion interacting with negatively charged π-electron cloud of benzene. The main force behind cation-π interaction is electrostatic, though modern theories also involve other forces like induced dipole, dispersion and CT [20].

Recently it was shown by Mandolini [18] that the cavity of calix[5]-arene **3**, fixed in the cone conformation by the presence of a polyoxyethylene bridge between the phenolic units, is suitable to host a large variety of quats (tetramethylammonium, acetylcholine, N-methylpyridinium salts) with medium to high affinities by cation- π interactions.



3

1.2.4 π - π interaction

This weak electrostatic interaction occurs between aromatic moieties, where one is relatively electron rich and one is electron poor. Two general types of π -interaction are face-to-face and edge-to-face [1,3,19] (figure 2). Dispersion energy plays an important role in stabilizing π - π interactions. Edge-to-face interactions are weak and are the result of the interaction between positively charged hydrogen atoms and negatively charged π -face of aromatic system. For example, these interactions are responsible for the characteristic herringbone packing in the crystal structures of a range of small aromatic hydrocarbons including benzene.

In the face-to-face interaction there is an orientation offset since direct overlap is repulsive. For example, this kind of π -stacking between the aryl rings of nucleobase pairs helps to stabilize the DNA double helix.

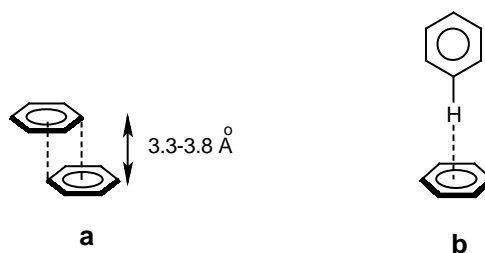


Figure 2. (a) face-to-face (interplanar distance about 3.3-3.8 Å).

(b) edge-to-face orientation

1.2.5 Hydrophobic effects

Hydrophobic interactions dominate many important processes, such as folding of proteins, protein-ligand (e.g. enzyme substrate) and protein-protein association, solubilization of non-polar substances by surfactant aggregates, and supramolecular complexation of guests with non-polar parts. The origin of hydrophobic interactions lies in the fact that non-polar molecules tend to avoid aqueous surrounding, as is evident from very low solubility of non-polar substances, in particular hydrocarbons, in water and in the positive transfer free energies of such substances from organic solvents to water. Water possesses a large internal cohesion energy density which is manifested in large vaporization enthalpy and high surface tension. Therefore, the unfavorable hydration free energy of the non-polar molecules can be partially compensated if such molecules associate in the aqueous solution, thus reducing the surface area accessible for water and causing it to form stronger intermolecular hydrogen bonding [1-4]. Such association represents hydrophobic interactions which is considered as a partial reverse of the transfer process 'solute in organic solvent → solute in water' in the sense that the nearest surrounding of the solute inside the associate is partially organic like.

These interactions to some extent compensate the inefficiency of polar interactions in water, which results from the high dielectric constant and strong proton-acceptor capacity of this solvent.

Hydrophobic effects are of crucial importance in the binding of organic guests by cyclodextrins and cyclophane hosts in water and are divided into an enthalpic and entropic energetic components. The association is accompanied by little change in enthalpy and is governed by entropy effects upon release of solvent molecules into the bulk.

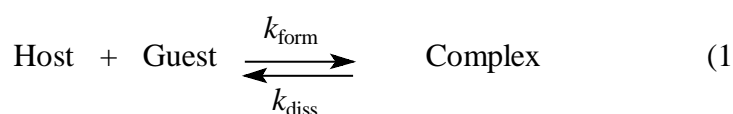
1.3 Design principles of supramolecular host

In general all compounds capable of binding another molecular species with a somewhat higher affinity than what must be expected from their fundamental molecular properties are termed molecular hosts. Association between host and guest molecules are usually based on simultaneous non-covalent interactions between single binding sites, acceptor and donor, which can be combinations like cation-anion, hydrogen-bond-acceptor-donor, etc.

In order to plan a suitable host for a target guest one should consider several parameters [1-3]. First, since non-covalent interactions are rather weak compared to covalent bonds, it is desirable to obtain multiple interaction sites to enhance complex formation and stability. The principle of multi-site complexation is very general in living systems, where it ensures the efficiency of replication, of enzyme-substrate and of antigen-antibody interactions etc. One can view multi-site complexation as a generalized chelate effect, well known in coordination chemistry, which refers to the increased stability of complexes with polydentate ligands, *e.g.*, as 1,2-diaminoethane with metal ion Ni^{2+} , as compared to those with chemically equivalent monodentate ligands, *e.g.*, ammonia, the chelate complex is more than 10^8 times more stable. An important requirement for multi-site binding is complementarity between binding sites in the correct disposition of host and guest molecules.

In designing a host that would bind a specific guest with a strong affinity and selectivity, one should bear in mind the necessary host-guest binding equilibrium. Equilibration is anticipated to be reached during the physical measurement time scale. Thus a prime target for host design is to enable kinetically labile complex formation, which allows rapid guest exchange. An upper limit for the association constant and the free energy of binding should be taken into account.

In host-guest complexation the equilibrium constant K_{ass} is determined from the ratio of the rate constants of complex formation (k_{form}) and dissociation (k_{diss}) reactions,



$$K_{\text{ass}} = \frac{k_{\text{form}}}{k_{\text{diss}}} \quad (12)$$

Where the dissociation rate,

$$v = k_{\text{diss}}[\text{complex}] \quad (13)$$

and dissociation half time,

$$\tau_{1/2} = \frac{\ln 2}{k_{\text{diss}}} \quad (14)$$

A crude estimate for a 1:1 stoichiometric association arrives at $K_{\text{ass}} \sim 10^{13} \text{ M}^{-1}$ ($\Delta G^\circ = -18 \text{ kcal mol}^{-1}$). The rate of bimolecular association is taken at the diffusion

limit of $10^9 \text{ M}^{-1} \text{ s}^{-1}$ and the half-time for dissociation of the complex at $T_{1/2} = 3 \text{ h}$. If a supramolecular complex formed with higher stability, one can predict that the bond formed must have a dissociation enthalpy ΔH_{diss} of less than 25-30 kcal/mol and $T\Delta S$ maximum at $-(13-14) \text{ kcalmol}^{-1}$. Therefore a formation of kinetically labile complex is a fundamental criterion in the definition of molecular hosts.

In addition to the above requirements, solvent effects play a fundamental role in host-guest design as their presence is obvious in all associations in condensed phases. Therefore, the net free energy of the complexation process depends strongly on solvent features that favor or impede host-guest association and stability. Hence, a qualified host that complexes the peculiar guest with activation of all the mutual interactions (according to the parameters discussed above) in one solvent may completely fail in another.

Unfortunately, however, due to the fundamental lock-and-key metaphor of Emil Fisher [9], which assumes that the mutual geometric fit of a host and guest dominates their thermodynamic affinity, the importance of the solvent in complexation was ignored for long time. Only recently, all the components of the structure-energy relationship, which depends on the host, guest and the solvent, have started being taken into account. Systematic exploration of the interplay between the various components of the structure-energy relationship is one of the main purposes of this dissertation.

1.4 A correlation between structure and energetics

For many years, the ultimate judge of successful complexation in studies launched to optimize the direct interactions between a host and a given guest by modifying the covalent structure of the host was the Gibbs free energy of complex formation ΔG° and the equilibrium constant for association (K_{assn}), not paying attention to the entropic components and solvent contributions. In many cases this approach didn't live up to the expectation and met with only limited success thereby exposing the shortcomings of the lock-and-key model.

The Gibbs free energy, ΔG° , which is a combination of enthalpic and entropic components that satisfy the Gibbs-Helmholtz equation, $\Delta G^\circ = \Delta H^\circ - T\Delta S^\circ$, may change only marginally with host structure because of enthalpy-entropy compensation [21,22]

that accompanies all weak interactions in solution and therefore does not reflect the structural achievements. The detailed knowledge of the energetic parameters allows a better determination of the nature of the complexation, *i.e.*, whether it is ΔH° or ΔS° driven, and therefore imposes more stringent constraints on explanatory attempts and on host design.

To demonstrate the last point we present three specific cases of complexation with ion-pairing and H-bonding. In these examples, it is shown that the Gibbs free energy alone fails to convey the accurate picture of the nature of the interaction and solvent contribution. However, when dissecting the energy components and following their behavior during complexation, separately, a better understanding of the true nature of the binding process in each case is achieved.

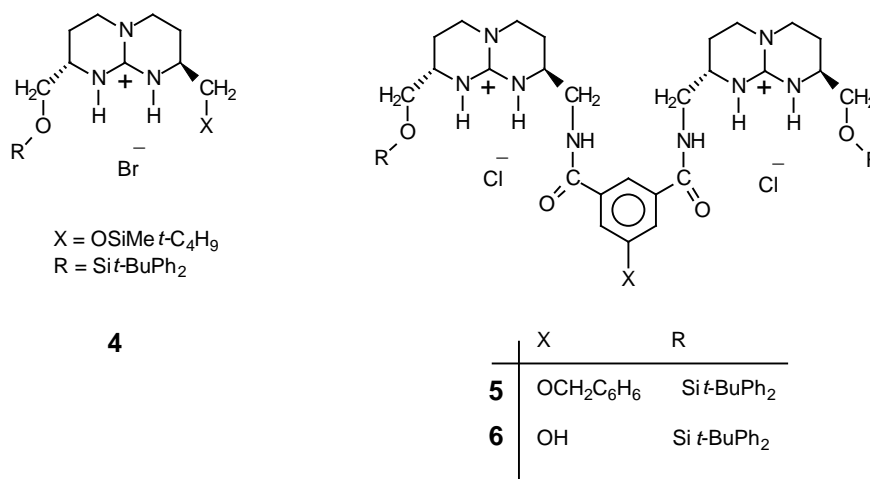
Case 1: The stability of the host-guest binding between tetraethylammonium acetate and the guanidinium **4** in acetonitrile at 30°C [23], is not only due to a strong exothermic enthalpic attraction, reflected in a strongly negative ΔH° (-3.7 kcal mol⁻¹) and a high affinity constant ($K_{\text{ass}} = 2.0 \times 10^5 \text{ M}^{-1}$), but also to a favorable positive entropic component ΔS° (+12.0 cal mol⁻¹ K⁻¹). This association process combines two molecular species to form one complex, yet the overall entropy of the system increases owing to the release of bound solvent molecules. Here, a non hydrogen-bonding solvent was chosen that at the same time would minimize unspecific ion-pairing by its high dielectric permittivity ϵ ($\epsilon = 36$).

Similar entropic effects are widespread in aqueous systems due to hydrophobic effects that have crucial importance in the binding of organic guests by hydrophobic host cavities in water. Here the binding process is driven by both the entropy and enthalpy that give rise to the high affinity of the complex.

Case 2: The binding of sulfate ions by host **5** in a highly polar and competitive solvent like methanol at 30°C [24], is strongly endothermic and gives $\Delta H^\circ = +7.7 \text{ kcal mol}^{-1}$ and $K_{\text{ass}} = 6.8 \times 10^6 \text{ M}^{-1}$. Thus, at room temperature association is strongly entropy-driven $\Delta S^\circ = +56.7 \text{ cal K}^{-1} \text{ mol}^{-1}$ by far outweighing the unfavorable ΔH° value. Since both the guanidinium group and the sulfate anions are solvated very effectively in protic solvents, the positive ΔH° value observed reflects the endothermic reorganization of the solvent shell upon complexation. The complex is less solvated

than the sum of its free components, and the release of solvent molecules thus leads to the entropic overcompensation of the unfavorable positive ΔH° of desolvation.

Case 3: Host-guest complexation of $\{\text{Na}^+\text{cryptand}[2.2.2]\}_2$ p-Nitrophenyl phosphate by compound **6** in acetonitrile [23] shows a strong negative enthalpy ($\Delta H^\circ = -9 \text{ kcal mol}^{-1}$) and a strong binding affinity ($K_{\text{ass}} = 1.6 \times 10^5 \text{ M}^{-1}$) which readily discloses a negative entropy contribution ($\Delta S^\circ = -5.9 \text{ cal K}^{-1} \text{ mol}^{-1}$). Owing to the very negative value of the enthalpy and the negative value of the entropy this complexation is enthalpy driven. The negative entropy implies that this interaction has reduced the degrees of freedom in the system and therefore, the complexation here is selective.



Case 4: Here we discuss a case in which the association between the host and the guest causes positive enthalpy ($+\Delta H^\circ$) and negative entropy ($-\Delta S^\circ$). This process is energetically unfavorable and hence unstable, and its time scale is normally very short rendering it practically undetectable. When the enthalpy response in an association process is exothermic then the binding of the two partners has occurred successfully. The entropy value depends on the amount of solvent release in the newly organized system and can, therefore, be positive or negative. Whereas, an endothermic enthalpy response necessitates a consumption of energy by the new noncovalent association, which is compensated in turn with entropy increase inducing the stabilization of the system. However, if the number of degrees of freedom in the system is significantly

decreased the interaction becomes energetically very expensive leading to a fast dissociation and to the break down of the noncovalent bond.

As a conclusion, the examination of the energetic parameters is very critical to understand the influence of the host character and the environment (*i.e.*, solvent molecules), on complexation. To measure these parameters, van't Hoff analysis derived from different instrumental methods like NMR and UV, and Isothermal Titration Calorimetry (ITC) [25] methods can be used. The NMR titration is an indispensable tool in the wide-range collection of information on supramolecular associations and can provide clues on the structural mode of host-guest relationships. However, the determination of the thermodynamic parameters ΔG° , ΔH° and ΔS° by this instrumental method requires the use of the laborious, insensitive, and error-prone, van't Hoff analysis of the binding data (see explanation below). A more direct access to those important energetic parameters is offered by isothermal titration calorimetry (ITC). The calorimetry method doesn't need any change in spectral characteristics to be induced by complexation. It requires, however, the reaction heat effect to be large enough to produce a measurable temperature change. This is at variance to spectroscopic methods for which the measured signal itself depends on the strength, specifically the ΔH° of the complex. Since calorimetric measurements faithfully report on the cumulative heat response of the entire system it is of utmost importance to design a host-guest system simple enough to allow deconvolution of all the processes happening simultaneously in solution and ascribe the heat effect to just one association reaction.

The main advantage of the ITC is that it allows the immediate determination of ΔH° as a primary parameter of measurement; ΔG° and the host-guest stoichiometry n are estimated from titration curve fitting. The reaction entropy ΔS° may then be easily calculated from the Gibbs-Helmholtz equation. The ITC can also provide a precise determination of heat capacity changes (ΔC_p) from measurements at different temperatures. There are clear advantages of the use of the ITC measured ΔH° and ΔC_p over the determination of the temperature dependence of an equilibrium constant by the van't Hoff equation,

$$\frac{d \ln K}{dT} = \frac{\Delta H}{RT^2} \quad (15)$$

The usual assumption is that in a small temperature interval, ΔH° can be considered as temperature-independent and, accordingly, the integral form of the equation can be presented as

$$R \ln K = -\Delta H / T + \Delta S \quad (16)$$

The temperature dependence of ΔH° is given by

$$\left(\frac{d\Delta H}{dT}\right)_p = \Delta C_p \quad (17)$$

and the aforementioned assumption of a constant ΔH° value implies that $\Delta C_p = 0$. The available data on ΔC_p values for various host-guest equilibria show, however, that this parameter can be even higher than $96 \text{ cal mol}^{-1} \text{ K}^{-1}$. With such values of ΔC_p the variation of ΔH° in a temperature interval of, for example, 50°C is more than $4.9 \text{ kcal mol}^{-1}$. Unfortunately the temperature dependence of ΔH° is often simply ignored.

1.5 Isothermal Titration Calorimetry (ITC)

In this work the ITC-MCS method introduced by MicroCal [26] was used for host-guest complexation study. This method directly measures the heat evolved or absorbed in liquid samples as a result of injecting precise amounts of reactants [27]. A spinning syringe is used for injecting and subsequent mixing. For other calorimetry methods see for instance [28].

In the ITC a pair of cells is enclosed in an adiabatic jacket (see figure 3), one cell is a sample cell filled with host or guest in a certain solvent, and the other cell is a reference cell, filled with a pure solvent. During an experiment the temperature of the reference cell is controlled and maintained constant by a steady small power supply, the reference offset. The temperature difference between the two cells is constantly measured and a proportional power is increased or reduced to the sample cell by the cell feedback system to keep the temperature difference very small. A signal proportional to the cell feedback (CFB), and with the instrument temperature and time, constitutes the relevant raw data. The CFB is calibrated in units of $\mu\text{cal/sec}$.

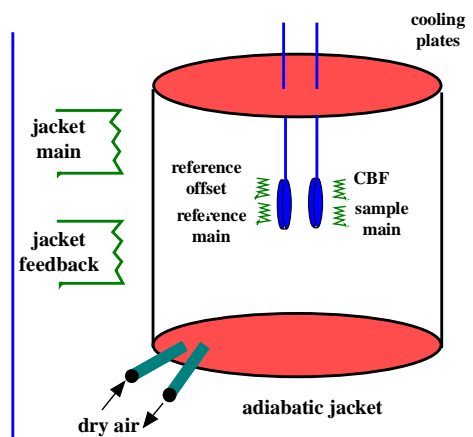
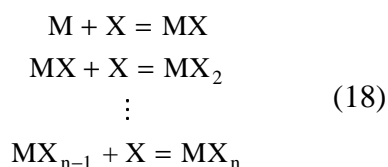


Figure 3. A schematic representation of the ITC unit.

A negative CFB signal occurs when an injection of a titrant into a sample cell causes a chemical evolution of heat (exothermic reaction). In this case, owing to the exothermic nature of the reaction, the cell feedback is no longer required to be active. The opposite is true for endothermic reactions that result in positive CFB signals. Here the temperature is reduced and the cell feedback is required to provide power for equilibrating temperature again. Since the cell feedback has units of power, the time integral of the peak, yields a measurement of thermal energy, ΔH° .

For a ligand X binding to a single set of n identical sites on a host molecule M, i.e.,



where the single-site binding constant is

$$K_{ass} = \frac{[\text{filled sites}]}{[\text{empty sites}][X]}
 \tag{19}$$

and

$$\Delta G^\circ = R T \ln K_{ass} = \Delta H^\circ - T \Delta S^\circ
 \tag{20}$$

Where ΔG° , ΔH° and ΔS° are the free energy, enthalpy, and entropy change for single site binding.

As mentioned before the parameters K_{ass} , ΔH° , and n are determined directly in a single experiment, by a non-linear least squares fit, and ΔG° and ΔS° are then calculated. Measuring the binding isotherm at a second temperature allows additional determination of the change in heat capacity of binding through the relation,

$$\Delta C_p = \frac{\Delta H_0(T_2) - \Delta H_0(T_1)}{T_2 - T_1} \quad (21)$$

It is worth mentioning here that ΔC_p is a good indicator of changes in hydrophobic interactions with binding, being negative if hydrophobic bonds are formed and positive if they are broken.

The critical parameter which determines the shape of the binding isotherm is the dimensionless constant c , defined as,

$$c = K_{\text{ass}} M_{\text{tot}} n \quad (22)$$

where M_{tot} is the total host concentration in the cell at the start of the experiment, and n is the stoichiometry parameter.

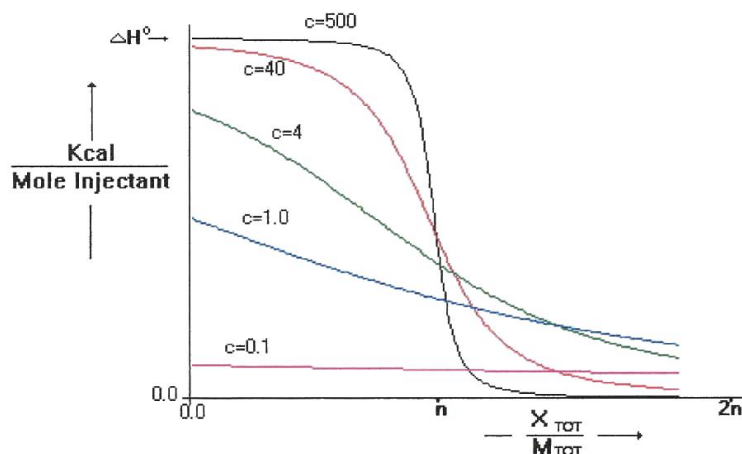


Figure 4. A plot showing the ITC binding isotherms with varying c values.

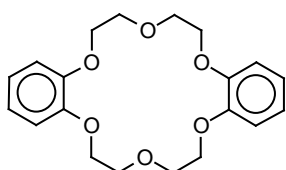
Very large c values lead to a very tight binding and the isotherm is rectangular in shape with the height corresponding exactly to ΔH° with the sharp drop occurring precisely at the stoichiometric equivalence point n in the molar ratio $X_{\text{tot}}/M_{\text{tot}}$ (see figure 4). The shape of this curve is invariant to changes in K_{ass} so long as the c value remains above 5000. As c is reduced by decreasing M_{tot} , the drop near the equivalence point becomes broadened and the intercept at Y axis becomes lower than the true ΔH° . In the limit of very low initial M_{tot} concentration (cf., $c = 0.1$), the isotherm becomes featureless and traces a nearly horizontal line indicative of very weak binding. The shape of these isotherms is sensitive to binding constant only for c values in the range $1 \leq c \leq 1000$. For ideal measurements the range is even more restricted $5 \leq c \leq 500$.

1.6 Hosts for cationic guest molecules

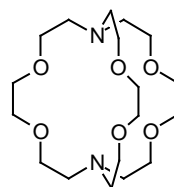
Many molecular receptors of varied structural types for binding cations, anions and neutral species have been investigated. The goal of their design was to achieve structural control through preorganization and led to the development of macrocyclic ligands from acyclic ones.

Crown ethers are macrocyclic receptors that are known for their selectivity and binding strengths towards alkali and alkaline earth metal cations [1-3]. The important characteristic of crown ethers are the number and type of donor atoms, the dimension of the macrocyclic cavity and the preorganization of the host molecule for most effective coordination. The so-called “macrocyclic effect” of crown ethers is related to the last two characteristics. Dibenzo-18-crown-6 **2**, which complexes Rb^+ ion, was first discovered by Pedersen in 1967. Similar inclusion in natural macrocycles takes place in ionophores such as valinomycin which gives a strong and selective complex with K^+ . The stability and selectivity of the complexes depend on the size of the polyoxyethylene crown ether ring, the best bound cation is the one that fits into the cavity. Crown ether complexes with other cations such as ammonium, guanidinium, arenediazonium and pyridinium have also been studied.

Shortly after Pedersen's work, Jean-Marie Lehn has designed three-dimensional analogues of the crown ethers called cryptates like host **7**. In this way it was anticipated that metal ions could be encapsulated entirely within a crown-like host with consequent gains in cation selectivity and enhancement in ionophore-like transport properties. The bicyclic cryptate ligands showed stability with alkali cations much higher than those of natural or synthetic macrocyclic ligands. The key to dramatically enhanced metal cation binding ability of cryptands over crown ethers is the three-dimensional nature of their cavity. They show selectivity as a function of relative sizes of the cation (complementarity) and the intramolecular cavity, which enables spherical recognition of the metal ion to take place [29].



2



7

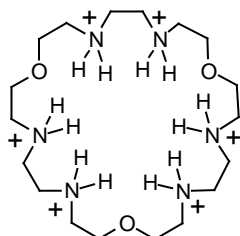
1.7 Hosts for anions in particular oxoanions like phosphate and carboxylates.

In comparison to cations, the area of supramolecular anion complexation has developed more slowly, but has attracted increasing attention in recent years [30]. Between 70 and 75% of enzyme substrates and cofactors are anions, very often phosphate residues (as in ATP and ADP) or inorganic phosphate. Anions such as sulphate and carboxylates also occur frequently in biochemical systems. In the gas phase almost all elements can form stable single-charged anions according to their electron affinities [31]. In condensed phases, especially in the presence of water and oxygen, many elements are more stable at higher oxidation states, which combine with water to form oxoanions in which the net charge is distributed over few atoms. Correspondingly, the charge density is lowered with notable changes in properties. Generally, anions possess larger ionic radii and higher solvation energy in protic solvents relative to cations. Electrostatic stabilization of anions is particularly efficient in polar protic solvents due to hydrogen-bonding interactions [32]. Although anions are strongly hydrated, the binding of oppositely charged species is not suppressed. Essential to hydrogen bonding stabilization of anions is their Lewis-base character [33]. The presence of lone electron pairs serving as H-bond acceptor sites (apart from exceptions like AlH_4^- , BPh_4^- , etc.) their Lewis basicity, however, varies within broad limits. Nevertheless, it is a common feature of anions and may be used as a basic interaction type in the construction of anion hosts. In combination with the covalently insured topology, it adds directionality to the system and renders it sensitive to the spatial arrangement and orientation of binding groups. These form the bases for the distinction between, for example, sulphate and hydrogen phosphate [34,35], which is vital to all biological processes involving these oxoanions. Anions are also of more diverse shapes than cations: spherical, linear, angular etc.

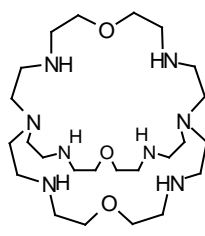
The mutual recognition pattern of host and guest must be defined with the aim of maximizing discrimination of similar guest species. But it is not the only matter, since the solvent shells around the binding partners will unavoidably be changed on complexation, and this can either be a costly process of the net free energy or restructuring the solvent may rather favor complex formation. The solvent will affect complex stability in a way that the association constant may change dramatically

depending on the sheer size of solvent molecules [36]. Therefore one should consider these points in anion host design.

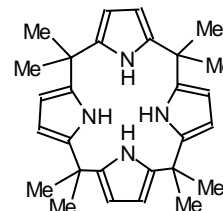
Anion receptors can be neutral Lewis acids, neutral proton donors, metal cations or positively charged organic groups, such as ammonium or guanidine centers, which can also serve as proton donors.



8



9



10

Cationic hosts capable of forming ion-pairs with anions in solution are most easily prepared by protonation of suitable basic compounds. Basic open-chain polyamine compounds like spermine or spermidine, are known [37] to bind to phosphate anions or polyanions in water at neutral pH, they most likely adopt a flexible extended conformation that presumably will not incorporate all the ammonium sites because of the far proximity to each other. In contrast, at low pH, polyprotonated monocycle azacrown ethers like **8** possess a greater charge density and thus a greater predisposition to anion binding. The hexaprotonated azacrown **8** shows strong complexes with a variety of anions in water ($\log K_{\text{ass}} = 4.7$ with AMP^{2-} , 7.7 with ADP^{3-} and 9.1 with ATP^{4-}). From the general trend that complex stability increases with guest charge, one can infer the dominance of coulombic interactions [38]. Complexation with fumarate²⁻ ($\log K_{\text{ass}} = 2.2$) and oxalate²⁻ ($\log K_{\text{ass}} = 4.7$) shows a good discrimination between anions of the same charge. A much greater improvement in stability and selectivity of anion complexation was achieved by rigidification of the binding sites, several bicyclic cryptands were prepared by Lehn such as cryptant **9**, which in its penta- or hexaprotonated forms, complexes a variety of well-solvated anions in aqueous solution [39-42]. Host **9** complexes anions like oxalate and malonate strongly by an inclusion process ($\log K_{\text{ass}} = 4.95, 3.10$ respectively), in which the guest anion penetrates the molecular cavity and is held there by an oriented set of hydrogen bonds. Furthermore, X-ray structures show the ellipsoidal shape of the host cavity and

the topology of nitrogen H-bonding sites provide an optimal complementarity with azide anion translating into an extraordinary high complex stability in water ($\log K_{\text{ass}} = 4.3$). Halides fit less well, and the decrease in binding free enthalpy from fluoride ($\log K_{\text{ass}} = 4.1$) to iodide ($\log K_{\text{ass}} = 2.15$) testifies to the importance of H bonding as the main attractive binding force.

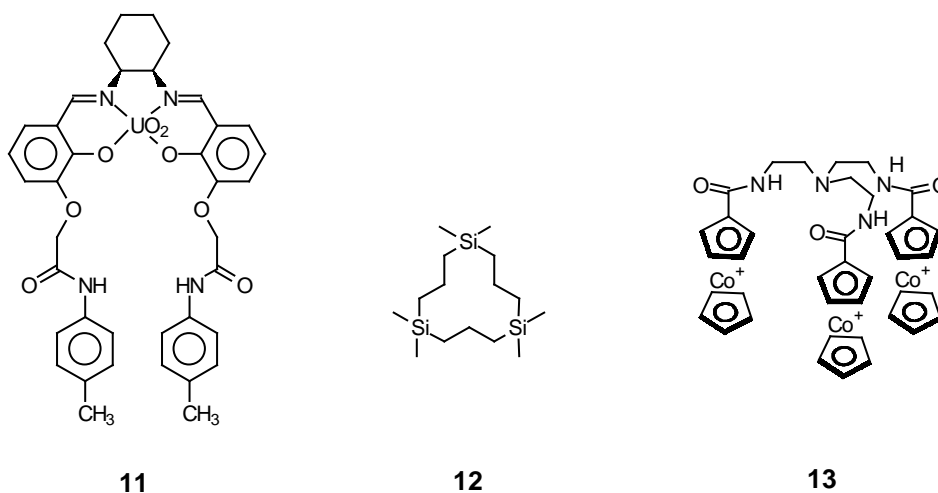
Calix[4]pyrrole **10** has been known for over a century but has been characterized only recently as an electroneutral host for halide anions [43] with a strong preference for fluoride ($K_{\text{ass}} = 1.7 \times 10^4 \text{ M}^{-1}$) over chloride ($K_{\text{ass}} = 350 \text{ M}^{-1}$) and dihydrogen phosphate ($K_{\text{assn}} = 97 \text{ M}^{-1}$) in dichloromethane. Recently it has been shown by Schmidtchen that complexation of **10** in dry acetonitrile resulted in a higher association constant by at least a power of 10 ($K_{\text{ass}} = 1.5 \times 10^5 \text{ M}^{-1}$ for fluoride, $1.8 \times 10^5 \text{ M}^{-1}$ for chloride and $1.6 \times 10^4 \text{ M}^{-1}$ for dihydrogenphosphate [44]). These results clearly repeat the message that in condensed phases selectivity, with competing guests is not a function of the host structure alone but is heavily dependent on the actual solvent used. Thus, the designation of calixpyrroles as a fluoride receptor at large appears not justified, because the fluoride specificity in dichloromethane or in the gas phase, too, is compromised and eventually vanishes totally in more polar solvents such as acetonitrile or DMSO.

The advantage behind the concept of crown ethers, the complexation of even very weakly coordinating cations, can be utilized for binding anionic species too. The placement of multiple Lewis-acid moieties with their electron-deficient sites in a preorganized molecular framework can result in a host-guest complexation with the lone electron pairs of anions. This is the mutual arrangement used in crown ethers and thus the term “anticrown chemistry” has been made up to clarify this relationship [45]. Electroneutral hosts do not face the problem of competitive counterion binding, which is unavoidable with cationic hosts. On the other hand Lewis-acid hosts have to encounter the natural competition of solvents with their guests. Most solvents except for hydrocarbons are quite Lewis basic and in general exceed the molar concentration of a guest anion by several orders of magnitude. (Therefore, solvation design is of great importance). But the examples of natural metalloproteins processing small inorganic anions clearly show that binding is to be possible even in Lewis basic

solvents, hence proposed that it might well be the preferable concept, if small anions are used.

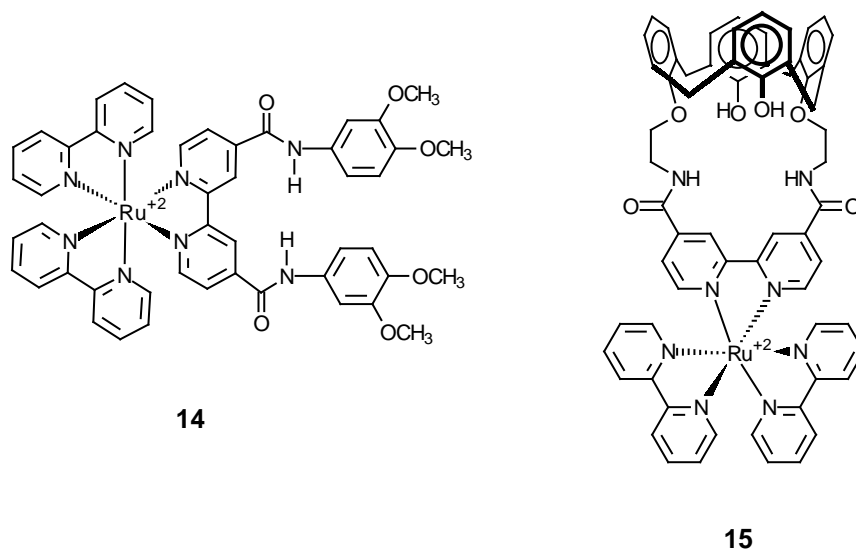
Examples of hosts that involve electron-deficient atoms such as uranium and silicon, are hosts **11** and **12**, respectively. Anion complexations of **11** in organic solvents (MeCN, DMSO) [46,47], reveal a general selectivity for H_2PO_4^- ($K_{\text{ass}} = 10^5 \text{ M}^{-1}$), over Cl^- ($K_{\text{ass}} = 10^3 \text{ M}^{-1}$) or NO_2^- ($K_{\text{ass}} = 10^2 \text{ M}^{-1}$) in MeCN. The analysis of the crystal structure reveals that dihydrogen phosphate is coordinated with the uranyl Lewis acidic center and builds supplementary hydrogen bonds to the methoxy and amido functions of the ligand.

Anion binding ($\text{Br}^- > \text{Cl}^- \gg \text{F}^-, \text{I}^-$) by macrocycle **12** [48] was tested due to its capacity to accelerate anion transport through water-organic solvent interface.

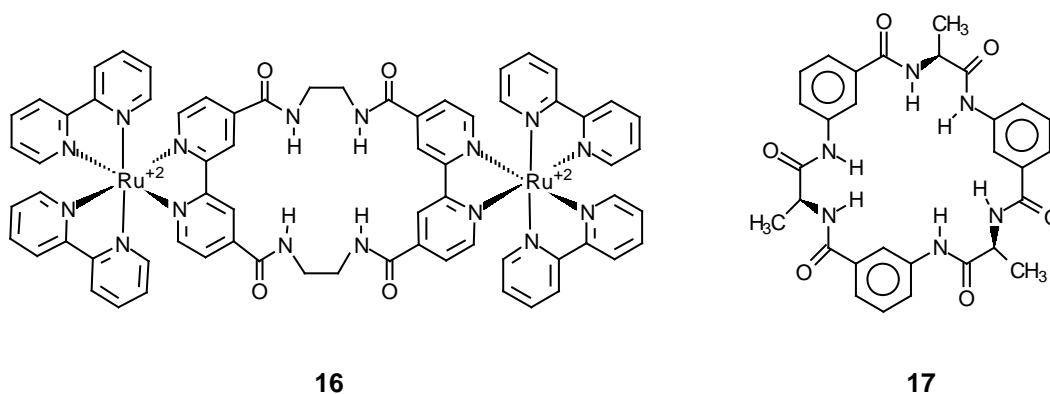


The majority of organic host compounds interacting by charge attraction with anionic species are based on cationic nitrogen compounds. However, the introduction of positive charge into the organic skeleton as an alternative to protonation can be very efficiently attained by metal cation ligation and as a result it requires the careful design of suitable coordination sites. Receptors which use transition metal cations as anion binding sites frequently have the ability to give readily detectable spectral or electrochemical signals upon anion binding, therefore they can act as anion sensors. The cationic acyclic receptors such as **13** [49,50] and **14** [50] are examples of designed receptors for this purpose and the uptake of anions was characterized by cathodic shifts of their reduction potentials. Structures **15** and **16** are more sophisticated macrocyclic derivatives of ruthenium(II) bipyridyl [51]. Anion binding was clearly

visible by optical or cyclic voltammetric methods. Host **15** shows, as expected, pronounced specificity to the more basic dihydrogen phosphate anion ($K_{\text{ass}} = 2.8 \times 10^4 \text{ M}^{-1}$ in DMSO), even in the presence of ten-fold excess of sulfate and chloride. Host **16**, which is a cyclic analog of host **14**, is specific for chloride ($K_{\text{ass}} = 4 \times 10^4 \text{ M}^{-1}$ in DMSO), but practically doesn't bind to dihydrogenphosphate. At the same time the acyclic compound **14** binds phosphate more strongly than chloride, the selectivity inversion is attributed to the rigid structure of the macrocycle.



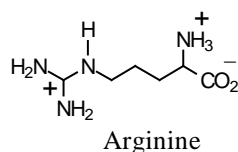
Anion binding by these hosts involves electrostatic and hydrogen bonding contributions.



Other receptors were prepared by utilizing peptide bonds in natural proteins for anion complexation. Cyclo-hexapeptide **17**, composed of dipeptide building blocks

containing *m*-aminobenzoic acid, possessed a structure with organized H-bonds donating groups converging to the center of the macrocycle [52]. Host **17** showed, through UV spectroscopic analysis, an exceptional binding with *p*-nitrophenyl phosphate in DMSO $K_{\text{ass}} = 1.2 \times 10^6 \text{ M}^{-1}$.

Of particular importance in anion binding of proteins and enzymes is the arginine residue **18**, which contains the guanidinium moiety. Guanidinium, the protonated and therefore positively charged, form of guanidine is an excellent anion binder. It stays protonated over an extremely wide range of pH ($\text{pK}_a = 13.5$ in water for the parent CN_3H_6), and therefore, in addition to the electrostatic attraction (ion-pairing), it can participate in double hydrogen bonding with oxoanions such as carboxylates, phosphates, etc. (figure 5), a structural motif that can be found in many crystal structures of enzyme complexes with oxoanions as well as in simple guanidinium salts [53,54]. Guanidinium is also involved in the stabilization of protein tertiary structures via internal salt bridges with carboxylate functions.



18

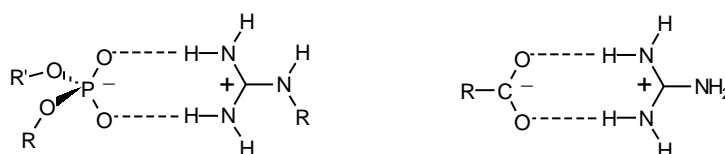
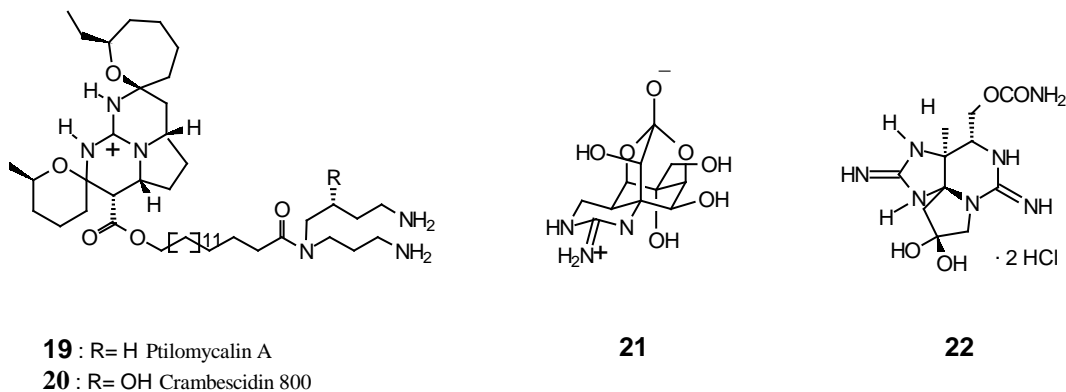


Figure 5. Schematic binding patterns of the guanidinium group with oxoanions as observed in many X-ray crystal structures.

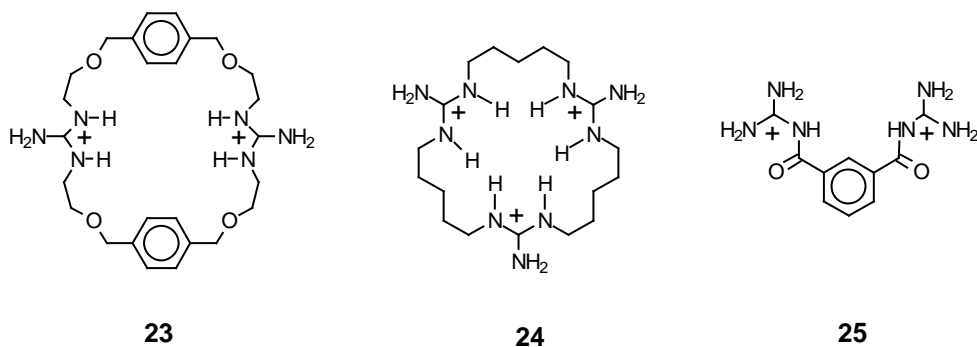
Some low molecular weight natural products contain a guanidino functionality as well. Alkaloids such as ptilomycalin A **19** was first isolated in 1989 [55] from the Caribbean sponge *ptilocaulis spiculifer* and the Red Sea sponge *Hemimycale*.. A related series of alkaloids such as crambescidines **20** were obtained from the mediterranean sponge *Crambe crambe*. These antitumor, antiviral and antifungal compounds possess a unique pentacyclic guanidinium core that has a hydroxyspermidine residue attached by a long chain of an ω -hydroxycarboxylic acid

spacer. Some toxins as well are characterized by their guanidinium moiety, *e.g.*, the puffer fish poison tetrodotoxin **21** [56], the paralytic shellfish poison saxitoxin **22** [57], the peptide antibiotics capreomycin, viomycin, tuberactinomycin, and the anti-fungal agent stendomycin.



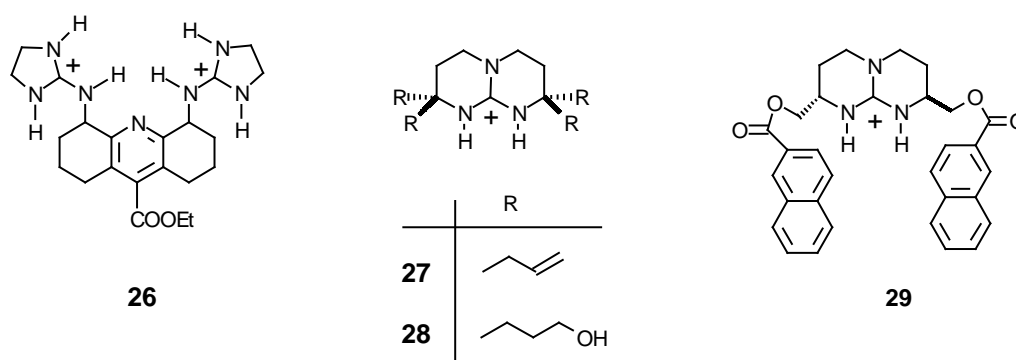
The hydrophilic guanidinium moiety enhances the receptor's solvation in water very efficiently, therefore ion-pairing and H-bonding with oxoanions in aqueous solution is negligible ($K_{\text{ass}} < 5 \text{ M}^{-1}$). In spite of these solvation properties that hinder the attempts to mimic the guanidines in artificial receptors, the aforementioned attractive features of this moiety and its participation in natural host-guest binding has encouraged researchers to design abiotic guanidinium host compounds.

The macrocyclic guanidinium based receptors **23** and **24** were prepared by Lehn *et al* [58]. to compare anion binding abilities relative to azacrown ethers. Binding of these receptors with PO_4^{3-} in methanol/water showed weak complexation with $\log K_{\text{ass}} = 1.7$ and 2.4, respectively. This result alongside many other similar examples [59] led to the conclusion that anion binding was governed by electrostatic interactions. Host **25** was designed by Hamilton [60] to mimic the enzymatic cleavage of phosphodiester [61]. compound **25** indeed complexes phosphodiester monoanions with $K_{\text{ass}} = 5 \times 10^4 \text{ M}^{-1}$ in



acetonitrile, and gave rate enhancements for transesterifications by a factor of 300. More preorganized hosts like **26** [62] showed that phosphate binding could stand up to more competitive aqueous solvation conditions and also showed an enhancement of imidazole-catalyzed mRNA hydrolysis by 20 folds in water [63]. Despite the catalytic effects in phosphate ester hydrolysis shown by these simple bis-guanidinium salts, they can't reach the degree of efficiency seen, for example, in the metalloenzyme mimics.

In order to maintain the structure of the guanidinium group and to enhance its binding abilities, one may incorporate it into a rigid bicyclic framework, which should reduce hydration of the charged moiety. The addition of hydrophobic hydrocarbon residues will lead to a well defined structure, therefore, binding to oxoanions can happen in only one mode with precise positioning of the guest relative to the host structure. The guanidinium moiety in the rigid, strain-free bicycle will make the host more chemically stable and more basic than the parent guanidine. Some natural products contain the guanidino functionality as part of a cyclic or bicyclic system.

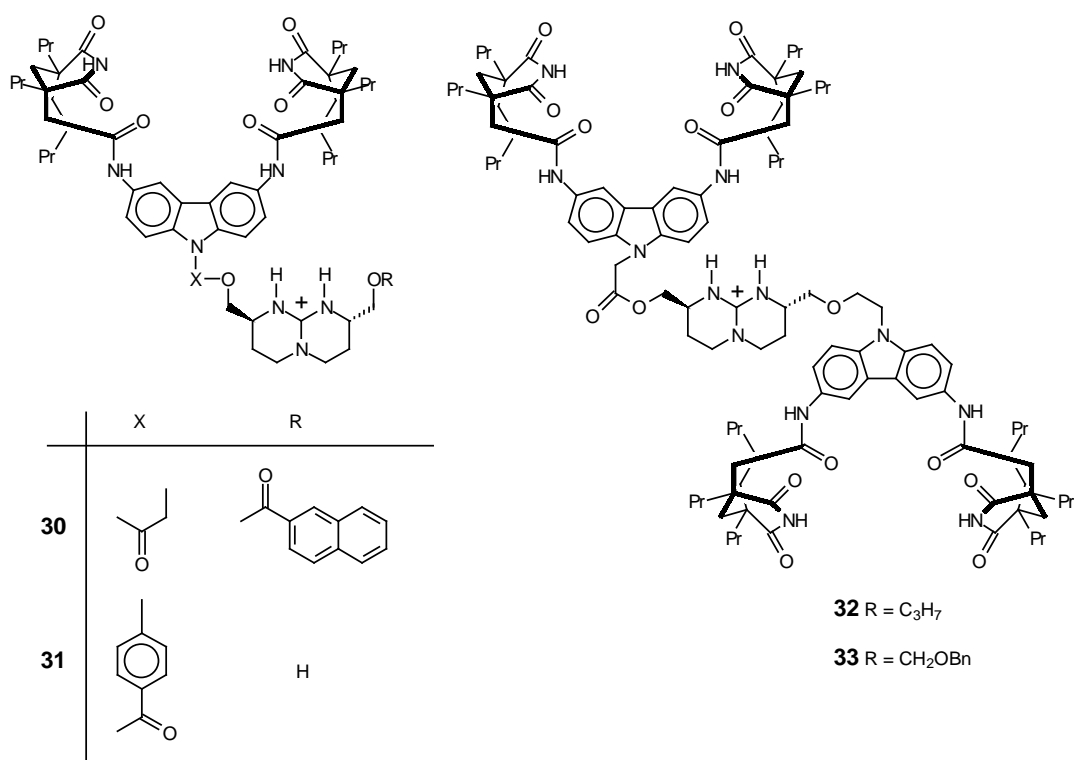


The desirable attributes of bicyclic guanidinium groups were recognized by Schmidtchen more than 20 years ago when symmetrically tetrasubstituted derivatives like **27** and **28** became available [64]. Host **27** forms a very stable ion-pair with p-nitrobenzoate in chloroform with $K_{\text{ass}} = 1.4 \times 10^5 \text{ M}^{-1}$ [54]. Host **28** with four hydroxypropyl substituents showed that the host-guest binding pattern with acetate was a part of a greater hydrogen bonding network. Later, chiral analogs of the bicyclic guanidines were obtainable [66,67]. Host **29** with its aromatic moieties allows two different recognition sites with aromatic carboxylate anions, ion-pairing and aromatic π -stacking [68,69]. Binding of **29** to chiral carboxylates, formed diastereomeric complexes. These

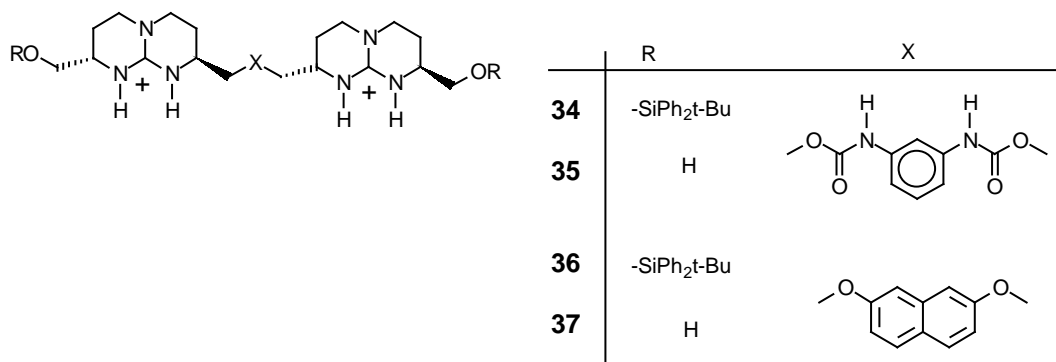
complexes were able to extract N-acetyl- and N-BOC-tryptophan from a racemic aqueous solution into chloroform with moderate selectivity.

Further addition of anchor groups to the bicyclic guanidinium framework can introduce other binding sites with certain guests and increase the specificity of guest binding. Many receptors were designed, with different anchor groups, to recognize amino acids in their zwitterionic form. Anchor groups like crown ethers [70], azacrown ethers [71] and calixarenes [72] will recognize the ammonium moiety of the amino acid.

Several guanidinium receptors were designed with complementary anchor groups, *e.g.*, tweezer-like Kemp acid derivatives, in order to selectively bind nucleotides [73]. Hosts like **30** could complex cyclo-adenosine monophosphate with some preference over guanosine analogs in two phase extractions. The guanidinium-phosphates ion-pairing adhered to in 1:1 stoichiometry. The binding pattern in these complexes as evident from NMR studies, is a combination of ion-pairing, π -stacking and a network of hydrogen bonds. Receptor **31**, prepared by Rebek, complexed 2'-3'-c-AMP with ion-pairing contributing about 0.6 kcal/mol on average to the total binding affinity of 3.65 kcal/mol [74].



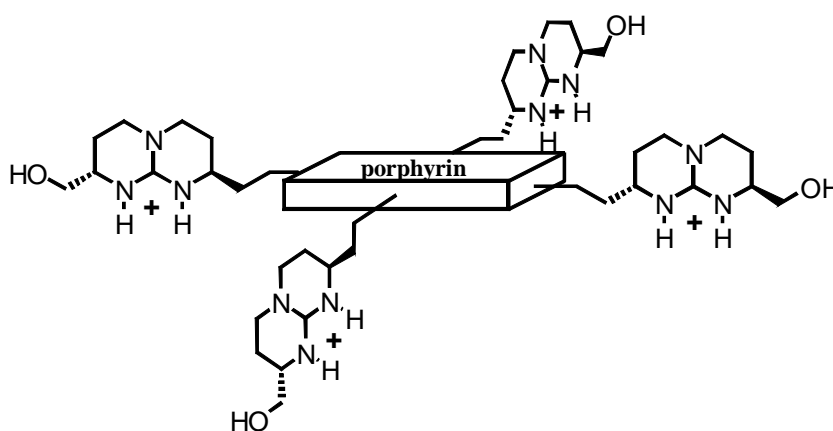
The development of these receptors to enhance binding of di- and oligonucleotides, led to the preparation of receptors **32** [75] and **33**. Receptor **32** showed high affinity for dinucleoside phosphate dApA, while **33** brought about phase transfer of nucleotides with a molecular weight of up to 25 kDa [76]. Hence these hosts show a high extraction affinity for oligonucleotides into organic solvents such as dichloroethane.



The continuous design improvements of guanidinium receptors to selectively bind tetrahedral oxoanions in more competitive solvents led to the development of ditopic and polytopic host molecules. In hosts **34-37** [77-81], two bicyclic guanidinium groups were linked by a linear and flexible spacer, a tetrahedral anionic guest binding would begin a folding of the receptor in order to place the main planes of the bicyclic moieties perpendicular to each other. Host **34** formed a 1:1 complex with nucleotides in methanol and **35** formed the same complexes even in water [77]. Compound **36** formed complexes with biologically important phosphates in methanol with binding constants of $(1.8-3.8) \times 10^4 \text{ M}^{-1}$. It also showed an impressive preference for binding malonate (dicarboxylate) over its shorter or longer chain analogs [80]. Removal of the silyl ether groups in **37** resulted in the formation of complexes with phosphates with higher stoichiometries in methanol, but in water 1:1 complexation was observed with $K_{\text{ass}} = 10^3 \text{ M}^{-1}$. The influence of spacer flexibility upon complexation was examined on rigidification by using mannitol-derived spacer units [81]. The varying K_{ass} led to the conclusion that spacer flexibility in these hosts does not play a major role in guest binding.

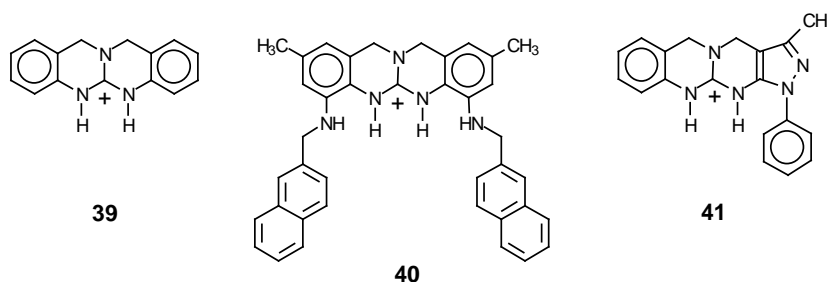
The synthesis, spectral properties, and anion-controlled assembly of porphyrin-bicyclic guanidine conjugates such as **38** in aqueous solutions has been recently

reported [82]. The design of the receptors was based on the concept of cooperative interactions of both porphyrin and the chiral bicyclic guanidine moieties with an anionic compound of interest. The coulombic and H-bonding attractive forces are predominantly governed by the peripheral bicyclic guanidines, which, in combination with π - π stacking of porphyrin units, impose additional geometrical restrictions with respect to the mutual distance and orientation of the guanidines. These porphyrin assemblies upon addition of small anions such as acetate, dihydrogenphosphate, terephthalate etc. form chiral structures controlled by the anion. Binding of these anions was indicated by UV/vis, fluorescence, and CD spectroscopy.



38

The reliable usefulness of the bicyclic guanidinium core in oxoanion complexation triggered the development of more rigid guanidinium systems, such as **39** [83], **40** [84] and **41** [85]. The conjugation of the nitrogen sites into the aromatic moieties make the compounds much less basic than ordinary guanidines and therefore complexation experiments is restricted to a smaller pH range. When host **41** was set up into a liquid membrane in slightly acidic solution it acted as an electrochemical sensor for hydrosulfite with great selectivity [86]. Receptor **40** also showed strong interactions with carboxylates [84]. Nevertheless, the utility of these systems needs further study and improvements.



2. Aim of this work

The aim of this work is to study the structure-energy relationship of a simple host-guest system in a non-hydrogen-bonding solvent in order to develop more reliable guidelines for molecular recognition. Evaluating the energetics means the dissection of ΔG° into its ΔH° and ΔS° components depending on host structure variation in order to understand the bimolecular association process and the role that solvent plays in binding. The latter point can donate a guideline for host-guest design into more competitive solvents, such as water. The importance of solvent participation was explicitly neglected in the earliest studies, therefore ignoring the entropic components of association as well as all solvent contributions.

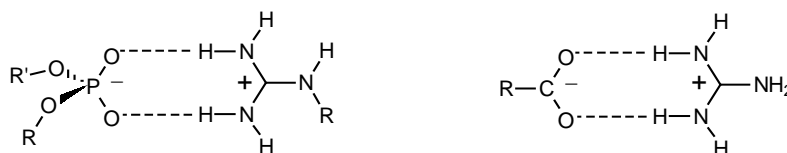


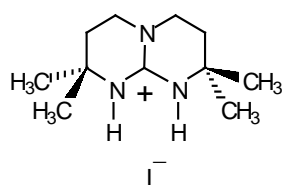
Figure 5. Hydrogen bonding and electrostatic interaction between the guanidinium moiety and oxoanions

In this study, the structure-energy relationship in guanidinium-oxoanion systems is explored. The interaction mode between the host and guest follows 1:1 stoichiometry and the prime structural motif features cation-anion arrangement, assisted by two parallel hydrogen bonds as shown in figure 5. Formation of hydrogen-bonded ion pair complexes is expected to depend on the competition with solvent. Thus, a non-hydrogen-bonding solvent was chosen that at the same time would minimize nonspecific ion-pairing by virtue of its high dielectric permittivity ϵ . Dry acetonitrile ($\epsilon = 36$) appeared to be an optimal choice for this kind of complexions.

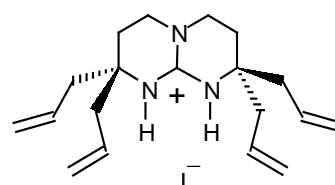
In order to unravel the structure-affinity correlation of host-guest binding modules based on guanidinium-oxoanion interaction, we have attempted to meet the following points:

1) The preparation of a series of bicyclic guanidines like compounds **48** and **70**. The concept behind the synthesis of the designed bicyclic guanidinium cations was to introduce substituents directly adjacent to the binding site with different steric

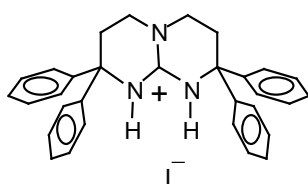
properties, such as phenyl groups or fluorene moieties in hosts **48** and **70** respectively, without harming the preferential binding mode. The importance of these residues lies in their ability to minimize the solvation shell near the binding site and thus reduce the enthalpy penalty paid to disrupt the solvation shell. Comparison with other hosts in the series like compounds **71** and **132** that were prepared with more flexible substituents will clarify if decreasing flexibility will affect binding properties. These guanidinium compounds constitute a suitable series for trend analysis.



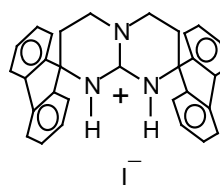
71



132



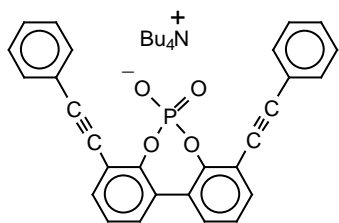
70



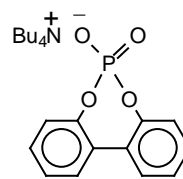
48

2) The preparation of optimal oxoanions building block, such as phosphate **78** and phosphinate **92** in an attempt to increase the binding directionality towards guanidines (the above hosts) assisted by the two side arms that will project above and beneath the main plain of the guanidinium moiety upon complexation. As a result the number of solvent molecules around the binding site will be reduced and consequently cut down on solvation effects. Although the intrinsic properties of the anionic moiety may not be touched, host-guest complexation is sensible to the overall structure of the guest and the nonionic part may well dominate the binding interaction.

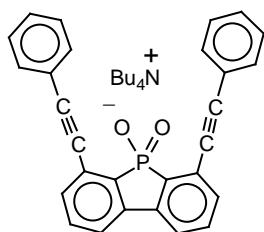
To evaluate the real effect of the newly designed guest anions, the parent anions **84** and **128**, which are missing the side substituents, will be used in a trend analysis as well.



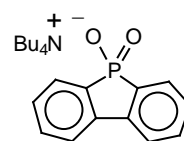
78



84



92



128

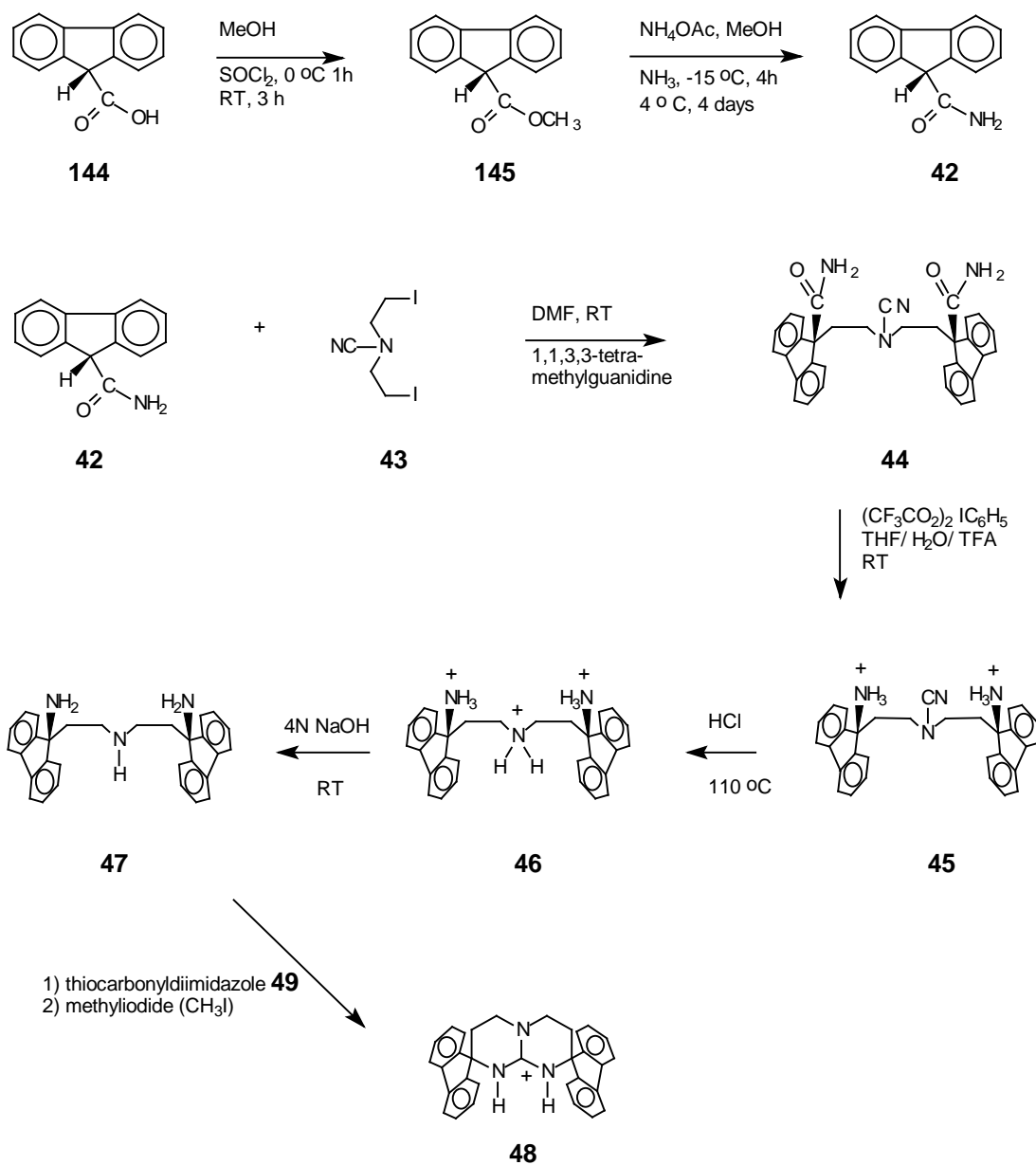
3. Synthesis

3.1 Synthesis of bicyclic guanidine hosts **48** and **70**

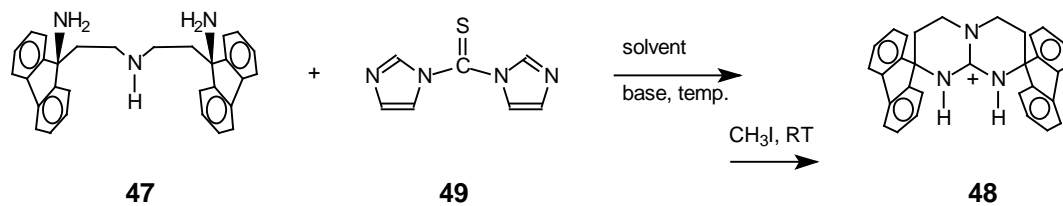
3.1.1 The synthetic strategies for host **48**

We have chosen to start off by preparing the fluorene bicyclic guanidine **48** through the reaction scheme strategy shown in scheme 1. The first stage in the step-wise reaction was successfully carried out, and fluorene dicarboxamide **44** was obtained in 80% yield by using the starting materials 9-fluorene carboxamide **42** and N,N-bis(2-iodoethyl)-4-cyanoamide **43**. Compound **42** was obtained from the amidation of 9-fluorene carboxylic acid methyl ester **145** starting from 9-fluorene carboxylic acid **144**. Compound **45** was then prepared in 85% yield by applying the Hofmann rearrangement to **44** using pifa ([Bis-(trifluoroacetoxy)-iodo]benzene) instead of sodium hypobromide as a modern oxidation reagent. Hydrolysis of the intermediate **45** offered the putative compound **46**. Deprotonation of **46** with 4N NaOH yielded **47**. In order to carry out the final step in the reaction, guanidylation of compound **47** was performed and compound **48** was produced. Although this last step has proven difficult (see below), fortunately, we managed to realize it.

The high basicity of the amino groups in compound **47** enables prompt protonation. In such a case the protonated **47** loses the amine's nucleophilicity and might therefore prevent the reaction with the reagent thiocarbonyldiimidazole **49**, which in turn contributes the additional carbon in compound **48**. Scheme 3 describes the mechanism of the guanidylation with thiocarbonyldiimidazole **49**. In order to insure complete deprotonation of **46** to **47** during the reaction, different bases were added (scheme 2, table 2, Experiments 1-3). However, despite base addition, the desired product was not observed. The reaction was repeated without the addition of base (Exp. 4 in Table 2) in the same solvent, CH₃CN, but did not generate any different result.



Scheme 1. A schematic representation for the preparation of fluorene-guanidinium **48**



Scheme 2

Table 2. Different conditions used for the guanidylation step of **47** .

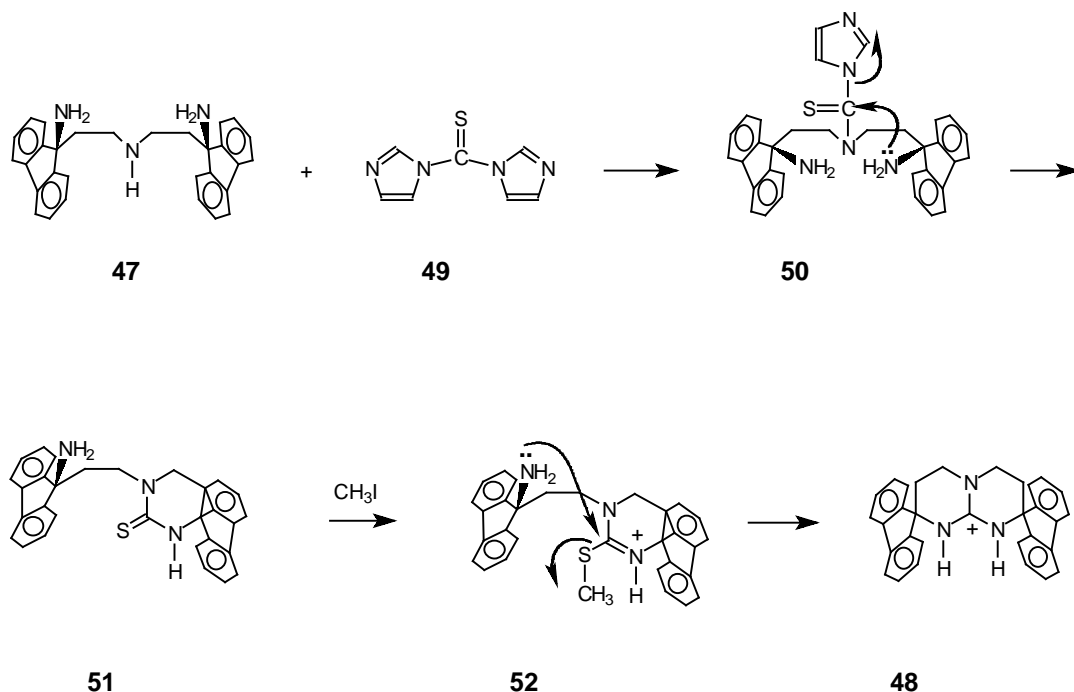
exp. #	solvent	base	T (°C)	product 48
1	acetonitrile	1,1,3,3-tetramethyl guanidine	85	no
2	acetonitrile	triethylamine	85	no
3	acetonitrile	ethyldiisopropylamine	90	no
4	acetonitrile	—	90	no
5	dimethylformamide	—	100	no
6	chloroform	ethyldiisopropylamine	0	no
7	chloroform	—	RT	no
8	1,4 dioxan	—	105	yes
9	diethyleneglycoldimethyl ether	—	140	yes

These negative results have provoked us to inspect whether the poor solubility of the compound **47** in CH₃CN acted as a hurdle in the guanidylation step. Therefore, the solvent as well as the temperature was varied (exp. 5-7). Unfortunately, however, the guanidylation of **47** still could not be achieved even with the new modifications.

The outcome of experiments 1-7 (Table 2) suggested to further restrict the potential solvents to those that satisfy the following characteristics: 1) Provide an efficient solvation environment for the starting materials. 2) Maintain the integrity of the reagent throughout the interaction. 3) possess a high boiling point as to enable higher reaction temp. It was found that such conditions are met by ethers with high boiling point, such as 1,4 dioxan (bp.102°C) or diethyleneglycoldimethyl ether (bp.162°C).

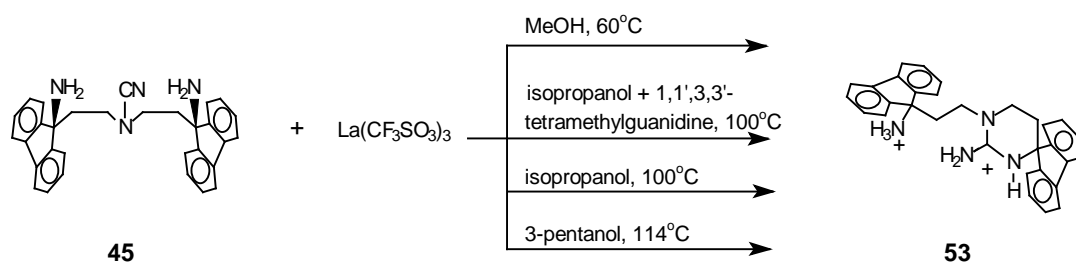
The experiments 8-9 (Table 2) using the same stoichiometries as in previous cases were conducted over night to the temperatures shown in Table 2. At the end of the heating period an oily precipitate was observed in Exp. 8, while in Exp. 9 a more solid precipitate was detected. In addition, monitoring the reaction by HPLC, a signal of the monocycle **51** was still observed, hence the alkylation reagent CH₃I was added to the reaction mixture to convert the remaining intermediate monocyclo compound **51** to the bicycle product **48** and subsequently to provide the I⁻ counter ion to the produced

charged bicyclic guanidine **48**. Analysis of the precipitated material by HPLC, NMR and MS confirmed it to be the desired compound **48**.



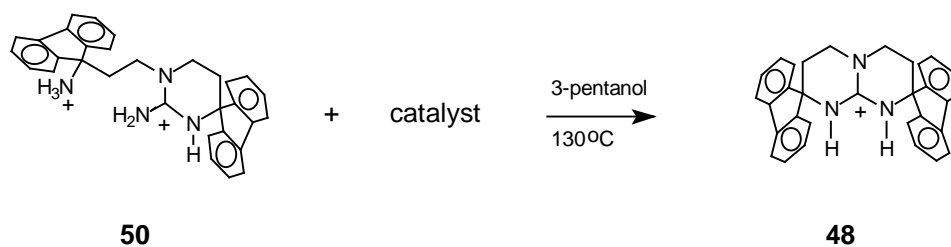
Scheme 3. The mechanism of guanidylation of **47** with thiocarbonyldiimidazole

The main goal of the use of the reagent thiocarbonyldiimidazole in the previously discussed guanidylation stage, is to provide the guanidinium carbon. Therefore, if the extra carbon atom required in cyclization of **47** were already present in the starting material, there will be no need for the reagent **49** in the guanidylation reaction. Actually, in the presence of a suitable catalyst, one can exploit the cyano (nitrile) group in compound **45** (scheme 1) as a donor of the guanidine carbon. This idea had been previously applied in the Lanthanide(III) ion-catalyzed reactions of amines with nitriles [88]. Here we have employed the same principle for compound **45** in the presence of the catalyst $\text{La}(\text{OTf})_3$, conducting the reaction in different alcoholic solvents at different heating temperatures (scheme 4). In all of our attempts, we obtained only the monocyclic product **53** and not the desired bicyclic one **48**.



Scheme 4.

In an attempt to complete the cyclization of the monocyclic product **53** to **48** we added different catalysts (scheme 5 and table 3) to a solution of the monocycle **53** in 3-pentanol and heated the mixtures in pressure tubes (scheme 5). Monitoring the reaction by HPLC analysis for several days, we didn't observe the desired product in any of the experiments.



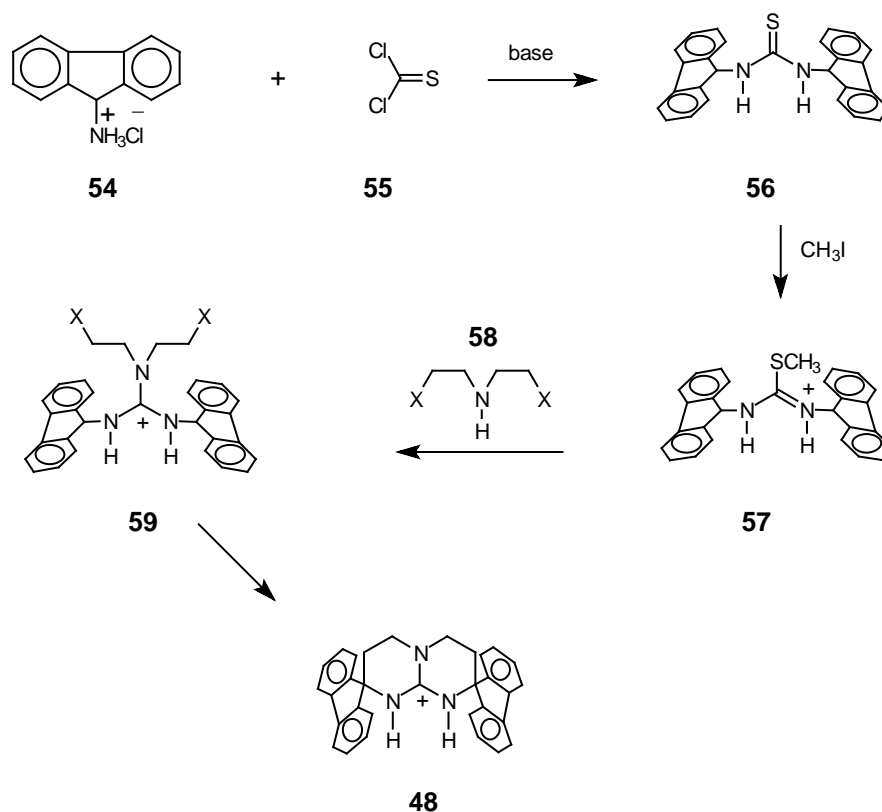
Scheme 5

Table 3. Different catalysts used for the reaction in scheme 5.

exp. #	catalyst
1	tris(dibenzylideneacetone) dipalladium /chloroform
2	tetrakis(acetonitrile)Pd(II) tetrafluoroborate
3	bis-(triphenylphosphine)- Pd(II) chloride

Due to reasons that will be discussed later, the route we followed for the preparation of fluoreneguanidinium iodide **48** (scheme 1), didn't give a sufficient yield (5%). Therefore, in order to synthesize compound **48** we tried the novel strategy shown in scheme 6. This route, however, proved to be even less productive than the previous one.

The strategy of the new route is to add the "guanidinium carbon" in compound **56** in the first step. Then, in order to facilitate the substitution of the secondary amine ligand **58**, thiourea **56** was activated by alkylation and produced **57**. A successful substitution should give compound **59**. Biscyclization of **59** by intramolecular interaction after deprotonation might occur under the reaction conditions to obtain the final product **48**.

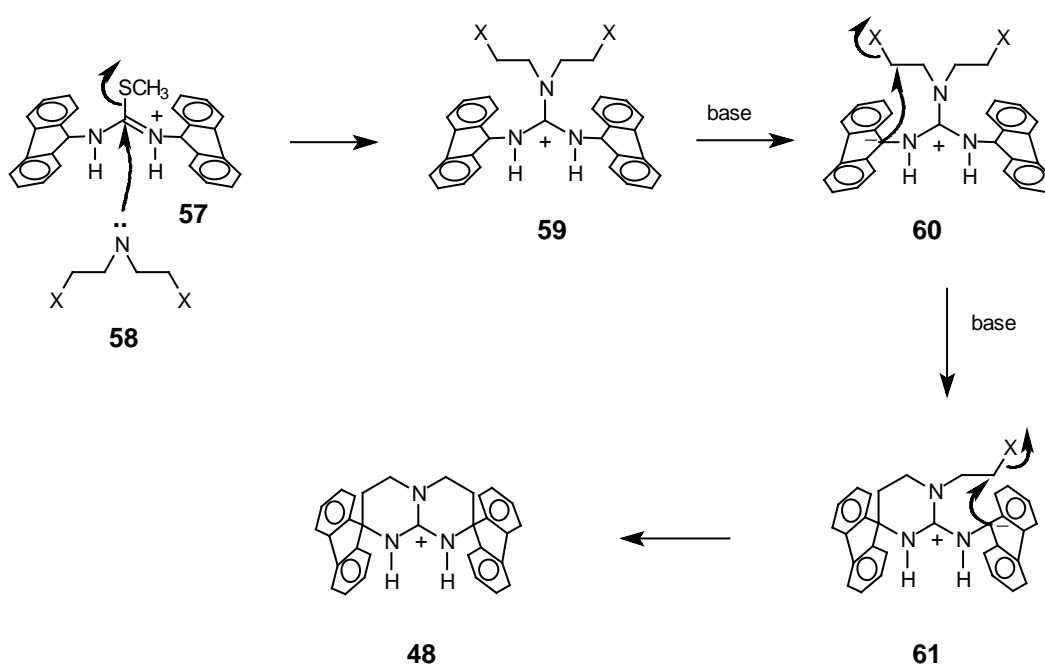


Scheme 6. A schematic representation of the new strategy for the fluorene-guanidinium preparation.

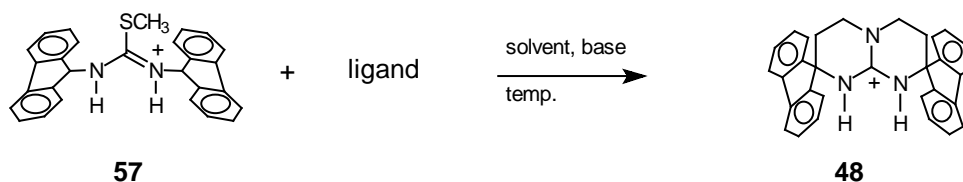
The preparation of fluorene-thiourea **56** was carried out successfully (50-70% yield) by addition of one half-equivalent of thiophosgene **55** to a dry solution of 9-aminofluorene hydrochloride **54** with a base like triethylamine in dichloromethane.

Activating the thiourea carbon in **56** with methyl iodide resulted in **57** in a yield range of 90-95%.

Different secondary amine ligands, presented in table 4, were used to carry out the reaction shown in scheme 8. To ensure the nucleophilicity of the secondary amine ligand and to facilitate cyclization (see scheme 7), a variety of bases were added. Unfortunately, none of these attempts (Exps. 1-7 in table 4) were successful. Possible explanations hinge on the fact that fluorene units are too bulky and therefore prevent the reaction by covering the interacting site. Another possibility is that the bases used are either too strong or too weak to promote such a reaction.

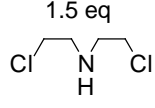
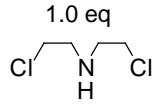
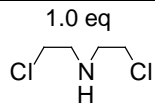
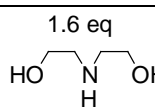
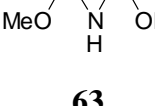
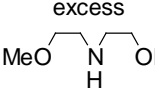
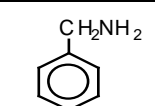


scheme 7. A proposed mechanism for the reaction route shown in scheme 6



Scheme 8

Table 4. Different conditions for the reaction in scheme 8.

exp	ligand	solvent	base	temp. (°C)	heating time
1	1.5 eq  HCl 58	diglyme	KOtBu, 4eq	140	24 h
2	1.0 eq  HCl 58	diglyme	KOtBu, 1eq	73	15 h
3	1.0 eq  HCl 58	acetonitrile	Et ₃ N, 3eq	85	16 h
4	1.6 eq  62	isopropanol	-----	82-100	15 h
5	excess  63	acetonitrile	-----	85	72 h
6	excess  63	dimethylacet- amide	-----	170	18 h
7	 64	acetonitrile	-----	85	18 h

Since the desired product couldn't be obtained even after testing many different conditions (exp.1-7, table 4), we decided to return to the first route and try to improve the yield of **48** produced in the guanidylolation stage (scheme 2). This stage was probed

several additional times all resulting in a varying, yet unsatisfactorily, low yield ($\leq 5\%$). To understand the variation of the yield in the repeated reactions, the starting material of the guanidation step, the triamine compound **47** in scheme 2 was re-characterized.

In revisiting the characterization issue it was realized that the existence of a very small peak in the ^{13}C -NMR results was initially ignored, which together with the ^1H -NMR data that pointed to the existence of symmetry in the compound, led to believe that the starting material was correctly obtained. On additional inspection of the compound with ESI-MS it was realized that the compound fed into the cyclization reaction did not have the correct mass for the triamine. Furthermore, the IR spectrum showed a vibration band of an amide unit that should not exist in the triamine. To add to the confusion, the results of the HPLC run that followed the hydrolysis of **45** by 6 N HCl showed a complete conversion of **45** to a new compound, which had a shorter retention time, consistent with what was expected from triamine **46** production.

After careful re-examination of the ESI-MS, IR- and ^{13}C -NMR results it was concluded that the compound used was the fluorene urea **65** (scheme 9), an intermediate compound produced during the triamine preparation, rather than the desired starting material **46**. Therefore the aim became to complete the last step of the hydrolysis procedure shown in scheme 9.

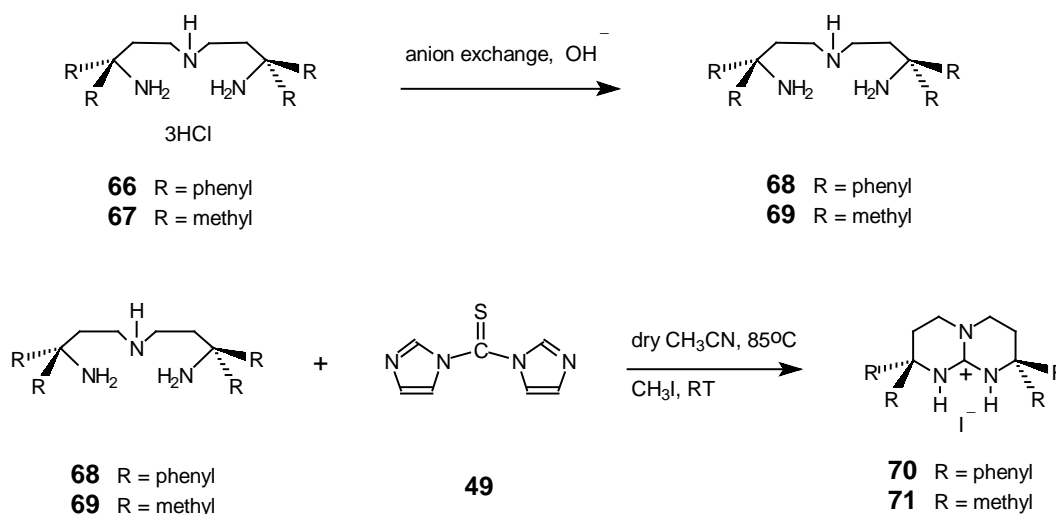
To obtain the triamine salt **46**, the urea product **65**, which was produced in 80-85% yield, was heated with concentrated HCl (35%-37%) at 145°C for 48h. The requirement of continuous heating under such extreme conditions might be explained by the existence of the two bulky fluorene units that could hide the reacting site and therefore hamper the hydrolysis with HCl. When the fluorene units were replaced by phenyl or methyl groups, the hydrolysis was completed in a much shorter time and under less harsh overnight conditions (6 N HCl at 110°C). After the unambiguous preparation of the triamine compound **46** in a yield of 45%, the guanidylation step (scheme 2) was carried out more successfully in a yield of 35%.

3.1.2 The synthesis of hosts **70,71**

The bicyclic tetraphenylguanidine **70** was prepared in a manner similar to compound **48** (see scheme 9). The triammonium salt **66** was converted to the free base **68** by filtration through a basic anion exchange column. The starting material **68** had a good

solubility in dry acetonitrile for the guanidylation step. The reaction with thiocarbonyldiimidazole **49** and subsequently with methyl iodide resulted in product **70** in 80% yield.

The guanidinium host **71**, first prepared in our lab. [64], was produced in large quantities so as to have relatively sizable amount of product for the ITC measurements. These different bicyclic guanidines **48**, **70** and **71** might probe the effect of host rigidity (hydrophobicity) on host-guest interactions.

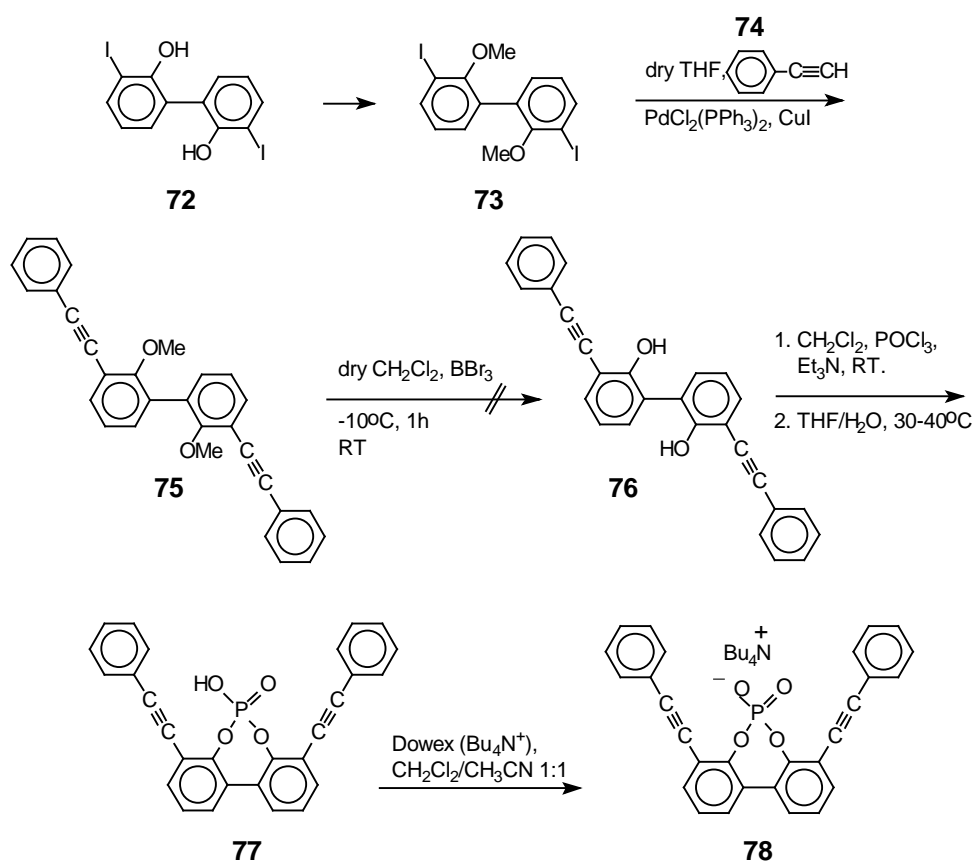


Scheme 9. The preparation of guanidinium compounds **70** and **71**.

3.2 Synthesis of the phosphate and phosphinate guests

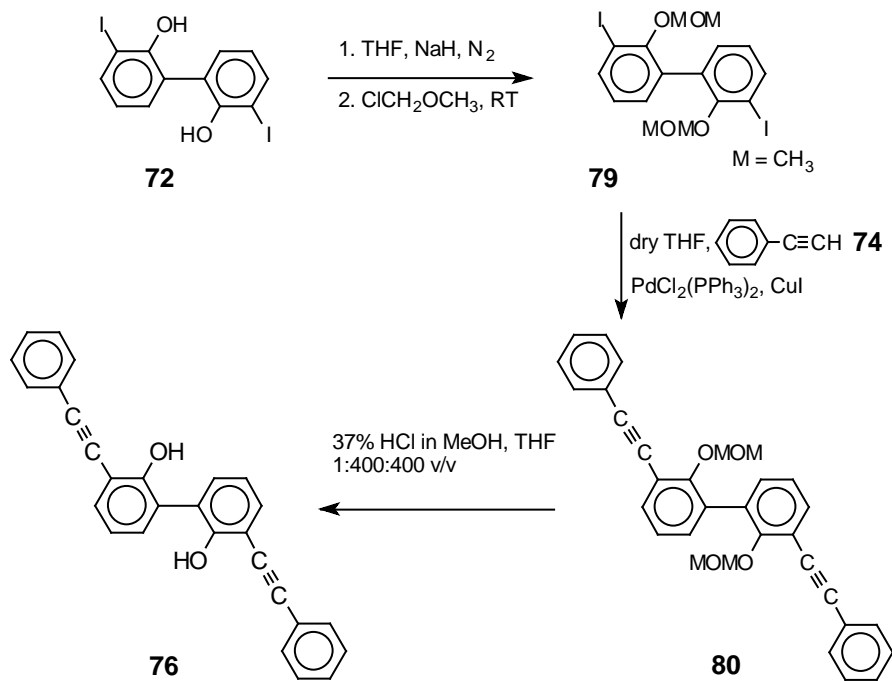
3.2.1 Synthetic strategy for phosphates **78** and **84**

To obtain the desired phosphate guest **78** we followed the synthetic strategy shown in scheme 10. The 2,2'-dihydroxy-3,3'-diiodo-1,1'-biphenyl **62** and 2,2'-dimethoxy-3,3'-diiodo-1,1'-biphenyl **73** were prepared according to the procedures given in [89]. A Sonogashira coupling of **73** with phenylacetylene **74** and Palladium catalyst gave **75** in 85% yield. Demethylation of **75** with BBr_3 [90] in dry dichloromethane failed to provide the dihydroxy compound **76**. Therefore the hydroxy groups in **72** were protected with methylmethoxy (MOM) groups [91] to obtain **79** (scheme 11), which in turn could be hydrolyzed more easily than the methyl groups in **75**.



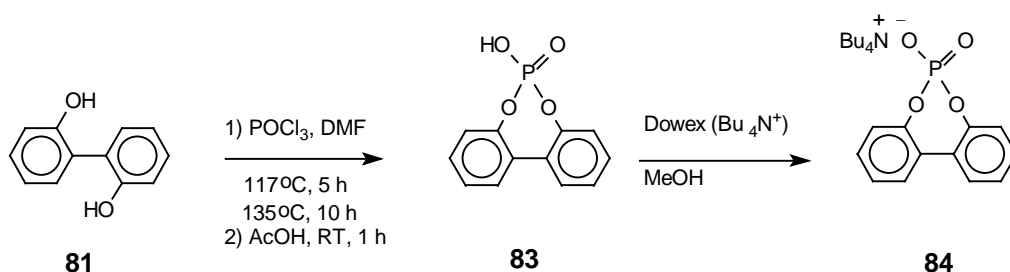
Scheme 10. The preparation of phosphate **78**

Compound **79** was obtained in 92% yield and then underwent a cross coupling reaction with phenylacetylene to afford **80** in 90% yield. For MOM-ether deprotection it was sufficient to use very mild acidic conditions in order to avoid the cyclization of the free OH groups with the adjacent ethynyl moieties [92]. Thus, the dihydroxy product **76** was available in 75% yield. When compound **76** was treated with POCl_3 (scheme 10) followed by $\text{H}_2\text{O}/\text{THF}$ hydrolysis the successful formation of the cyclic phosphordiester **77** was observed (60% yield). Compound **77** was converted to the final TBA-salt **78** by ion-exchange in an organic solvent mixture. This conversion was necessary for obtaining the phosphate guest anion in a soluble form which will be used later in the complexation with the guanidinium cations.



Scheme 11. The preparation of the dihydroxy **76**

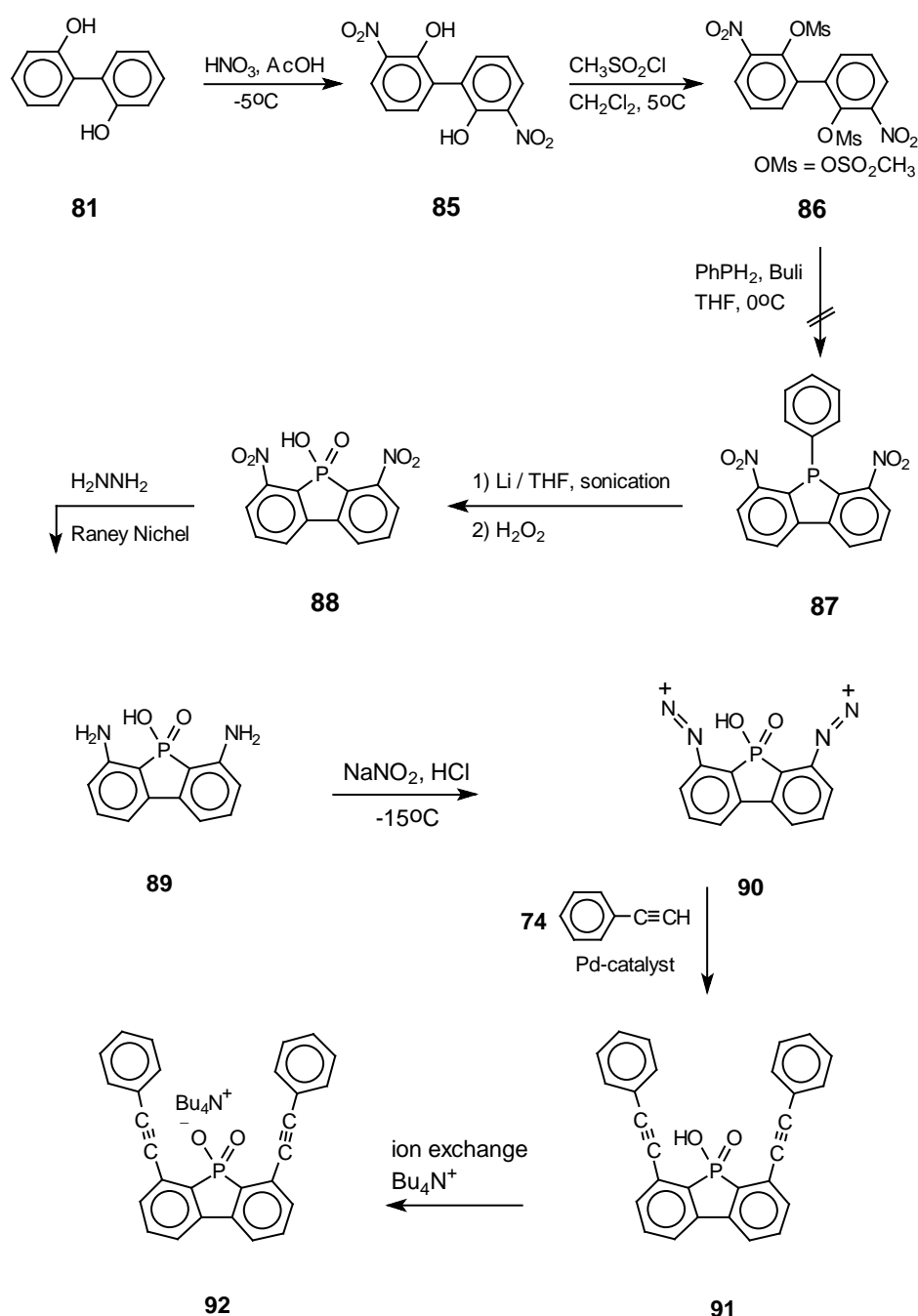
When the desired product **78** became available, the parent phosphate anion **84** was prepared, which lacks the two side arms. The phosphate **83** (scheme 12) was prepared according to the hints provided by reference [93]. 2,2'-dihydroxy-1,1'-biphenyl, **81**, reacted with POCl_3 in the presence of a catalytic amount of DMF, then the intermediate acid chloride **82** was hydrolyzed with acetic acid to give **83** (70% yield). The acid **83** in MeOH was transformed into the TBA-salt using a TBA-charged ion-exchange column to produce the phosphate salt **84**, ready for ITC measurements.



Scheme 12. The preparation of the parent phosphate **84**

3.2.2 Synthetic strategy for the phosphinate **92**

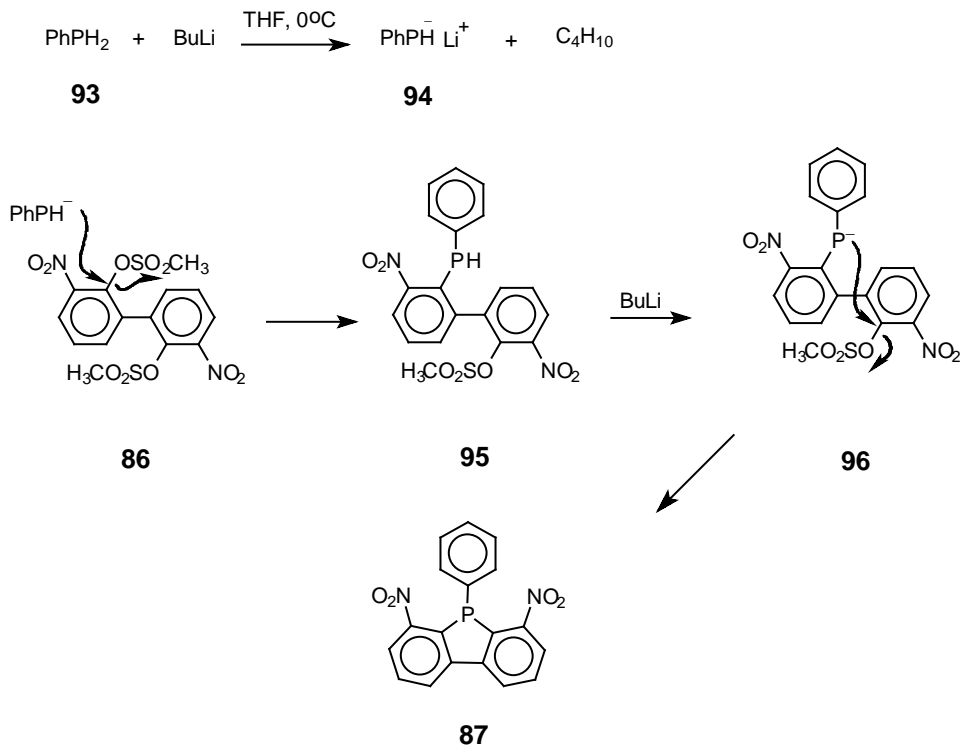
The preparation of phosphinate **92** starting from 2,2'-dihydroxy-3,3'-dinitrobiphenyl **85**, (scheme 13). The rationale behind this strategy included the mesylation of the hydroxy groups in **85** to facilitate in the next step the reaction of **86** with phenylphosphine and butyllithium producing compound **87**. Then, a cleavage of



Scheme 13. A schematic representation for the preparation of phosphinate **92**

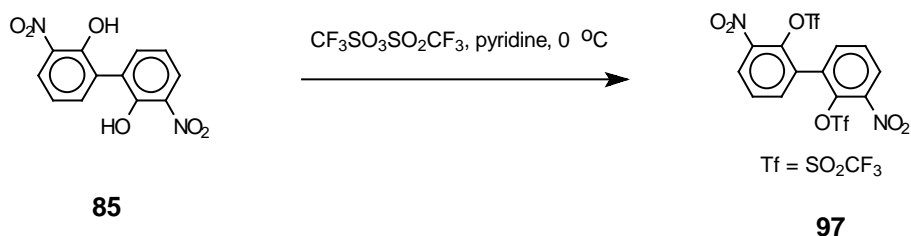
the phosphole **87** by an alkali metal in THF, followed by oxidation with H₂O₂ would result in the phosphinic acid product **88**. Hydrogenation of **88** would give **89**. Bis-diazotization of compound **89** was presumed to give **90**. The coupling reaction of phenylacetylene and **90** in the presence of a Pd-catalyst should give the desired product **91**. Finally, conversion to **92** would be achieved by transfer of **91** through cation exchange column, loaded with tetrabutylammonium cation.

2,2'-dihydroxy-3,3'-dinitro biphenyl **85** was prepared in 30% yield by reacting 2,2'-dihydroxy biphenyl **81** with nitric acid in AcOH as described in the literature procedure [94]. In this reaction several isomers, related to the substitution partition of the nitro groups on the phenyl rings, were obtained. The desired isomer **85** was acquired after purification. For characterization in this case it was insufficient to rely solely on the NMR and ESI-MS spectra as both **85** and the isomer 2,2'-dihydroxy 6,6'-dinitrobiphenyl lead to exactly the same results. Consequently, verification the offered isomer was sought from acid-base titration for pK_a determination and comparison with literature data. Fortunately, the obtained pK_a matched that of the desired isomer **85** [95] thereby confirming the isolation of the correct isomer.



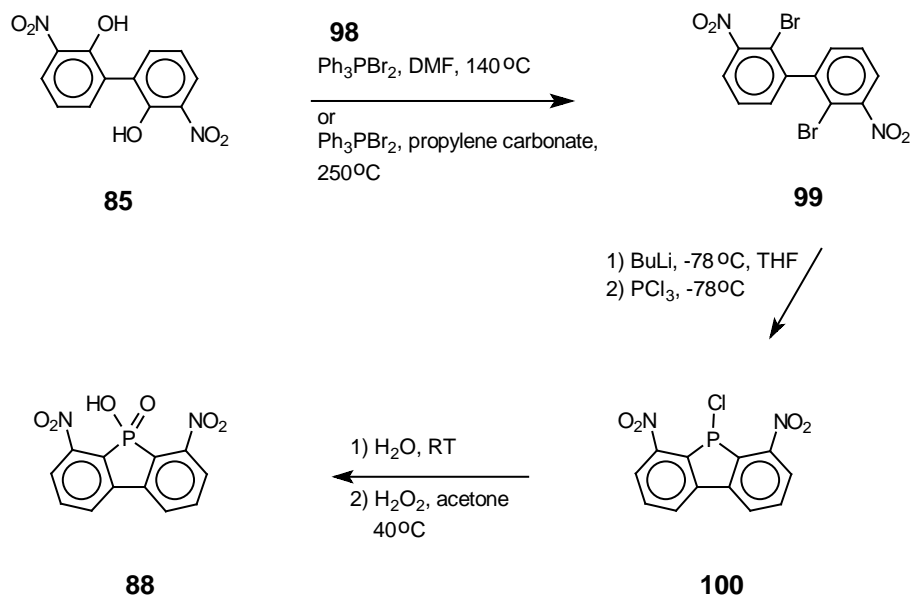
Scheme 14. The mechanism for obtaining the phosphole **87**

The hydroxy groups in **85** were converted into better leaving groups by reaction with mesylchloride; compound **86** was then readily obtained in 73% yield. The leaving groups in compound **86** were reacted with phenylphosphine **93** and butyllithium (see mechanism in scheme 14) in order to obtain the phosphole **87**. Unfortunately, despite several attempts using freshly dried solvents and authentic reagents, product **87** was never observed. In order to obviate the possible deprotonation of the mesyl groups in **86** their replacement by less acidic and more reactive leaving groups was necessary. Therefore, compound **97** possessing the triflate groups was produced as shown in scheme 15 in 85% yield. However the reaction with phenylphosphide **94** did not yield product **87** either.



Scheme 15.

It is worth noting that phenylphosphine **93** can be rapidly oxidized to a higher oxidation state, requiring storage under argon. Despite the extra precautions taken to avoid contact with air or humidity, there is no absolute guarantee that the reaction was not hampered by oxidation. The failure to produce the expected compound might be attributable to adventitious oxidation resulting from the small scale conduction of this reaction.

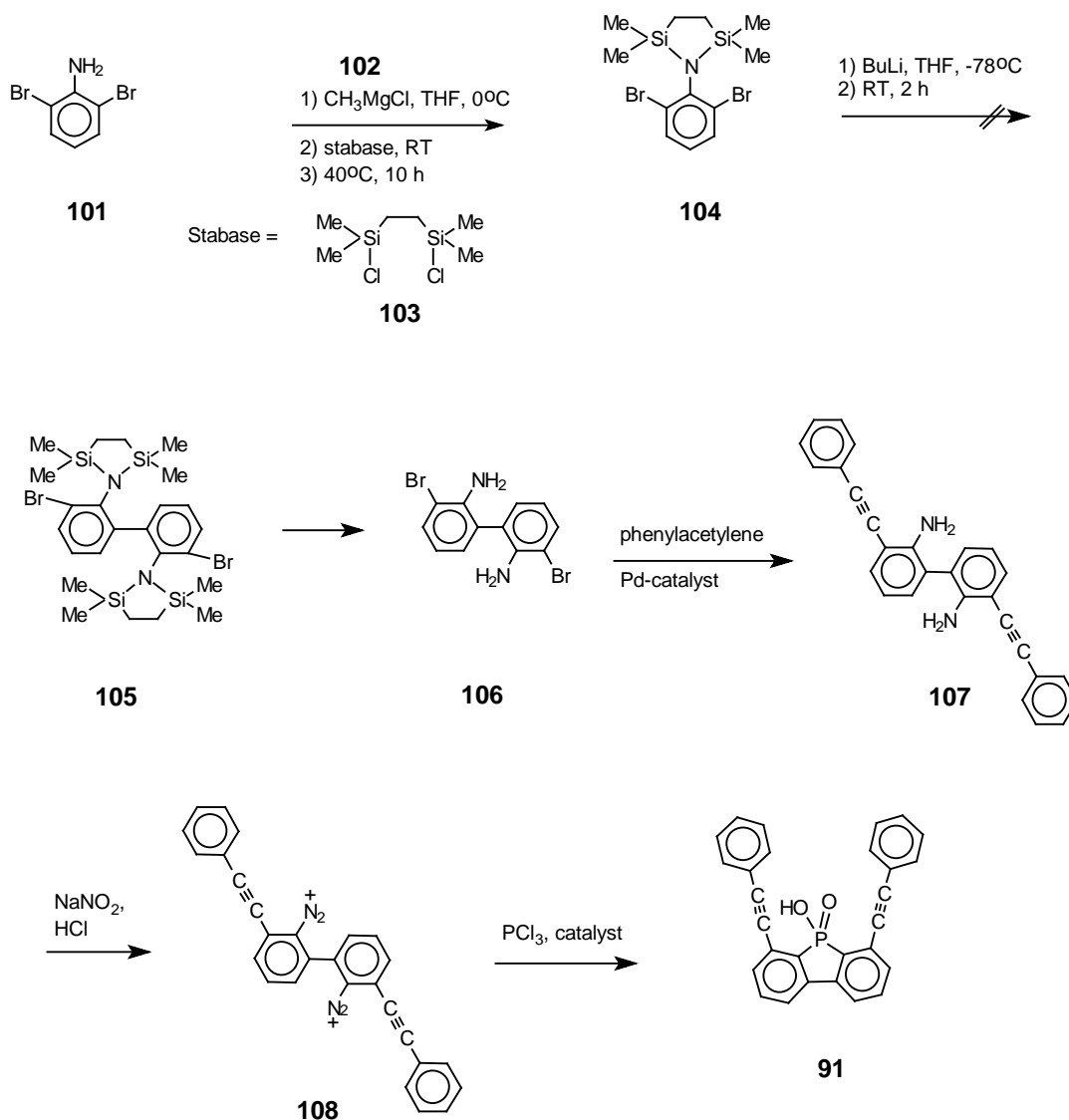


Scheme 16. A strategy for preparing compound **88**

To salvage this approach a modification was attempted so that the two hydroxy groups in **85** were to be replaced by halides, *e.g.*, the bromides in compound **99** (see scheme 16). The advantage of this change lies in the easy metalation of compound **99** by butyllithium, which, upon addition of phosphorotrichloride (PCl_3), would lead directly to product **100**. In the same reaction mixture this product can be hydrolyzed by water and oxidized with H_2O_2 to yield product **88**. Attempts to replace the hydroxy groups in **85** by bromide using triphenylphosphine-dibromide **98**, as described in reference [96], were unsuccessful. More attempts to convert the triflate groups in **97** to iodides by reacting **97** with NaI in refluxing acetone or in dry DMF heated to 140°C , did not yield any positive results as well.

Owing to these disappointing results, a completely new strategy which utilizes the commercially available compound 2,6-dibromoaniline, **101**, was adopted (see scheme 17). A protection of the amino group in aniline **101** is favorable due to the acidic amino protons that could be reactive and functional in the various stages of the reactions. For this purpose, compound **101** was reacted with the Grignard reagent methylmagnesium chloride (MeMgCl) **102** and subsequently with the protecting group bis(dimethylchlorosilyl)ethane (stabase) **103** to produce product **104** in 51% yield. A complete conversion of the aniline **101** by adding a large excess of the stabase reagent

led to the formation of side product, which was very difficult to separate from **104**, while a stepwise conversion by which only 2.3 equivalents of stabase **103** were added to the reaction mixture allowed a simple separation from the starting material **101** in a standard chromatographic procedure. This explains the relatively low reaction yield.

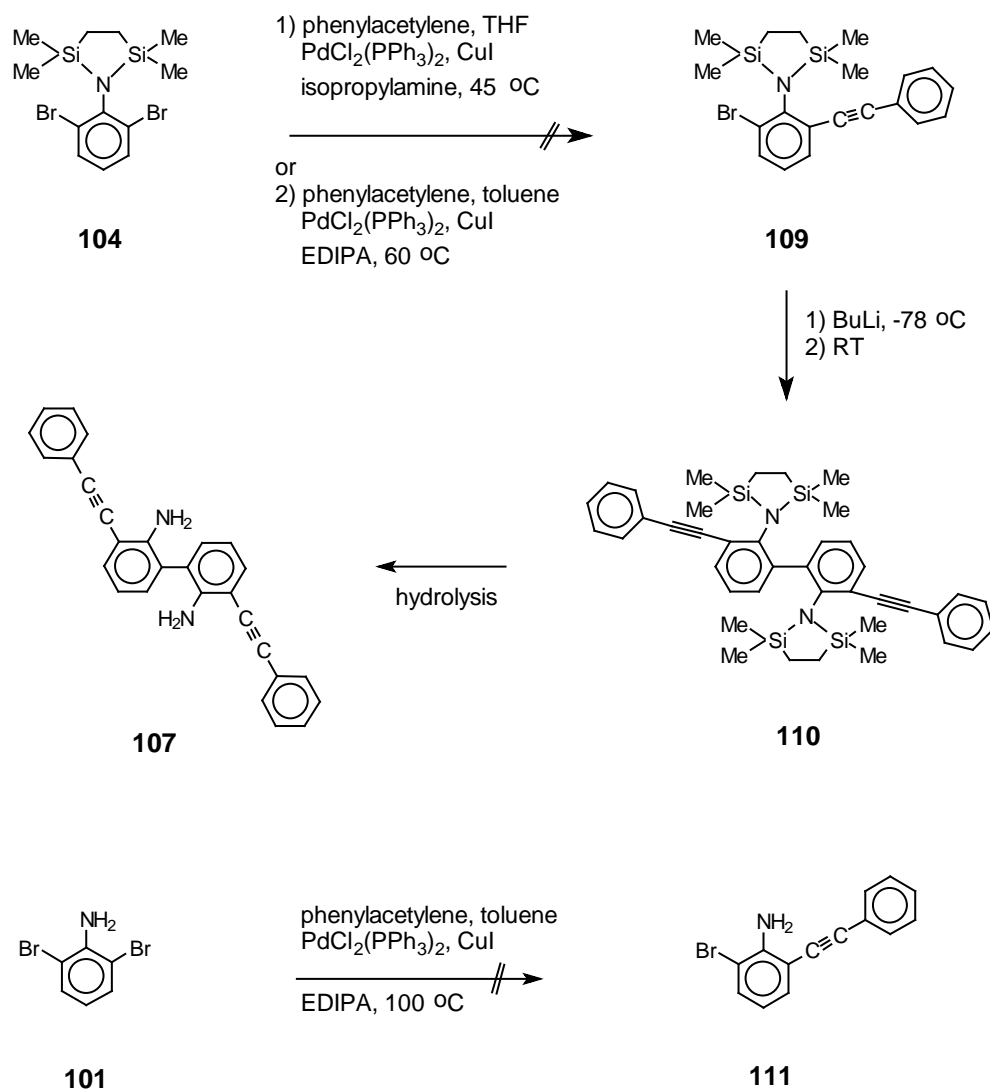


Scheme 17. A schematic representation for the preparation of compound **91**

Surprisingly, an attempt to carry out the coupling reaction of **104** with butyllithium to yield the biphenyl **105** was not successful, probably due to the complexity of the structure involved in the reaction.

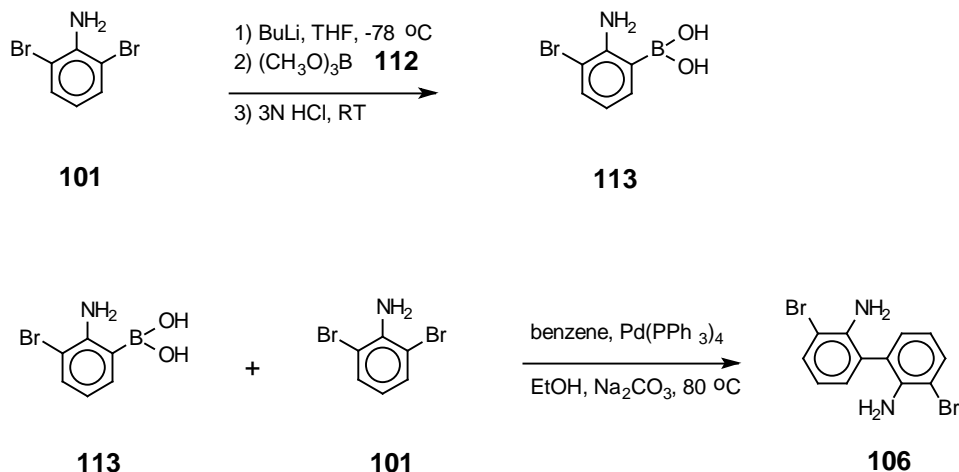
To overcome the last hurdle and decrease the complexity of the reaction, we tried Sonogashira coupling of **104** with phenylacetylene to arrive at compound **109**, (scheme 18). In this case one bromide is left and the coupling reaction of **109** with itself might

hopefully yield **110** in one step. However, this approach, even with the reaction repetition with different bases and temperatures, did not yield product **109**. The reaction was repeated with aniline **101** to produce **111** and no product formation was observed as well. The unsuccessful coupling might be due to the electron donating amino group in **104** and **101** that causes the low reactivity of the bromides.

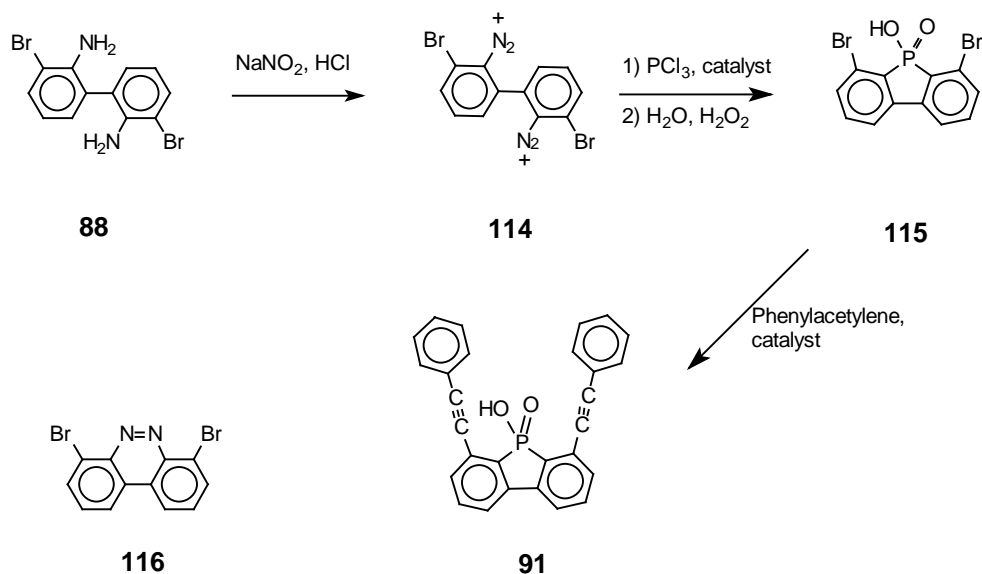


Scheme 18. A different strategy for the preparation of **107**

Within the framework of the adopted strategy, we attempted to synthesize the main building block **106**, from the starting material **101**, and then pass it through several modifications to reach the final product. A search in the literature revealed that a Suzuki coupling between compound **101** and any boronic acid in the presence of a catalyst was successful without protecting the amino group in the aniline **101** [97]. Therefore, applying a similar strategy as shown in scheme 19 was the next step to try.



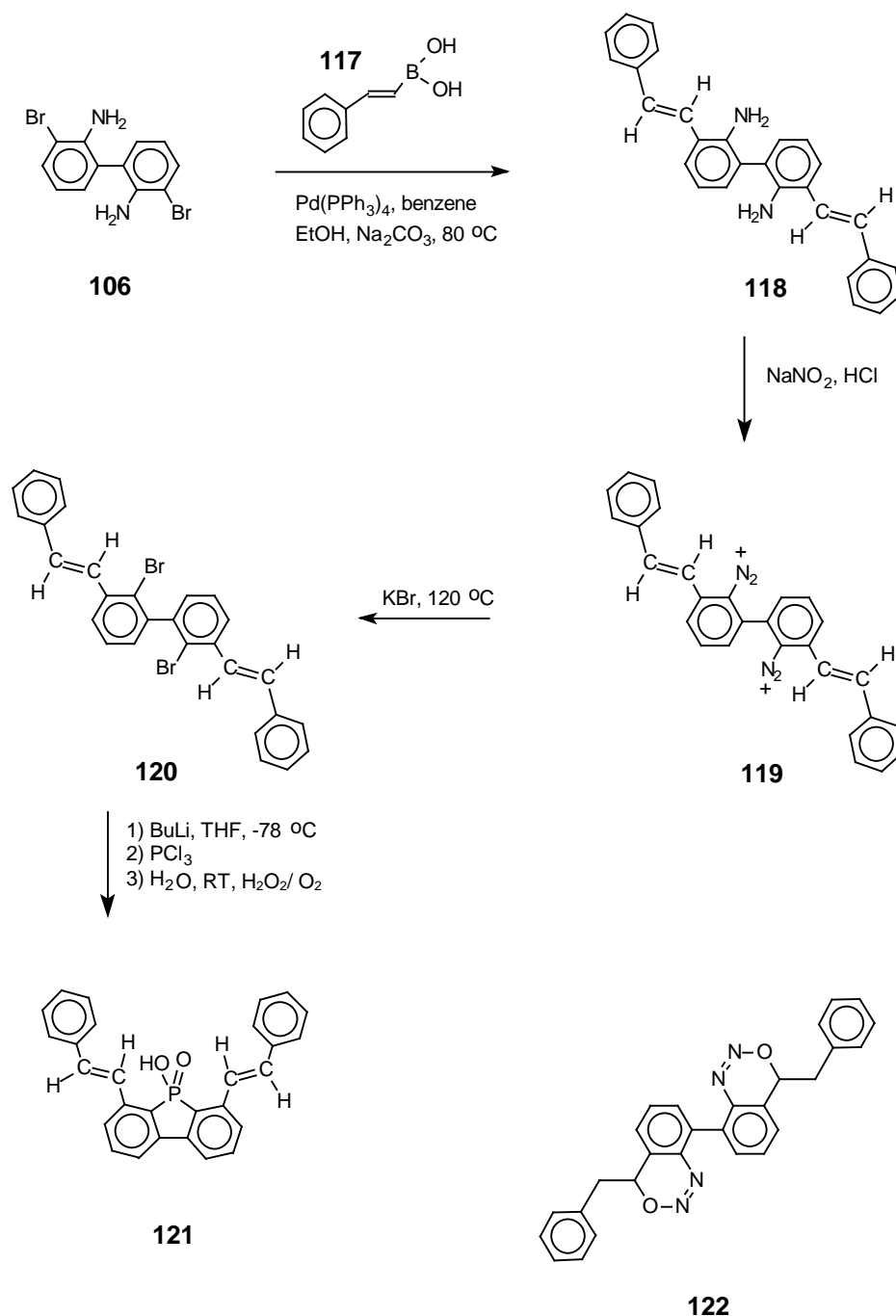
Scheme 19. The preparation of the biphenyl **106**



Scheme 20. An alternative route for preparing **91**

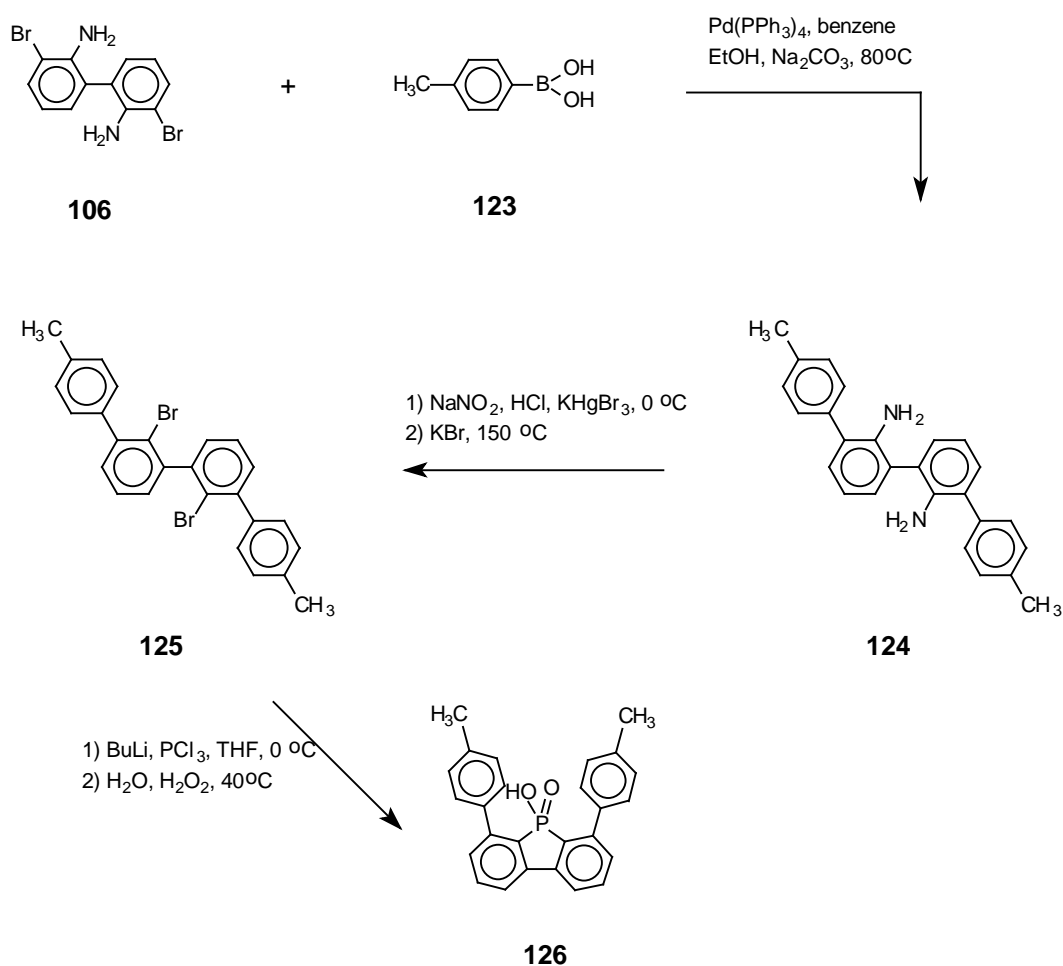
The addition of 3 equivalents of BuLi to compound **101** led to metalation in three positions, the two protons of the amino group and one bromide. A subsequent addition of trimethyl borate **112** to the metalated compound followed by hydrolysis produced the desired boronic acid **113** in 60% yield. Suzuki coupling between the intermediate compound **113** and 2,6-dibromoaniline **101** in the presence of a catalyst finally gave the building block **106** in 66% yield. A bis-diazotization of **106** by sodium-nitrite in a concentrated acid gave the salt **114** (scheme 20). After careful drying of the salt the reaction with phosphotrichloride (PCl_3) and Cu^{1+} -catalyst to form the dibenzophosphole derivative was applied. In this reaction the desired product **115** was not observed instead mainly product **116** was formed (scheme 20), perhaps due to

incomplete tetra-azotization of **106**. A similar observation was found in the literature [98] as well. To counter this problem the complete conversion of all the amino groups to the diazonium moiety must be insured. After extensive drying, this salt can be introduced into the next steps. Unfortunately, the reaction with PCl_3 and $[\text{Cu}^+(\text{CH}_3\text{CN})_4]\text{PF}_6$ in THF at 0°C then at 40°C did not produce the required product.



Scheme 21. A schematic representation for preparing the phosphinate **121**

On the basis of this experience the conventional route using halides instead of diazonium groups in the reaction with PCl_3 appeared more reliable. The metalation of halides, like bromides, by BuLi followed by an addition of PCl_3 has already been shown to easily proceed in the desired direction [99]. Therefore, to follow this route, a Suzuki coupling between **106** and trans-2-phenylvinylboronic acid **117** in benzene (a commercially available boronic acid) taking Pd-catalyst was performed to obtain compound **118** (scheme 21). The reaction proceeded successfully in 70% yield. The next step required bis-diazotization of **118** to yield the salt **119**. The subsequent conversion to the bromide **120** would be carried out by heating with KBr . Only then, a reaction between a metalated **120** by BuLi and PCl_3 might furnish the product **121**.

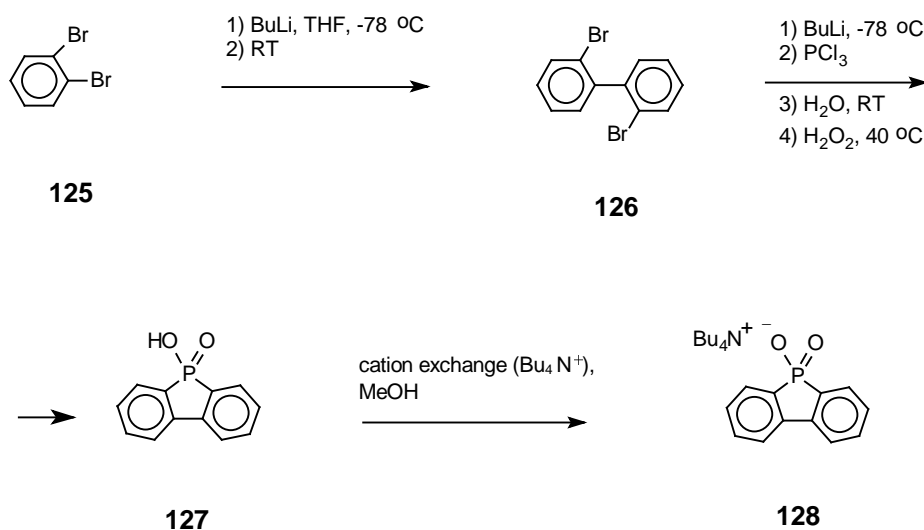


Scheme 22. A schematic representation for the preparation of phosphinic acid **126**

Disappointingly, the diamine **118** underwent bis-diazotization at -20°C by sodium-nitrite to a compound different than **119**. A careful analysis of the ESI-MS spectrum

strongly suggested that a cyclization to compound **122** had probably happened instead of **119**. This could occur following addition of diazotate to the double bond (or its prior hydration followed by ring closure) on the “arm” followed by cyclization with the diazonium moiety.

In order to obviate the complications seen with the styryl substituent the target was switched to phosphinic acid **126**. Presumably the preparation would not suffer from problems with diazotization step. *p*-Tolueneboronic acid **123** was chosen to couple with compound **106** as shown in scheme 22. Following the standard procedure for this coupling we obtained the tetraphenyl product **124**. Further inspection of the literature in order to find some extra insight regarding the diazotization step, revealed good chances for success. For instance, the Cornforth group had applied many bis-diazotization reactions on starting materials similar to **124**. In addition, they had converted the bis-diazonium salt in the tetraphenyl framework to the iodide or bromide and prepared, thereafter, phosphinic acids [99]. These are exactly the steps we planned to carry out to obtain our product. At this stage the bis-diazotization step of **124** is still under experimentation.



Scheme 23. A schematic route for preparing the parent phosphinate **128**

In a separate attempt, the preparation of the phosphinic acid **128**, as a parent for compound **126**, was carried out as shown in chart 23. 1,2-dibromo benzene was reacted with 1 equivalent of BuLi in THF to yield compound **126** [100]. The dibromo-biphenyl **126** was metalated with 2 equivalents of BuLi in THF followed by the addition of PCl₃. Hydrolysis and oxidation were continued to obtain the phosphinic

acid **127** in 70% yield. The phosphinic acid was converted to the required TBA-salt **128** by using a TBA-charged cation exchange column.

4. Results and discussion

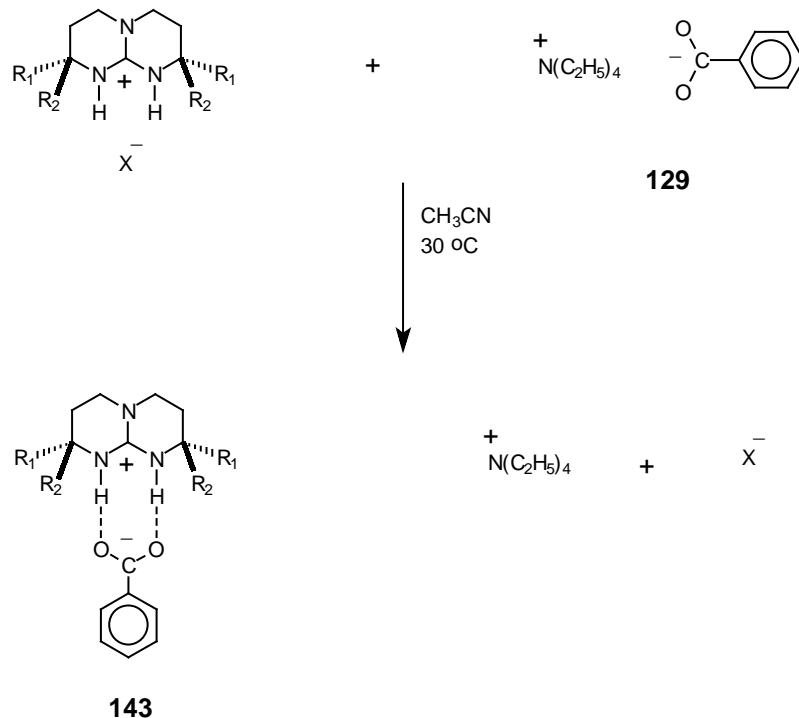
4.1 Complexation of different guanidinium cation hosts with carboxylate 129.

Here we describe an experimental attempt to evaluate the energetics of a simple host-guest system based on guanidiniums and oxoanions to develop more reliable guidelines for molecular recognition. Namely, one does not only focus on the free energy of association ΔG° , that may not reflect the real contributions of host-guest association and solvent influence, but rather on the dissection of this parameter (ΔG°) into its enthalpy (ΔH°) and entropy (ΔS°) components. In condensed phases all weak interactions are accompanied by enthalpy-entropy compensation [21,22], therefore, the factorization into the energetic components is necessary to measure the enthalpic gain on binding of host and guest and the magnitude of its entropy counteraction. As the enthalpy and entropy components can compensate, the free energy of association ΔG° may change only marginally and will not reflect the structural achievements. Connection of the structural modification in a tailored host-guest relationship to the experimental energetics, can be determined by using the ITC diagnostic method [27]. Since calorimetric measurements faithfully report on the cumulative heat response of the entire system it is required to design a host-guest system simple enough to allow the disentanglement of all the processes happening simultaneously in solution and ascribe the heat effect to just one association reaction.

Studying a series of structurally related compounds should unfold the structure-affinity correlation, and in addition, the risk of misinterpretation is lowered by using trend analysis.

After completing the preparation of the guanidinium compounds they were kept in non-basic solution in order to prevent hydrolysis of the guanidinium moiety by a strong nucleophile to the cyclic urea. Based on various experimental data the hydrolysis of cyclic guanidinium salts seems to be affected by the antiperiplanar or syn lone pairs of the amino groups in the guanidine [65]. The stereoelectronic effects of the lone pairs in the cleavage of guanidinium salts is still not completely determined. If stereoelectronic control by antiperiplanar lone pairs is operative, then they are expected to hydrolyze

with endocyclic C-N cleavage to acyclic ureas. However, hydrolysis in basic media produces mixtures of cyclic and acyclic products, as determined by $^1\text{H-NMR}$ analysis. The results reported in [65] show that in the six-membered ring antiperiplanar lone pairs provide a weak acceleration of the breakdown of the tetrahedral intermediate, but in five- and seven-membered rings there is no evidence for such acceleration, which instead can be provided by syn lone pairs.



$R_1 = R_2$	$X^- = \text{Cl}^-$	Br^-	I^-	BF_4^-	PF_6^-
$-\text{CH}_2\text{CH}=\text{CH}_2$	130	131	132	133	134
$-\text{C}_6\text{H}_5$	135	136	70	----	137
$R_1, R_2 =$	138	139	48	----	140

Scheme 24. Overview of the associations between different bicyclic guanidinium- X^- compounds and **129**.

The association of bicyclic guanidinium cations (e.g. **130**) with carboxylate **129** (scheme 24) may provide a suitable host-guest system. The interaction mode follows strict 1:1 stoichiometry and was characterized in solution and in the solid state in numerous examples [23, 53, 101]. The prime structural motif features an almost planar

cation–anion arrangement, assisted by two parallel hydrogen bonds as shown by the X-ray crystal structures of the tetraphenylguanidinium-benzoate (figure 6a), tetraallylguanidinium-trifluoroacetate (figure 6b), and fluoreneguanidinium-trifluoroacetate complexes (figure 6c).

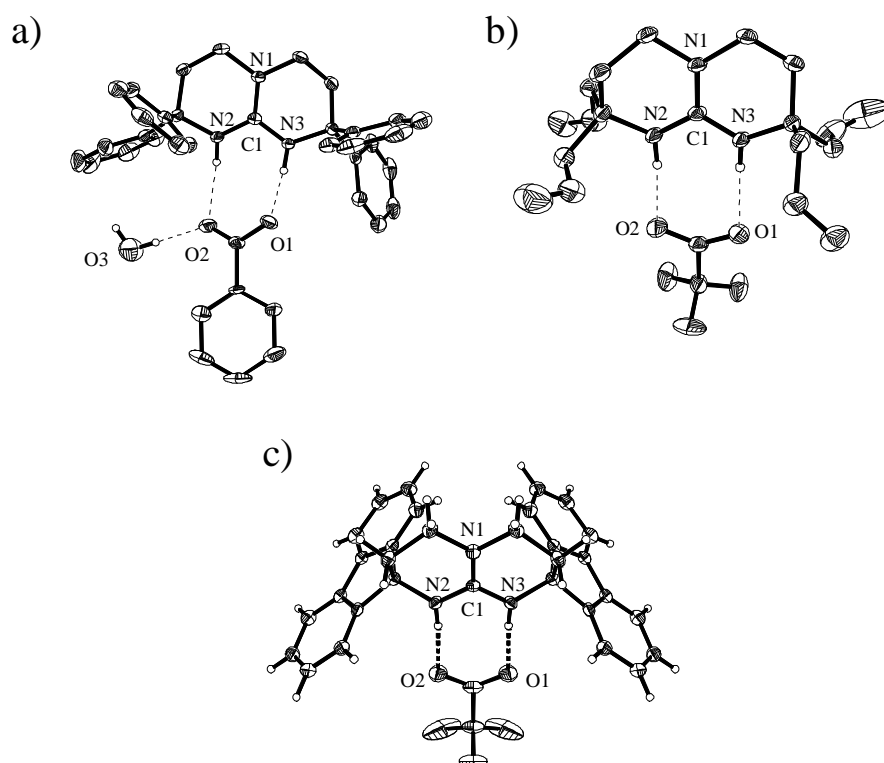


Figure 6. X-ray crystal structures of tetraphenylguanidinium benzoate (a), tetraallylguanidinium trifluoroacetate (b) and fluoreneguanidinium trifluoroacetate (c).

Formation of the dedicated hydrogen-bonded ion-pair complex **143** is expected to depend on the competition with solvent. Thus, the non-hydrogen-bonding solvent acetonitrile was, among other grounds, chosen due to its high dielectric permittivity ϵ ($= 36$) which minimizes the unspecific ion pairing. A typical ITC plot from the titration of **136** with **129** in acetonitrile at 30°C is depicted in Figure 7. The top panel displays raw data; heat evolution over time. Initial injections produce a large signal from complete complexation of added guest, but this response decreases over time as binding sites become saturated. A binding isotherm is generated by integrating each peak and plotting the resulting data versus the mole ratio. Elevated concentrations of

injectant result in a sizable heat of dilution which is measured in a separate titration and subtracted from the raw data to produce the final binding curve, shown in the bottom panel. Also shown is the non-linear least squares fit of the subtracted curve using a one-site-binding model. The integration of the heat pulses obtained in each titration step gives a titration curve rendering the molar enthalpy ΔH° as the step height and the free energy ΔG° from the slope in the inflection point. The stoichiometry n is derived as an independent parameter from the curve fit, and the molar entropy ΔS° is calculated from the Gibbs-Helmholtz equation. The binding isotherm of the tetraphenyl guanidinium bromide **136** with TEA-benzoate **129** is characteristic of a strong, exothermic 1:1 complex ($\Delta H^\circ = -4.17$ kcal/mol and $K_{\text{ass}} = 2.18 \times 10^4 \text{ M}^{-1}$) displayed in figure 7. The exothermic nature of the association suggests a complex held together by strong hydrogen bonding such as the bidentate interaction shown in scheme 24.

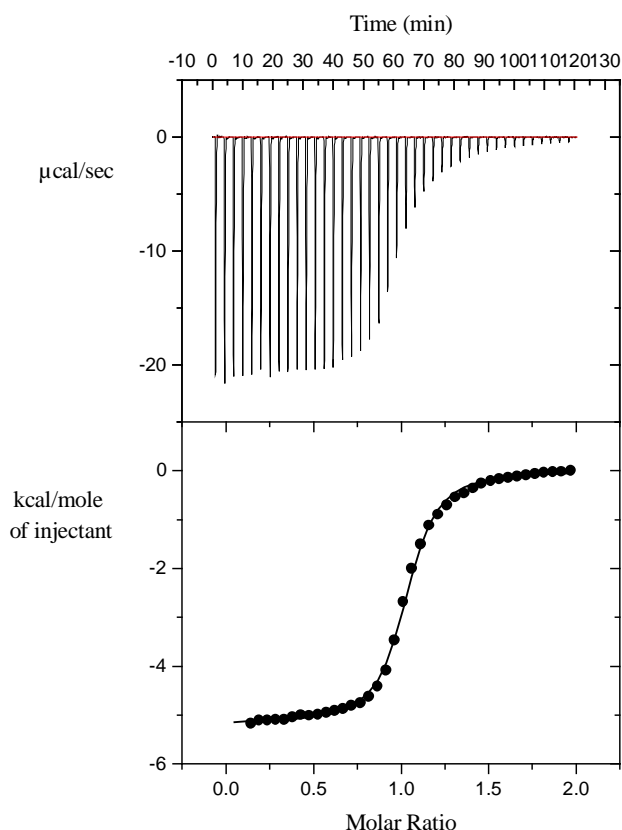


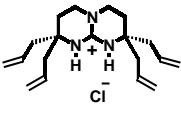
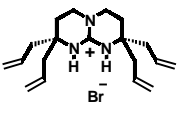
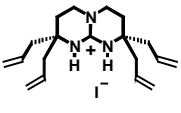
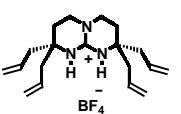
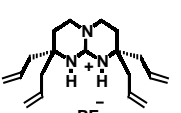
Figure 7. The raw data (CFB = cell feedback current, upper panel) and the integration isotherm (lower panel) is a typical ITC plot of the titration of tetraphenylguanidinium iodide **70** (1.09 mM) with TEA-benzoate **129** (22.48 mM) in acetonitrile at 30°C.

Competition of the desired guest species with the counter ions is inevitable when using charged abiotic hosts. Though straightforward deliberations can reduce this interference its influence has occasionally been noted [102, 103] but has seldom been quantified. The calorimetric determination of host–guest binding in acetonitrile of the tetraallyl-substituted guanidinium compounds **130-134** [64] with **129** revealed a surprisingly strong dependence on the counter ion (Table 5) [104]. Switching the counter anion from chloride to hexafluorophosphate shifts the experimental host–guest affinity by more than a power of ten, with the larger, less hydrogen-bonding anions yielding the higher K_{ass} values. The anion influence is easily detectable even at submillimolar concentrations in high dielectric solvent acetonitrile. The clear-cut dependence on charge density points to an unspecific ion-pairing process which is also indicated by inspection of the entropy of host–guest binding. In all cases the association is accompanied by a positive entropy contribution testifying to the inadequacy of the lock-and-key principle [105] to explain the experimental outcome. While the combination of just two binding partners to form a tight complex must superficially result in a more negative ΔS° because of the loss of degrees of freedom for translation and rotation [106] the observation of the opposite result can be explained by the release of solvent molecules and counter ions engaged in the solvation of the binding sites. The contribution of the entropic component $T\Delta S^\circ$ to the free energy ΔG° is not a marginal factor but may even constitute the major part of ΔG° (e.g. in the case involving chloride; Table 5). Again a subtle enthalpy–entropy compensation ensures the more drastic change in the association enthalpy ΔH° is not expressed in the resulting Gibbs enthalpy ΔG° .

The results listed in Table 5 suggest that there is a grading in the formation of ion-pairs between the guanidinium host and the series of counter anions. Chloride forms the most stable complex with the host, thus showing the lowest exothermicity ($-\Delta H$) in the exchange of chloride for benzoate, while the PF_6^- ion, at the other extreme, obviously enables the strongest enthalpic response because of its weak binding to the guanidinium group (see figure 8). There is no direct evidence that the limit of complete dissociation of the host-counterion ion-pair has been reached even with the least hydrogen-bonding ion PF_6^- nor that the second process to be considered in the trend

analysis, the interaction of the counter anion released on benzoate binding with the tetraethylammonium cation, would perturb the result significantly. In fact tetraalkylammonium halides have been characterized as strong electrolytes in acetonitrile [107] and any ion-pairing there would rather strengthen the differences within the series.

Table 5. Experimental stoichiometries n , binding affinities K_{ass} , and thermodynamic parameters of the reactions of tetraallyl-guanidinium⁺-X⁻ with TEA benzoate **129** in acetonitrile at 30°C (303°K), from ITC titration (the error limits refer to the fit of the data).

Tit. #	Host	TEA Benzoate [mM]	n	K_{ass} [M ⁻¹]	ΔH° [kcal M ⁻¹]	ΔS° [cal K ⁻¹ M ⁻¹]	T ΔS° [kcal M ⁻¹]	ΔG° [kcal M ⁻¹]	c
1	1.02 mM  130	23.70	1.17	38 000 ± 3 000	- 2.93 ± 0.05	+ 11.3 ± 0.3	+ 3.42	- 6.35 ± 0.05	39
2	1.07 mM  131	23.17	1.07	118 000 ± 7 000	- 4.13 ± 0.02	+ 9.5 ± 0.2	+ 2.89	- 7.03 ± 0.05	121
3	1.03 mM  132	23.17	1.05	280 000 ± 22 000	- 4.52 ± 0.02	+ 10.0 ± 0.2	+ 3.03	- 7.55 ± 0.05	289
4	1.04 mM  133	23.17	1.09	414 000 ± 8 000	- 4.58 ± 0.01	+ 10.6 ± 0.1	+ 3.20	- 7.78 ± 0.02	180
5	1.14 mM  134	21.40	1.00	380 000 ± 17 000	- 5.21 ± 0.01	+ 8.3 ± 0.1	+ 2.52	- 7.73 ± 0.03	211

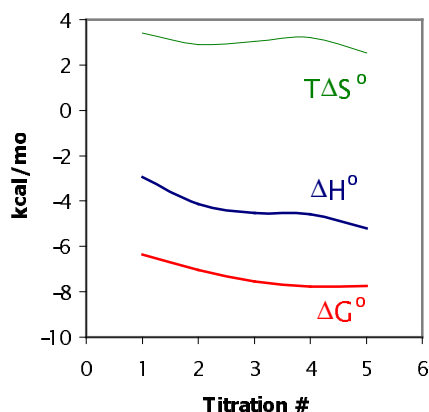
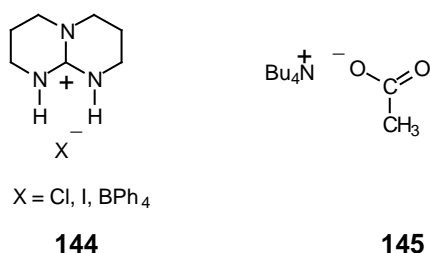


Figure 8. A plot showing ΔG° , ΔH° and $T\Delta S^\circ$ in (kcal M^{-1}) of table 5 as they vary with the host counteranion (titrations 1-5).

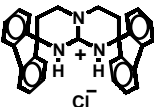
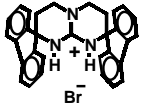
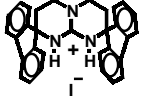
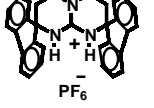
In a similar study Hamilton and Linton [108] had reported that association characteristics between the simple guanidinium host **144** and TBA-acetate **145** in DMSO are dependent on counterion and solvent as well, while they found that the association strength of the guanidinium chloride counterion with **145** is smaller ($2.9 \times 10^3 M^{-1}$) in comparison to that of the iodide ($5.2 \times 10^3 M^{-1}$) or tetraphenylborate (TPB) ($5.6 \times 10^3 M^{-1}$) counterions. This could be attributed to the chloride-guanidinium attraction which reduces the net energy gain from acetate complexation. This finding is consistent with the trend analysis result shown in table 5. They also reported a similar, albeit weaker, trend for the enthalpy values.



The calorimetric determination of the fluorenyl-substituted guanidinium compounds with **129** (table 6) in acetonitrile revealed results almost similar to those shown in table 5. Switching the counter anion from chloride to iodide shifts the experimental host-guest affinity by a ratio of about 28, with the large iodide ion yielding the highest K_{ass}

values. In all cases the association is accompanied by a positive entropy contribution that again is explained by the release of solvent molecules and counter anions to the bulk.

Table 6. Energetics of the complexation between fluorenyl-guanidinium⁺ X⁻ with benzoate **129** in acetonitrile at 30°C (303K).

Tit. #	Host	TEA Benzoate [mM]	<i>n</i>	<i>K</i> _{ass} [M ⁻¹]	Δ <i>H</i> ^o [kcal M ⁻¹]	Δ <i>S</i> ^o [cal K ⁻¹ M ⁻¹]	TΔ <i>S</i> ^o [kcal M ⁻¹]	Δ <i>G</i> ^o [kcal M ⁻¹]	<i>c</i>
6	1.05 mM  138 Cl ⁻	22.47	0.99	21 300 ± 1 170	- 3.56 ± 0.03	+ 8.0 ± 0.2	+ 2.44	- 6.00 ± 0.03	22
7	0.96 mM  139 Br ⁻	21.86	1.08	51 600 ± 5 500	- 4.07 ± 0.05	+ 8.1 ± 0.4	+ 2.46	- 6.53 ± 0.06	50
8	0.2 mM  48 I ⁻	5.30	1.06	592 000 ± 34 000	- 6.03 ± 0.03	+ 6.5 ± 0.2	+ 1.97	- 8.00 ± 0.04	115
9	0.91 mM  140 PF ₆ ⁻	22.57	1.00	67 400 ± 3 000	- 5.07 ± 0.02	+ 5.4 ± 0.2	+ 1.63	- 6.70 ± 0.03	59

The results in table 6 show the lowest exothermicity ($-\Delta H^o$) in the exchange of chloride for benzoate, while the I⁻ ion enables the strongest enthalpic response (see figure 9). Surprisingly the affinity of the larger, less hydrogen-bonding PF₆⁻ counter anion is smaller than that of the iodide by a factor of about 9, and its enthalpy is less negative by 1 kcal, contradicting the expected behavior of these anions, namely, that it should display the strongest enthalpic response upon complexation with carboxylate because of its weak, mainly electrostatic binding to the guanidinium group. An

explanation of this amazing result can emerge from the assumption that part of the PF_6^- counterion had been hydrolyzed to the difluorophosphate stage. An inspection of the X-ray crystal structure of the tetraphenyl-guanidinium salt (figure 12c), which nominally was expected to be the PF_6^- -salt, shows a hydrogen bonding between a tetraphenyl-guanidinium cation and one of the oxygen atoms in the tetrahedral difluorophosphate (PF_2O_2^-) anion indicating that a hydrolysis of the PF_6^- counter anion of the tetraphenylguanidinium host had occurred resulting in an X-ray structure different from what was expected with the PF_6^- . This structure proves the adventitious presence of hydrolyzed anion species and thus might explain the unusual energetic data obtained for the PF_6^- anion (table 6). During the titration experiment the counter anion PF_6^- had probably been hydrolyzed and simultaneously associated by hydrogen bonding with the guanidinium moiety which will definitely lead to a stronger complex because of the additional hydrogen bonding. The enthalpy of the guanidinium- PF_2O_2^- will result in a lower exothermicity in the exchange for benzoate than with guanidinium-iodide.

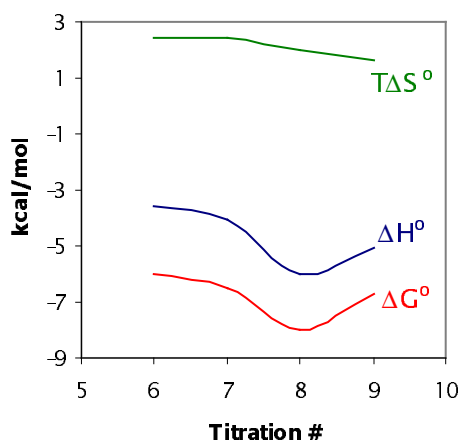
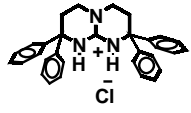
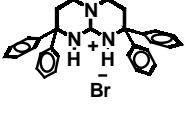
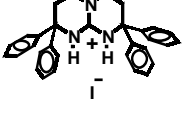
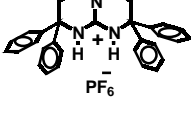


Figure 9. A plot showing ΔG° , ΔH° and $T\Delta S^\circ$ in (kcal M^{-1}) of table 6 as they vary with the host counteranion titrations 6-9.

The titration results of the tetraphenylguanidinium hosts with benzoate **129** shown in table 7, mark an increase in the association constant when replacing the chloride counter anion with the largest PF_6^- counter anion. The enthalpic values show higher exothermicity when shifting the counter anion to the iodide and not the PF_6^- . The positive entropy component is the highest for the PF_6^- counter anion indicating that

more solvent molecules were released to the bulk (see figure 10). Again, this unexpected result can arise from the assumption that part of the PF_6^- counter anion had been hydrolyzed to the difluorophosphate. It seems that the percentage of the PF_6^- counter anion involved in the hydrolysis process varies from one experiment (see differences between tables 6 and 7) to the other therefore, the trend behavior of this anion upon complexation is ill determined.

Table 7. Energetics of host–guest binding of the tetraphenylguanidinium cations with benzoate **129** in acetonitrile at 30°C (303K).

Tit. #	Host	TEA Benzoate [mM]	<i>n</i>	K_{ass} [M^{-1}]	ΔH° [kcal M^{-1}]	ΔS° [cal $\text{K}^{-1}\text{M}^{-1}$]	$T\Delta S^\circ$ [kcal M^{-1}]	ΔG° [kcal M^{-1}]	<i>c</i>
10	2.02 mM  135	51.22	1.03	7 600 ± 172.0	- 3.59 ± 0.02	+ 5.9 ± 0.2	+ 1.80	- 5.38 ± 0.02	115
11	1.01 mM  136	21.40	1.06	21 800 $\pm 1 700$	- 4.17 ± 0.06	+ 6.0 ± 0.2	+ 1.81	- 5.99 ± 0.03	21.8
12	1.09 mM  70	22.48	1.01	111 000 $\pm 7 000$	- 5.18 ± 0.02	+ 6.0 ± 0.2	+ 1.81	- 6.99 ± 0.04	289
13	0.91 mM  140	22.36	1.01	125 000 $\pm 8 500$	- 4.61 ± 0.03	+ 8.1 ± 0.2	+ 2.50	- 7.07 ± 0.04	180

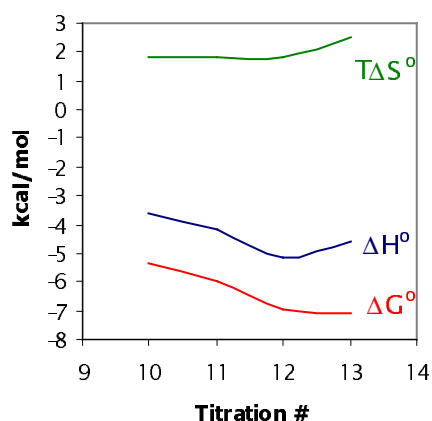


Figure 10. A plot showing ΔG° , ΔH° and $T\Delta S^\circ$ in (kcal M^{-1}) of table 7 as they vary with the host counteranion (titrations 10-13).

The enthalpy results presented in tables 5, 6, and 7 – concisely collected in table 8 – clearly indicate that the complexation of guanidinium chloride counter anion with benzoate produce the lowest enthalpy values in the series, ranging from -3.0 to -3.6 kcal/mole. Switching the counter anion to bromide shifts the experimental enthalpy values to about -4.1 kcal/mole. The highest enthalpic response range (-4.5 to -6 kcal/mole) is obtained with iodide, the largest halide counter anion. Note that, as discussed earlier, the enthalpy values obtained with the largest counter anion in the series, PF_6^- , has values unexpectedly lower than those with iodide. Therefore, it is sufficient to use the guanidinium iodide ion-pair in the exchange for the oxoanions examined in the experiments performed hereafter.

Table 8. The enthalpy values in kcal/mol for the different counter anions of the guanidinium hosts with benzoate **129**.

X^-			
Cl^-	-2.93	-3.56	-3.59
Br^-	-4.13	-4.07	-4.17
I^-	-4.52	-6.03	-5.18
PF_6^-	-5.21	-5.07	-4.61

The impact of host design on binding affinity represents the ultimate goal of molecular-recognition studies. Here this was evaluated using an ensemble of bicyclic guanidinium iodides **48**, **70**, **132**, **141**, **142** (table 9). All of these compounds contain the same primary binding motif and are probed by complex formation with the same guest species **129**. However, the lining of the binding site was modified synthetically to introduce substituents with different steric properties, but without harming the preferential binding mode. Some of these compounds were newly prepared and the others were previously obtained in our lab [64, 109]. This specific set of differently substituted guanidinium compounds was chosen due to their varying hydrophobicity properties, from the more flexible allyl groups in **132** to the more rigid fluorenyl units in **48**. The logic behind complexing these substituted guanidinium cations with the same guest anion is to investigate the effect of the guanidinium hosts rigidity on the complex desolvation. Solvation effects may be supplemented to some degree by a field effect that lowers the dielectric constant in the vicinity of the charged guanidinium function which results in desolvation enhancement near the binding site and thereby enhances the coulombic attraction and hydrogen bonding for the anionic guest [104].

The approach is analogous to the site-directed mutagenesis of biological receptors in which single amino acid residues in the substrate binding pocket may be deliberately exchanged to probe or alter the binding characteristics. Unlike the biological example, in the present artificial host–guest system the substituents available are not restricted to the natural amino acids side chains.

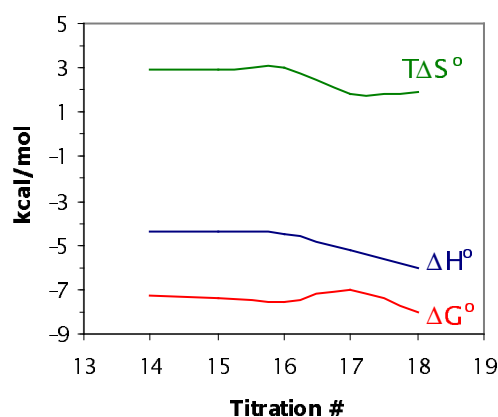
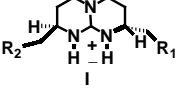
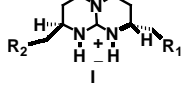
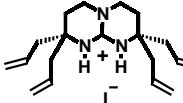
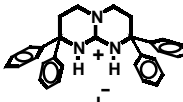
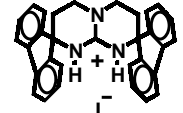


Figure 11. A plot showing ΔG° , ΔH° and $T\Delta S^\circ$ in (kcal M^{-1}) of guanidinium iodide hosts, table 9 as they vary with benzoate **129** (titrations 14-18).

Table 9. Energetics of host – guest binding of different guanidinium iodide host compounds with benzoate **129** in acetonitrile at 30°C (303K).

Tit. #	Host	TEA Benzoate [mM]	<i>n</i>	K_{ass} [M^{-1}]	ΔH° [kcal M^{-1}]	ΔS° [cal $K^{-1}M^{-1}$]	$T\Delta S^\circ$ [kcal M^{-1}]	ΔG° [kcal M^{-1}]	<i>c</i>
14	1.08 mM  $R_1 = \text{OSi}t\text{BuPh}_2$ $R_2 = \text{OSi}t\text{BuMe}_2$ 141	24.51	1.03	167 000 $\pm 8\ 000$	- 4.36 ± 0.01	+ 11.5 ± 0.1	+ 2.88	- 7.25 ± 0.03	180
15	1.04 mM  $R_1 = R_2 = \text{OSi}t\text{BuPh}_2$ 142	24.51	0.90	203 000 $\pm 12\ 000$	- 4.40 ± 0.02	+ 11.8 ± 0.3	+ 2.95	- 7.35 ± 0.04	211
16	1.03 mM  132	23.17	1.05	280 000 $\pm 22\ 000$	- 4.52 ± 0.02	+ 10.0 ± 0.2	+ 3.03	- 7.55 ± 0.05	289
17	1.09 mM  70	22.48	1.01	111 000 $\pm 7\ 000$	- 5.18 ± 0.02	+ 6.0 ± 0.2	+ 1.81	- 6.99 ± 0.04	121
18	0.2 mM  48	5.30	1.06	592 000 $\pm 34\ 000$	- 6.03 ± 0.03	+ 6.5 ± 0.2	+ 1.96	- 8.00 ± 0.04	115

The calorimetric results (Table 9) report a clear trend that assigns a decisive role to solvation even in a typical organic solvent, such as acetonitrile. We observe a distinct variation of the binding free energy ΔG° with the substitution pattern of the host (see figure 11). The differences are manifest in the enthalpies as well as in the entropies of association. The less positive ΔS° values seen in **70** and **48** with the aromatic substituents indicate the release of fewer solvent molecules on benzoate binding than in

132 or **142** or **141**. In view of the considerable distance of the guest from the residues in the α -positions of the host (see Figure 6), a direct influence of the guest on the internal motility of the host is unlikely. Thus, it is most plausible to assume that the receptor site in **70** and **48**, lined by aromatic residues, is less solvated than the others and thus the enthalpic penalty paid to disrupt the solvation shell is smaller (see figure 11). This smaller unfavorable contribution results in an enhancement of the total exothermicity. The same arguments serve to explain the energetics of binding to the hosts **132**, **141** and **142**. The tetrasubstitution with “lean” residues directly adjacent to the binding site in **132** or by disubstitution with much more bulky silylether groups in **141** and **142** gives states of solvation that seem to be very much alike.

The fluorenyl compound **48** shows solvation changes almost identical to those of the tetraphenyl analogue **70** (cf. ΔS° values), but exhibits a significantly enhanced enthalpic contribution. The result relates to the presumed higher rigidity of **48** which opposes the reorientation of the solvent dipoles to cope with the change of the electrostatic field on complex formation. Comparison of **132** and **70** also provides a good example for the benefit of dissecting ΔG° into the enthalpy and entropy components. Considering affinity only (K_{ass}) the allyl compound **132** would be a better host than **70**. Most molecular recognition studies, however, would rather select for better structural definition of the noncovalent complex since this constitutes the basis of goals from selectivity to self-assembly. With respect to precise structuring of the host–guest complex, **70** holds an edge over **132** because of the stronger enthalpic interaction and thus provides a strong argument to take enthalpy instead of the almost exclusively used free energy as a ranking criterion.

4.2 Different conformations of the tetraphenylguanidinium cation with different counter anions.

The tetraphenylguanidinium compound is considered to be less flexible than the tetraallyl- **132** and the tetramethyl- **71** hosts. Several X-ray structures for the tetraphenyl compound with different counter anions (figure 12) show that this host in the solid phase can adopt different conformations due to a degree of flexibility that allows the conversion from one conformation to another depending on the nature of the counter anion. Tetraphenylguanidinium iodide and bromide shown in figures 8a and

8b respectively, adopt a trans conformation in which one phenyl group is in the axial position perpendicular to the plane of the bicyclic guanidine while the other axial phenyl group in the neighboring ring is below the plane. The other two phenyls groups are in the equatorial positions. On replacing the counter anion to benzoate the structure adopts the cis conformation (figure 12d) where the two axial phenyls point in the same direction, however, when the counter anion is replaced with PF_2O_2 the structure adopts a conformation in between cis and trans (figure 12c). These observation reveals that the tetraphenylguanidinium compound can not be considered rigid.

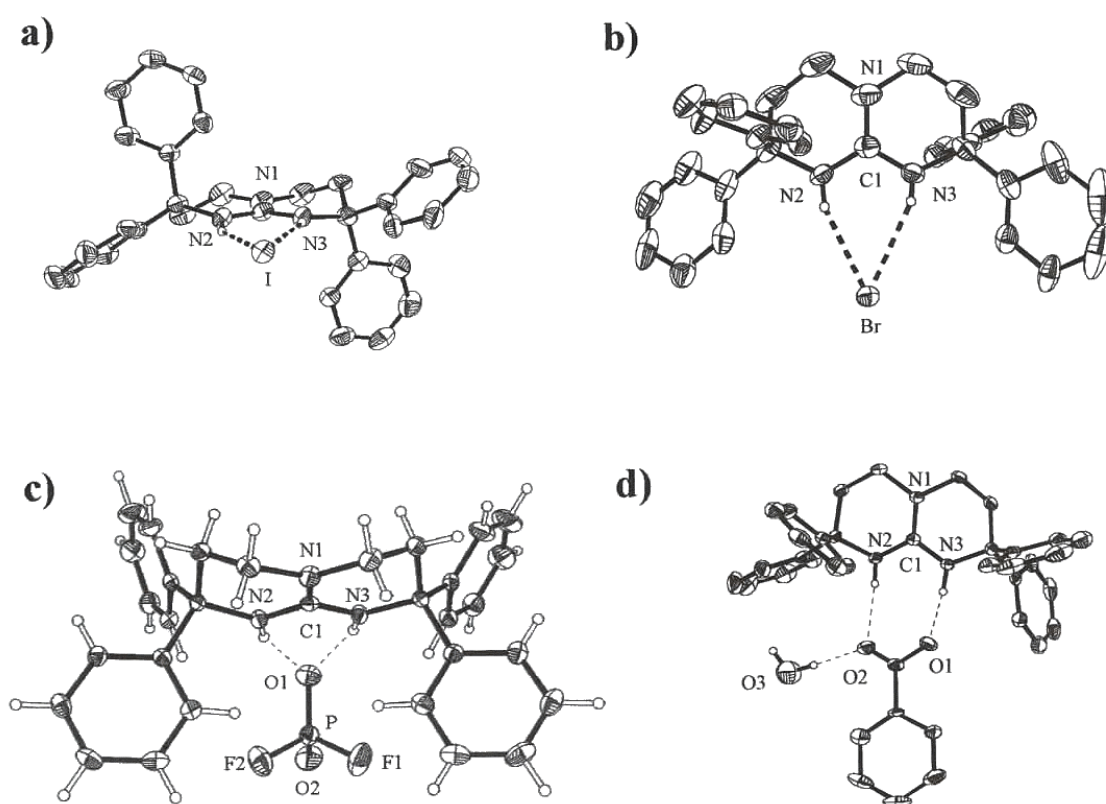


Figure 12. X-ray crystal structure of tetraphenyl guanidinium–iodide (a), –bromide (b), –difluorophosphate (c), –benzoate (d).

An examination of the association properties with ITC of the different guanidinium hosts with carboxylate **129** in methanol, did not show any marked binding characteristics. The complexation is hampered due to the strong polar and competitive hydrogen bonding solvent that decreased the association constant to a limit that was

not detectable from the ITC experiment. An increase in the concentration of both host and guest did not result in a significant association as well.

About a decade ago, a theoretical Monte Carlo study [110] of the free energy profile for the guanidinium-acetate ion-pair in water was carried out in order to model putative interactions between solvated arginine and glutamic or aspartic acid residues. These simulations showed that best geometric configuration for the ion-pair is to be maintained in a C_{2v} symmetry. The determined potential showed three minima, corresponding to an ion-pair, solvent separated and “infinitely” separated ion-pairs. There was no clear preference within the ion-pairs. Whereas, the intermediate state displayed cooperative binding between the ions via two water molecules forming a double hydrogen-bond bridge. The two extreme states of ion-pair and infinitely separated ions have a large energy barrier. Therefore, the weak association in methanol between the guanidinium compounds and the benzoate found in the current study could be caused by an intermediate state in which binding between the two ions has taken place through methanol molecules.

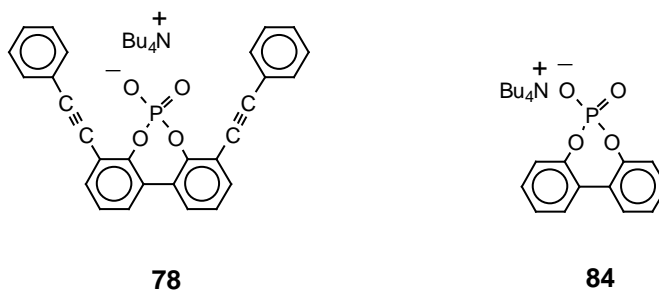
In this work, the guanidinium host molecules were complexed with carboxylate or phosphate oxoanions in acetonitrile. It is wise to note that despite the similar preferential binding mode of these oxoanions with the guanidinium moiety, there are some differences in their stereochemistry when each interacts with Lewis acid [111].

The stereochemistry of carboxylate–Lewis acid interaction is defined as syn or anti, the carboxylate group typically prefers a syn-oriented interaction with metal ion, a hydrogen bond donor, or a covalently bound proton. Additionally, the interaction preferably occurs in the plane of the carboxylate, presumably in order to complex the oxygen sp^2 lone electron pair. The anionic phosphinyl portion ($-PO_2^-$) of the phosphate group, as it comprises the backbone of nucleic acids, may interact with Lewis acids such as metal ions or hydrogen bond donors as well. However, the geometry of phosphate–Lewis acid interactions has been examined by using the Cambridge Structural Database [111]. Interactions involving metal ions display preferentially syn, unidentate, and out-of-plane coordination stereochemistry with regard to the phosphinyl ($-PO_2^-$) group. In contrast, hydrogen bond donors display a very slight preference for anti stereochemistry with the phosphinyl group, and these interactions also do not tend toward in-plane interaction with the phosphinyl group.

Therefore, in general, the preferential phosphate–Lewis acid geometry contrasts markedly with carboxylate–Lewis acid geometry. These results were useful in the interpretation of nucleic acid structures and protein–nucleic acid interactions observed by macromolecular X-ray crystallography.

4.3 Complexation of different guanidinium cation hosts with phosphate **78**.

The impact of guest design on binding affinity with different guanidinium iodide hosts was evaluated using a newly designed phosphate anion **78** (figure 13 shows the X-ray crystal structure of the phosphoric acid form of **78**) with comparison to the parent **84**. The new phosphate anion contains the same primary guanidinium binding motif as in all oxoanions, however, the lining of the guest binding site was modified synthetically to introduce substituents (arms) at positions adjacent to it but without harming the preferential binding mode. The motive behind the additional substituted arms in the guest anion, is to strengthen the directionality towards the guanidinium binding site and restrict it into one possible direction only. The new phosphate might wrap around the host in order to reach an optimal orientation upon complexation that will lead to selectivity enhancement within this specific guest anion.



The calorimetric results (table 10) of the complexation between the phosphate guest anion **78** and the different guanidinium iodide hosts, starting from the more flexible tetramethyl-substituted guanidinium compound **71** down to the most rigid fluorene-guanidinium compound **48**, report again a clear trend of increasing host-guest affinity with host rigidity, yielding the highest K_{ass} for the fluorene-guanidinium compound **48**. A variation of the binding enthalpy ΔH° , where the tetraphenylguanidinium compound **70** shows the strongest enthalpic response despite having the lowest affinity (K_{ass}) in the series (see slope of ITC plot, figure 15). A

variation in the ΔS° values was noticeable as well, for example, the complexation between the phosphate **78** and compound **70** yields the first negative entropy value that was observed in this work (see $T\Delta S^\circ$ in figure 14 titration # 21).

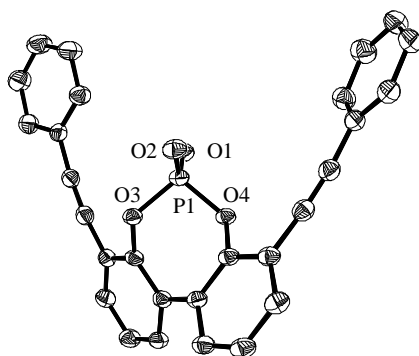


Figure 13. X-ray crystal structure of the Phosphoric acid **9**, the acid form of the **78**.

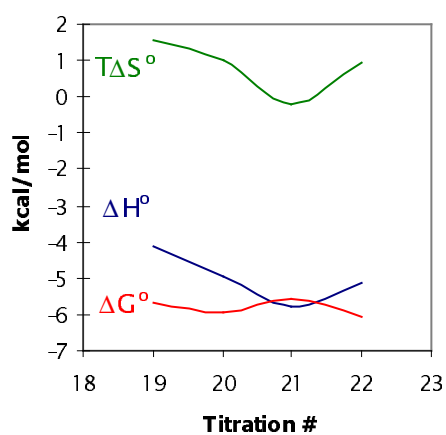
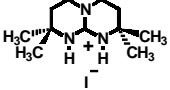
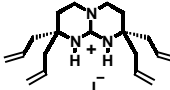
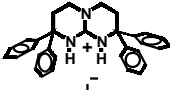
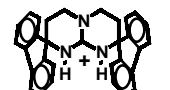


Figure 14. A plot showing ΔG° , ΔH° and $T\Delta S^\circ$ in (kcal M^{-1}) of guanidinium iodide hosts, table 10 as they vary with phosphate **78** (titrations 19-22).

Table 10. Energetics of host–guest binding of different guanidinium iodide hosts with phosphate **78** in acetonitrile at 30°C (303K).

Tit. #	Host [mM]	phosphate 78 [mM]	<i>n</i>	K_{ass} [M^{-1}]	ΔH° [kcal M^{-1}]	ΔS° [cal $\text{K}^{-1}\text{M}^{-1}$]	$T\Delta S^\circ$ [kcal M^{-1}]	ΔG° [kcal M^{-1}]	<i>c</i>
19	0.52 mM  71	16.00	1.04	12 500 ± 290	- 4.14 ± 0.02	+ 5.0 ± 0.1	+ 1.54	- 5.68 ± 0.01	7
20	0.50 mM  132	16.00	0.94	19 800 ± 680	- 4.97 ± 0.03	+ 3.3 ± 0.2	+ 0.99	- 5.96 ± 0.02	10
21	0.75 mM  70	16.00	1.09	9 900 ± 466	- 5.77 ± 0.05	- 0.8 ± 0.3	- 0.23	- 5.54 ± 0.03	7
22	0.20 mM  48	4.60	0.92	23 000 $\pm 1\ 000$	- 5.10 ± 0.07	+ 3.15 ± 0.3	+ 0.95	- 6.04 ± 0.03	5

The negative entropy value might reflect a release of few solvent molecules near the binding site upon complexation and formation of a tight complex that results in the loss of degrees of freedom. The other guanidinium hosts have more positive entropy values compared to **70**, however, lower than the entropy values obtained from complexation of the same hosts to carboxylate (tables 5-7 and 9). It is clear that the tetraphenyl-compound **70** shows, unexpectedly, the highest ΔH° and ΔS° values within this series. The energetic values of fluorene-guanidinium host **48** is the second in order in this family in terms of binding strength. Comparison between the host-guest complexes in table 10 is another good example of the insight provided by dissecting ΔG° into its enthalpy and entropy components. Considering the affinity (K_{ass}) and the Gibbs energy

of complex formation (ΔG°) only, the tetraphenyl compound **70** would be the weakest host in this group. However, by studying the detailed energetic parameters of complex formation, host **70** holds a benefit over the others due its strongest exothermicity ($-\Delta H^\circ$) and its negative entropy value, pronouncing the higher selectivity toward the guest anion **78** with respect to the rest of the series.

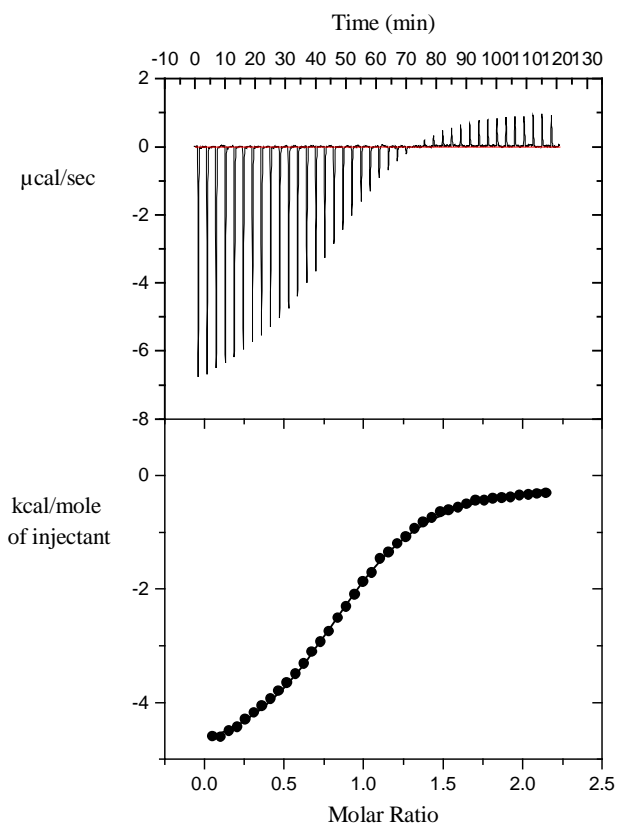
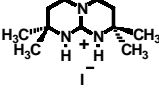
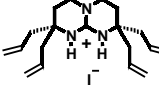
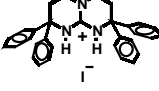
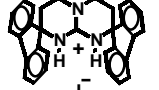


Figure 15. ITC plot for the association between tetraphenylguanidinium iodide **70** (0.75 mM) with phosphate anion **78** (16 mM) in acetonitrile at 30°C.

Table 11 shows the association properties of the same hosts as in table 10 with the parent phosphate anion **84** which resembles phosphate **78** but lacks the two side arms. The trend behavior of these hosts with the guest anion **84** is very much like the results shown in table 10 (see figure 16). A comparison between the two tables 10 and 11 highlights the differences in binding properties of the same guanidinium hosts with anion **78** and the parent anion **84**. The comparison unveils the influence of the two side substituents in phosphate **78** on the binding properties.

Table 11. Energetics of host–guest binding of different guanidinium hosts with phosphate **84** in acetonitrile at 30°C (303K).

Tit. #	Host	Phosphate 84 [mM]	<i>n</i>	K_{ass} [M^{-1}]	ΔH° [kcal M^{-1}]	ΔS° [cal $\text{K}^{-1}\text{M}^{-1}$]	$T\Delta S^\circ$ [kcal M^{-1}]	ΔG° [kcal M^{-1}]	<i>c</i>
23	1.04 mM  71	22.56	1.10	10 000 ± 150	- 3.21 ± 0.02	+ 7.7 ± 0.06	+ 2.33	- 5.54 ± 0.01	10
24	0.54 mM  132	11.56	0.98	18 000 ± 1 129	- 3.51 ± 0.04	+ 7.8 ± 0.3	+ 2.39	- 5.90 ± 0.04	10
25	0.60 mM  70	23.12	1.05	10 400 ± 517	- 5.19 ± 0.06	+ 1.3 ± 0.3	+ 0.38	- 5.57 ± 0.03	6
26	0.20 mM  48	4.62	1.09	22 000 ± 873	- 4.54 ± 0.05	+ 4.9 ± 0.3	+ 1.48	- 6.02 ± 0.02	5

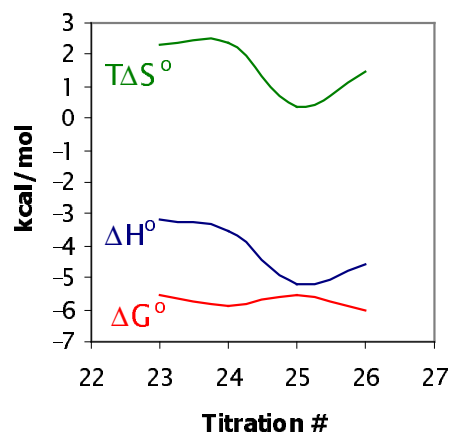


Figure 16. A plot showing ΔG° , ΔH° and $T\Delta S^\circ$ in (kcal M^{-1}) of guanidinium iodide hosts, table 11 as they vary with phosphate **84** (titrations 23-26).

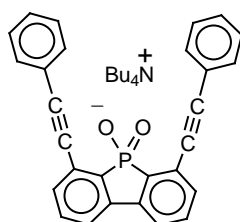
Inspection of the binding affinity between pairs of titration experiments (19-23, 20-24, 21-25, 22-26) of the same guanidinium host with phosphate **78** and phosphate **84**, indicates that there is no significant difference in the association affinity (K_{ass}) toward either guest anions. However a clear enhancement in the binding enthalpy ΔH° is evident when the phosphate anion **78** is used. The value of the binding enthalpy of tetramethyl compound **71** with anion **78** is 1kcal greater than its value with anion **84**. The enthalpic response of the tetraallyl compound **132** with **78** shows an exothermicity of about 1.5 kcal higher than with the parent anion, **84**. When using anion **78**, the tetraphenyl-**70** and the fluorenyl compound **48** have an increased exothermicity of about 0.5 kcal more than those obtained with **84**. Therefore, it is clear that the binding strength of all the guanidinium hosts was higher on binding with phosphate **78**. The less positive ΔS° values seen in all the titration experiments with anion **78** indicate the release of fewer solvent molecules than on phosphate **84** binding.

The unchanged affinity constant (K_{ass}) together with the increase in the affinity strength (ΔH°) and decrease in the entropy (ΔS°) values within every pair of experiments indicates very clearly the enhancement of the binding directionality and selectivity upon complexation with phosphate **78**. In the complexation process there might be an additional cation- π or π - π interaction between the tetraphenylguanidinium host or the fluorenyl host **48** and the phosphate anion **78**. This additional interaction could be caused by the aromatic moieties attached to the hosts and to the guest anion, which explains the enhanced enthalpic response upon complexation in comparison with anion **84**. The additional cation- π and π - π interactions between guanidinium moieties and benzylic oxoanions were noticed and studied before. Certain benzylic biphosphonates are known to bind strongly to guanidinium cations, however, these guests showed enhanced selectivity for aromatic guanidines. The specific recognition pattern of these molecules includes additional π - π interactions, that are absent in the arginine-selective molecular tweezer [112].

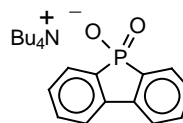
Hamilton and de Mendoza [113] have designed a new protein surface that utilizes cation- π interactions to enhance binding between an α -helical peptide that contains the aspartic acid and the tryptophan carboxylate residues and a cationic bicyclic guanidinium molecule in even aqueous-methanol solution. Therefore, in principle these interactions could occur with the compounds used in the current study, however more

robust data should be obtained, *e.g.*, an X-ray crystal structure, in order to validate the existence of such interactions.

If the determination of the strongest host-guest complex in both tables 10 and 11 would be according to the ΔG° values alone, that do not vary with significant values for all complexes, it would be not possible to reach the above conclusions nor the structural achievement in phosphate **78** would be observed.



92

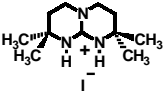
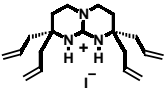
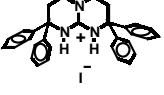
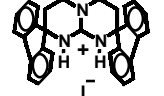


128

In an attempt to increase the selectivity of the guanidinium hosts towards a specific oxoanion, the synthesis of the new phosphinate anion, **92**, was envisaged. The guest anion **92** has the same organic framework as the phosphate anion **78** but with the phosphate diester unit in the latter replaced with phosphinic acid while maintaining the same binding motif to the guanidinium compound hosts. In complexation, the whole anion molecule is expected to be much closer to the guanidinium host molecule. The phosphorus atom in the phosphinate guest anion is part of a 5-membered ring and directly bound to the biphenyl framework, whereas in the phosphate diester **78** the phosphorus atom is a part of a 7-membered ring within which the oxygen atoms are the ones directly attached to the biphenyl framework. Owing to the geometrical difference between the two structures, the opening angle between the two side arms in **92** is tighter which increases the directionality upon complexation. Since the opening angle between the arm substituents in **92** is smaller than in **78**, the abundance of solvent molecules in the vicinity of the binding site is diminished. It seems likely that anion **92** will deliberately form tighter complexes with guanidinium hosts like **48** and **70** than those achieved with anion **78**. This tightening is surely assisted by the two side arms

that will project above and beneath the main plain of the host to reach optimal orientation at the time of complex formation. Anion **92** is still in preparation.

Table 12. Energetics of host–guest binding of the different guanidinium iodide compounds with phosphinate **128** in acetonitrile at 30°C (303K).

Tit. #	Host	phosphinate 128 [mM]	<i>n</i>	K_{ass} [M^{-1}]	ΔH° [kcal M^{-1}]	ΔS° [cal $\text{K}^{-1}\text{M}^{-1}$]	$T\Delta S^\circ$ [kcal M^{-1}]	ΔG° [kcal M^{-1}]	<i>c</i>
27	0.52 mM  71	23.08	1.24	24 700 ± 1393	- 3.62 ± 0.03	+ 8.2 ± 0.2	+ 2.47	- 6.09 ± 0.03	13
28	0.54 mM  132	23.08	0.94	49 500 ± 3057	- 5.13 ± 0.04	+ 4.5 ± 0.3	+ 0.93	- 6.51 ± 0.04	27
29	0.20 mM  70	11.54	0.97	33 000 ± 758	- 10.09 ± 0.06	- 15.3 ± 0.3	- 4.62	- 6.27 ± 0.01	7
30	0.50 mM  48	11.54	0.95	78 000 $\pm 2 288$	- 5.14 ± 0.02	+ 5.4 ± 0.1	+ 1.65	- 6.79 ± 0.02	39

A calorimetric study of the complexation between the parent phosphinate **128**, prepared for a planned comparison with **92**, and different guanidinium cations was obtained (table 12). In this series we observe yet again that affinity to the phosphinate becomes stronger with host rigidity as in the fluorenyl compound **48**. The unexpected result reported in table 12 is the strong exothermicity ($-\Delta H^\circ$) of the tetraphenyl compound **70** (see also table 11) which differs from the other enthalpy values by about 5 kcal. The unusual negative entropy in the same host indicates a pronounced selectivity to the guest (see figure 17). The high exothermicity and negative entropy

achieved during binding to tetraphenyl guanidinium provide a clear testimony to the strong structural definition toward this phosphinate guest. It is expected that complexation of the same host series with the desired guest anion **92** would reveal even higher energetic values than what is shown in table 12.

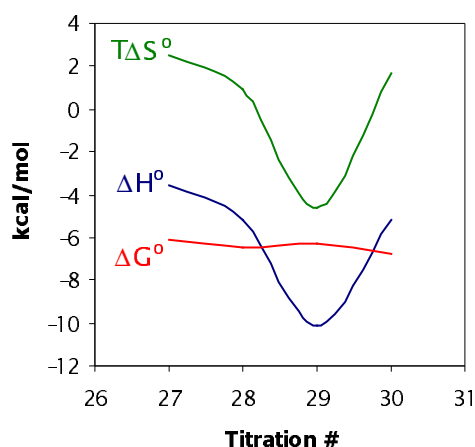


Figure 17. A plot showing ΔG° , ΔH° and $T\Delta S^\circ$ in (kcal M^{-1}) of the guanidinium iodide hosts, table 12 as they vary with phosphinate **128** (titrations 27-30).

Most of the guanidinium host samples for the titration experiments were prepared in dry acetonitrile of about 1mM concentration. Owing to the association between the tetraallylguanidinium iodide (1.03 mM) and TEA-benzoate (23.17 mM) the first several injections in the titration experiment, as seen in figure 18a, deviate from ideal binding behavior. This deviation probably reflects the effect of multiple guanidinium molecules association with the limited benzoate present, or other unspecific interactions. To ensure that this behavior is due to unspecific interactions and not part of the association between the guanidinium and the anion guest, the guanidinium sample was diluted to reach a concentration of 0.27 mM and then complexed with the same guest anion (5.3 mM). Figure 18b shows that the anomaly of the initial injections has disappeared testifying to the specificity of the host-guest interaction in the diluted samples. The energetic values in both cases (figure 18) were identical. In the rest of the titration experiments, when a similar behavior occurs, the first several injections were not included in the curve fitting analysis.

The dilution option can be only used when the association constant of the two partners is relatively high, otherwise the dilution effect might weaken the association.

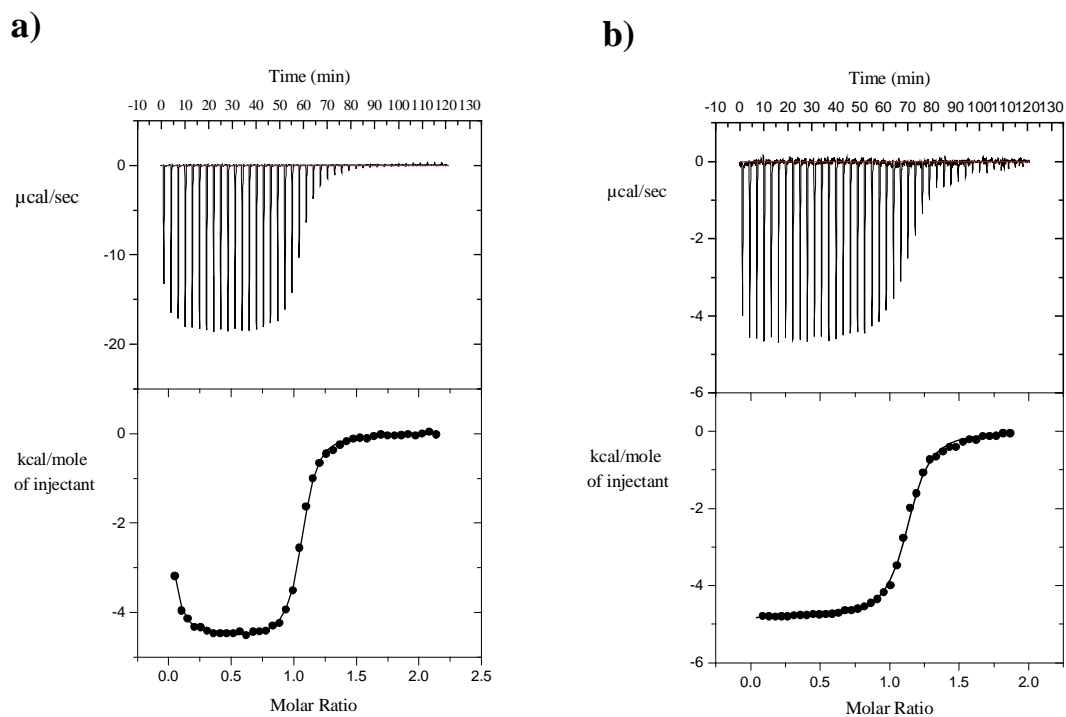


Figure 18. ITC plots for the association of tetraallyl guanidinium iodide **132** and TEA-benzoate **129** in acetonitrile at 30°C with (a) concentration of 1.03 mM and 23.17 mM respectively and (b) concentration of 0.27 mM and 5.3 mM respectively .

5. Experimental part

5.1 General methods and materials.

Proton and ^{13}C -NMR spectra were recorded on a Bruker AM 250 or 360 (MHz) and were calibrated to tetramethylsilane as internal standard. ^{31}P and ^{19}F NMR were recorded on a Bruker 250 MHz and were calibrated to H_3PO_4 as external standard and to C_6F_6 internal standard, respectively. Mass spectra were obtained on :

- Varian MAT CH5 : Fast-Atom-Bombardment (FAB)
- Varian MAT 112S : Electron-Ionization (EI)
- Finnigan LQC : Electrospray-Ionization (ESI, HPLC-MS)

IR spectra were measured on a Perkin-Elmer FTIR 1600 instrument. HPLC-analysis were performed on Merck-Hitachi instrument L6200 or 655A-11 pump connected to Knauer UV-detector or to a Eurosep DDL-31 light-scattering detector.

Solvents were distilled before use except for DMF which was purchased in anhydrous quality from Aldrich and acetonitrile which was purchased in HPLC-quality from Baker. All other chemicals were purchased in reagent quality and used as received. Aqueous solutions were prepared from deionized, glass-distilled water. Most reactions were carried out in an atmosphere of nitrogen and solvents (CH_2Cl_2 , CH_3CN) were passed for drying through a small column of activated alumina directly into the reaction vessel.

HPLC analyses were carried out under six sets of conditions which will be referred to as HPLC1, HPLC2, HPLC3, HPLC4, HPLC5 and HPLC6 analysis.

HPLC1 analysis: Nucleosil C18 (250×4.6 mm) column, UV detection at 254 nm, flow = 1 ml/min, gradient from 50% MeOH to 90% MeOH in 15 min, 30 mM $\text{NaClO}_4/\text{H}_3\text{PO}_4$ as buffer.

HPLC2 analysis: Nucleosil C18 (250×4 mm) column, UV detection at 254 nm, flow = 1ml/min, gradient from 50% MeOH to 90% MeOH in 15 min, 30 mM $\text{NaClO}_4/\text{H}_3\text{PO}_4$ as buffer.

HPLC3 analysis: Nucleosil C18 (250×4 mm) column, LS detector, UV detection at 254 nm, flow = 1 ml/min, gradient from 50% MeOH to 90% MeOH in 15 min 0.1% TFA as buffer.

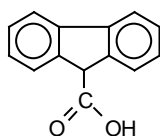
HPLC4 analysis: Nucleosil C18 (250×4 mm) column, UV detection at 254 nm, flow = 1 ml/min, gradient from 50% MeOH to 90% MeOH in 10 min and holding 90% MeOH for 5 min, 30 mM NaClO₄/H₃PO₄ as buffer.

HPLC5 analysis: Nucleosil C18 (250×4 mm) column, LS detector, UV detection at 254 nm, flow = 1ml/min, gradient from 50% MeOH to 90% MeOH in 5 min and continuing at 90% MeOH for 25 min 0.1% TFA as buffer.

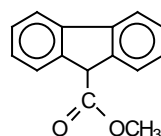
HPLC6 analysis: Nucleosil C18 (250×4 mm) column, LS detector, UV detection at 254 nm, flow = 1ml/min, gradient from 50% MeOH to 90% MeOH in 10 min and 90% MeOH for 5 min, 0.1% TFA as buffer.

5.2 Synthetic procedures

9-Fluorenicarboxylic acid methyl ester 145



144



145

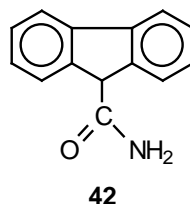
10 g (47.5mmol) of 9-fluorenicarboxylic acid **144** were dissolved in 200 ml of MeOH in 1 liter flask, and 7 ml of thionyl chloride (SOCl₂) were added. The reaction mixture was stirred in a 1 liter flask at RT. At the beginning observed a non homogeneous solution, but after 1.5 h the mixture had a clear yellow colour. After 2 hours all of the starting material was completely converted to 9-fluorenicarboxylic acid methyl ester (HPLC analysis). The solvent and SOCl₂ were removed by a stream of N₂ or evaporation in vacuum. 9 g (40mmol, 84%) of product **145** were obtained after recrystallization from MeOH.

145: C₁₅H₁₂O₂ (MW 224.2)

mp: 65°C (lit): 63-63.5°C

HPLC1 analysis: R_V(**144**)= 10.4 ml, R_V(**145**)= 11.8 ml

9-Fluorene carboxylic acid amide 42



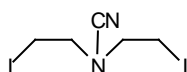
100 g (1.3 mmol) of ammonium acetate (NH_4OAc) were dissolved in 200 ml of MeOH in a 1 liter flask. The mixture was stirred at 0°C , then a stream of ammonia gas was passed through the solution. When the solution was saturated with ammonia, 9 g (40 mmol) crystals of 9-fluorencarboxylic acid methyl ester **145** were added. It took 5 min until the reaction mixture reached homogeneity again. The reaction mixture was kept at 5°C for 3-5 days. A precipitate of 9-fluorencarboxylic acid amide **42** was obtained and collected by filtration, washed with H_2O and dried by N_2 gas. The white residue was crystallized from ethanol to give 5 g (23.8 mmol) of product (60% yield).

42: $\text{C}_{14}\text{H}_{11}\text{NO}$ (MW 209.2)

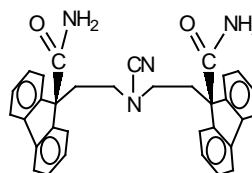
mp: 258°C (lit): 250°C

HPLC1 analysis: $R_V = 5.8$ ml.

N,N-Bis[2-(9'-carboxamidefluoren-9'-yl)ethyl]cyanoamide 44.



43



44

2 g (9.57 mmol) of dry 9-fluorencarboxylic acid amide **42** were suspended in 9 ml of dry DMF (nonhomogeneous solution) and 4.2 ml (33.5 mmol) of 1,1,3,3-tetramethylguanidine was added. Within 2 min of stirring at RT the reaction mixture became a clear yellow solution. Then 1.34 g (3.83 mmol) of bis(2-iodoethyl)-cyanoamide **43** were added slowly. The reaction mixture was stirred at RT over night, then 10 ml diluted acetic acid (50%) was added and the mixture was extracted repeatedly with

chloroform (3-4 times). The combined organic phases were dried over MgSO₄ and then filtered and evaporated. A white product **44** was obtained and crystallized from THF/EtOH or THF/ Ether to give 2.4-3.9 g (4.78-7.65 mmol, 50%-80% yield) of **44** (enforced dryness of the starting materials and the solvent resulted in higher yield of product).

44: C₃₃H₂₈N₄O₂ (MW 512.6)

mp: 195°C

HPLC2 analysis: R_V(**42**)= 10 ml, R_V(**43**)= 8 ml, R_V(**44**)= 14 ml.

¹³C-NMR of (**44**) (62.90 MHz; MeOD): δ= 172.0 (carboxamide), 145.9, 142.3, 129.8, 129.2, 125.0, 121.7 (aromatic carbons), 117.5 (cyanoamide), 61.2 (C-9 of fluorene units), 48.3, 34.4 (aliphatic carbons).

¹³C-NMR of (**44**) (62.90 MHz; DMSO-d₆): δ= 172.8 (carboxamide), 145.0, 140.4, 128.1, 127.7, 123.8, 120.4 (aromatic carbons), 116.4 (cyanoamide), 59.7 (C-9 of fluorene units), 46.8, 33.2 (aliphatic carbons).

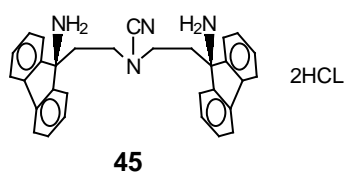
¹H-NMR of (**44**) (250 MHz; MeOD): δ= 7.6, 7.3-7.1 (m, 16H aromatic), 2.28 (t, *J*= 7.2, 4H aliphatic), 1.7 (t, *J*= 7.3, 4H aliphatic).

¹H-NMR of (**44**) (250 MHz; DMSO-d₆): δ= 7.82-7.29 (m, 16H aromatic), 6.88, 6.06 (2×br s, 4H carboxamide), 2.33, 1.86 (8H aliphatic).

¹H-NMR of (**44**) (250 MHz; CDCl₃): δ= 7.72-7.30 (m, 16H aromatic), 5.14, 4.93 (2×br s, 4H carboxamide), 2.50 (t, *J*= 7.7, 4H aliphatic), 2.0 (t, *J*= 7.7, 4H aliphatic).

IR (KBr): 2208 cm⁻¹ for cyanoamide, 1672 cm⁻¹ for carboxamide

Bis-[2-(9-fluorene amine)ethyl]-cyanamide hydrochloride **45**



1 g (1.95 mmol) of **44** was added to 20 ml of THF, 3 ml of H₂O and 166 μl of TFA. After 5 min of stirring of the resulting solution at RT 2.6 g (6 mmol) of [bis-(trifluoroacetoxy)-iodo]benzene (CF₃CO₂)₂IC₆H₅ (pifa) were added. The reaction mixture was protected from light and was kept at RT over night. After 15 hours the

THF was evaporated, and 10 ml of 6% HCl were added to the reaction mixture. After 15 min at RT the reaction mixture was shaken with ethyl acetate which extracted most of the undesired byproducts (repeated 3-4 times). The desired product **45** stayed in the water phase as a salt. The water phase was evaporated by rotavapor or lyophilization to get 700 mg (1.32 mmol) 85% yield of an oily product.

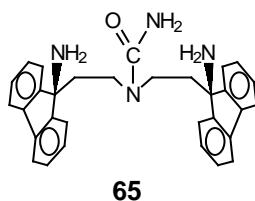
45: C₃₁H₃₀N₄Cl₂ (MW 529.6)

HPLC2 analysis: R_v = 4.0 ml

¹³C-NMR (62.9 MHz; MeOD): δ= 142.2 (CN), 142.0, 141.7, 131.9, 129.8, 124.6, 122.2 (aromatic carbons), 64.7 (C-9 of fluorene units), 44.9, 35.0 (aliphatic carbons).

¹H-NMR (250 MHz; MeOD): δ= 7.59-7.12 (m, aromatic-H), 2.27 (t, *J*= 7.3 Hz, aliphatic-H), 1.72 (t, *J*= 7.4 Hz, aliphatic-H).

N,N-Bis-[2-(9-aminofluorenyl)ethyl]-urea 65



500 mg (0.94 mmol) of **45** were dissolved in 5 ml of 6N HCl and heated to 110°C for 2 hours, the conversion to **65** was followed by HPLC analysis, the reaction mixture contained two phases (brown and light yellow, respectively). Product **65** was distributed between both phases, mostly however, the light yellow phase contained **65** in much higher purity. The two phases were separated and both were washed with ethyl acetate. The light yellow (water) phase was evaporated and a yellow brown salt of **65** was obtained. The product was treated with 20 ml of 4N NaOH and extracted with 20 ml of CHCl₃, the organic phases were combined and dried over MgSO₄. After filtration and evaporating the solvent, product **65** (367 mg, 0.77 mmol) was obtained in 80%-85% yield, and crystallized from EtOH/ CH₃CN.

65: C₃₁H₃₀N₄O (MW 474.6).

mp: 246-249°C

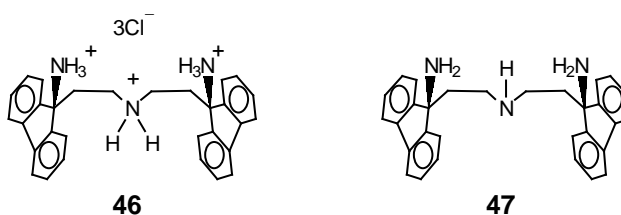
HPLC4 analysis: R_v = 4 ml

MS-ESI: $m/z = 476$ (M^+ 100%)

$^1\text{H-NMR}$ (360 MHz, DMSO-d_6): $\delta = 7.70, 7.42, 7.28$ (d, d, m, $J = 6.5, 6.5$ Hz respectively for aromatic-H), 2.40, 1.92 (8H aliphatic).

$^{13}\text{C-NMR}$ (90.56 MHz, DMSO-d_6): $\delta = 157.6$ (the amide carbon), 151.0, 138.7, 127.7, 127.5, 123.2, 119.8 (aromatic carbons), 63.8 (C-9 of fluorene units), 42.5, 38.9 (aliphatic carbons).

Bis-[2-(9-aminofluoren-9-yl)-ethyl]-amine 47



5 ml of concentrated hydrochloric acid were added to 367 mg (0.77 mmol) of **65** and the mixture was heated in a glass pressure tube at 145°C for 2-3 days. A precipitate appeared which proved to be the desired product **46** and was collected. The ammonium tris-hydrochloride salt **46** was dissolved in H_2O and DMSO , then 4N NaOH were added until the precipitate of the triamine free base **47** appeared. The product was extracted with 2×10 ml CHCl_3 . The organic phases were combined, dried over MgSO_4 and evaporated to yield a brown solid was partly soluble in methanol. The yield of **47** after crystallization from $\text{EtOH}/\text{CH}_3\text{CN}$ amounted to 40%-45% 151.2 mg (0.35 mmol).

47: $\text{C}_{30}\text{H}_{29}\text{N}_3$ (MW 431.6)

mp: $61-64^\circ\text{C}$

HPLC4 analysis: $R_v = 8$ ml

MS-ESI: $m/z = 432$ (M^+ 100%)

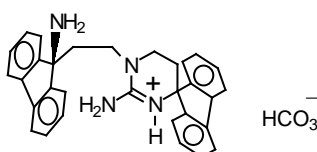
$^1\text{H-NMR}$ of (**46**) (360 MHz, MeOD): $\delta = 7.71-7.64$ (m, aromatic-H), 7.42-7.33 (m, aromatic-H), 2.7, 1.9 (8H aliphatic).

$^{13}\text{C-NMR}$ of (**46**) (90.56 MHz, MeOD): $\delta = 141.8, 141.4, 132.2, 130.1, 125.1, 122.2$ (aromatic carbons), 64.3 (C-9 of fluorene units), 43.7, 33.3 (aliphatic carbons).

$^1\text{H-NMR}$ of (**47**) (250 MHz, CDCl_3): δ = 8.0-7.65 (m, 16H aromatic), 2.50-2.40 (m, 8H aliphatic).

$^{13}\text{C-NMR}$ of (**47**) (62.90 MHz, CDCl_3): δ = 150.4, 139.2, 128.1, 127.8, 123.0, 120.0 (aromatic carbons), 64.5 (C-9 of fluorene units), 45.5, 40.1 (aliphatic carbons).

2-Amino-3-(2'-[9''-aminofluorene-9''-yl)ethyl)-6-(9''-fluorenylidene)-3,4,5,6-tetrahydro pyrimidine hydrogen carbonate 53.



53

Product **45** was basified with 4N NaOH and extracted with CHCl_3 . After drying and evaporating the solvent the free base of **45** was obtained as an oily product.

50 mg (0.1mmol) of the oily product were dissolved in 2ml of isopropanol, MeOH or 3-pentanol. The reaction mixture stirred at RT over night. During this period **45** cyclized quantitatively to monocycle **53**. When the same starting reaction mixture was heated at 60°C , complete conversion to **53** occurred within half an hour.

The solvent was evaporated and the product was dried over night by a stream of N_2 .

53: $\text{C}_{32}\text{H}_{29}\text{N}_4\text{O}_3$ (MW 517.6)

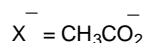
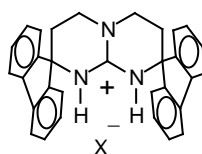
HPLC2 analysis: $R_V = 10$ ml.

MS- ESI: $m/z = 457$ (M^+ 100%)

$^{13}\text{C-NMR}$ (90.50 MHz; CD_3CN): δ = 155.5, 151.9, 148.4, 140.7, 140.4 (aromatic carbons, C-2 of the monocycle), 131.1, 130.0, 129.80, 129.6, 125.3, 124.8, 122.0, 121.8 (aromatic carbons), 65.5, 63.5 (C-9 of fluorene units), 48.0, 45.0, 39.1, 33.1 (aliphatic-carbons)

$^1\text{H-NMR}$ (360 MHz; CDCl_3): δ = 7.67, 7.61, 7.59, 7.42-7.28 (d, d, d, m, $J = 7.5, 7.4, 7.6$ respectively, aromatic-H), 3.47, 3.40, 2.45, 1.96, (m, aliphatic-H).

3',4',6',7'-Tetrahydrodispiro[9H-fluorene-9,2'-[2H]pyrimido[1,2-a]pyrimidine-8'(1'H),9''-[9H]fluorene] acetate 48.



48

600 mg (1.37 mmol) of **47** were dissolved in 15 ml of diethyleneglycol dimethyl ether, then a solution of 316 mg (1.78 mmol) of thiocarbonyl diimidazole **49** in 15 ml diethyleneglycol dimethyl ether was added slowly. The reaction mixture was stirred at 130°C over night. A precipitate was observed and the reaction mixture was cooled to RT. The precipitated product was isolated by centrifugation and was purified by preparative HPLC using a prontosil nitrile column, 30 μ m (UV detection at 245nm, 50% MeOH in 50 mM NH_4OAc , isocratic eluent, flow = 3 ml/min), The product was eluted after 180 ml or after 120 min. Recrystallization from MeOH/ toluene yielded 205 mg (0.41 mmol) 25%-30% yield.

48: $C_{33}H_{30}N_3O_2$ (MW 500.6)

mp: 250°C

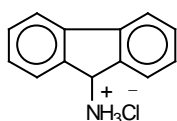
HPLC2 analysis: $R_V = 12.8$ ml.

ESI MS: $m/z = 440.3$ (M^+ 100%)

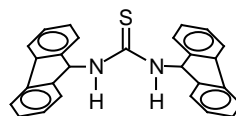
^{13}C -NMR (360 MHz; MeOD): $\delta = 153.3$ (guanidinium carbon), 148.4, 140.5, 130.8, 129.6, 124.9, 121.6 (aromatic carbons), 63.5 (C-9 of fluorene units), 45.9, 33.0 (aliphatic carbons).

1H -NMR (360 MHz; MeOD): $\delta = 7.72, 7.63, 7.35$ (d, d, m, $J = 7.0, 6.8$ Hz respectively, 16H aromatic), 3.91, 2.28 (8H aliphatic).

N,N'-9-Fluorenyl thiourea 56



54



56

500 mg (2.3 mmol) of dry 9-aminofluorene hydrochloride **54** were suspended in 10 ml dry CH₂Cl₂, (the solubility improved after the addition of 4-6 eq of Et₃N). The reaction mixture was stirred for 15 minutes at RT, then 88 μl (1.15mmol) of thiophosgene (CSCl₂) **55** were slowly added and the color of the mixture turned brown. The mixture was heated to 60°C for 3-4 hours, until all the starting material was converted to the thiourea product (HPLC analysis). The dichloromethane solution was washed with diluted acetic acid pH 4-5, in order to extract the base and the salts that were produced during the reaction. The organic phase was evaporated and the product was washed with the minimum amount of CH₃CN, a white solid product appeared and crystallized from hot acetonitrile to yield 325.6 mg (0.8 mmol, 69%). The yield ranged between 50%-70% and dependent on the dryness of the starting material. When **54** was kept under N₂ over night or in a desiccator the yield improved.

56: C₂₇H₂₀N₂S (MW 404.5)

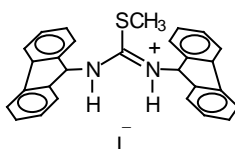
HPLC1 analysis: Rv (**54**)= 6 ml, Rv (**56**)= 20 ml

¹H-NMR for (**54**) (360 MHz, MeOD): δ= 7.72 (m, 4H aromatic), 7.39 (m, 4H aromatic), 5.27 (s, aliphatic-H).

¹³C-NMR for (**54**) (90.56 MHz, MeOD): δ= 142.2, 140.4, 131.2, 129.1, 126.0, 121.6 (aromatic carbons), 55.2 (aliphatic carbon)

¹H-NMR for (**56**) (250 MHz, MeOD): δ= 7.65, 7.27 (m, 16H aromatic), 5.12 (s, 2H aliphatic).

¹³C-NMR for (**56**) (62.90 MHz, MeOD): δ= 139.8, 128.6, 127.6, 124.8, 120.2 (aromatic-carbon), 57.3, 56.4 (aliphatic carbons).

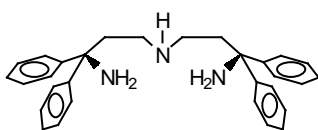
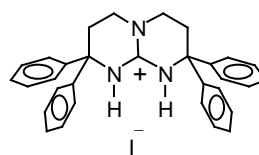
1,3-Bis-(9H-fluoren-9-yl)-2-methyl-isothiourea- iodide 57**57**

100 mg (0.25 mmol) of **56** were suspended in 5 ml dry CH₃CN and heated to 80°C, when 8 eq (2 mmol, 125 µl) of CH₃I were added. After 1-2 hours at 80°C the reaction was completed and the product was crystallized from the reaction mixture after cooling. 123 mg (0.225 mmol, 90%) of **57** were obtained.

57: C₂₈H₂₃N₂IS (MW 546.46)

HPLC1 analysis: R_v = 14.4 ml

¹³C-NMR for (**57**) (90.56 MHz, MeOD): δ= 142.4, 142.1, 130.9, 129.3, 126.0, 121.7 (aromatic carbons), 60.51, 60.3 (aliphatic carbons), 15.75 (CH₃).

2H-Pyrimido[1,2-a]pyrimidine,1,3,4,6,7,8-hexahydro-2,2,8,8-tetraphenyl- iodide 70**68****70**

673 mg (1.55 mmol) of **68** [114] were dissolved in 10 ml of dry CH₃CN (dried over Al₂O₃ activity-I) and heated to 85°C. A solution of 364 mg (2 mmol) thiocarbonyldiimidazole in 4 ml of dry CH₃CN was then added. The reaction was kept at 85°C for 4 h. When the reaction was cooled to RT, 170 µl (2.68 mmol) of CH₃I were added. A precipitate appeared, the mixture was stirred for another 16 hours at

RT. The precipitate, was identified as product **70**, and was filtered and crystallized from nitromethane (CH₃NO₂) yielding 700 mg (1.24 mmol), 80% yield.

70: C₃₁H₃₀N₃I (MW 571.5)

mp.(**70**): 340°C

MS ESI: 444.4 (100% M⁺).

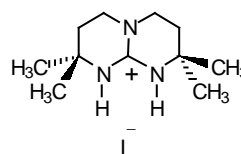
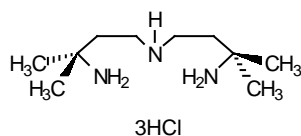
HPLC2 analysis: R_V(**70**)= 13.9 ml.

¹³C-NMR for (**70**) (62.9 MHz; DMSO-d₆): δ= 162.1 (the guanidinium carbon), 143.6, 129.0, 127.9, 126.0 (phenyl carbons), 60.6, 44.0, 31.2 (aliphatic carbons).

¹³C-NMR for (**70**) (62.9 MHz; MeOD): δ= 162.0 (the guanidinium carbon), 144.7, 130.1, 129.2, 127.3 (phenyl carbons), 62.6, 45.6, 33.2 (aliphatic carbons).

¹H-NMR for (**70**) (250 MHz; MeOD): δ= 7.36-7.26 (m, 20H aromatic), 3.08, 2.70 (8H aliphatic).

2H-Pyrimido[1,2-a]pyrimidine,1,3,4,6,7,8-hexahydro-2,2,8,8-tetramethyl-iodide 71



30 g of Dowex resin (2×8 50-100 mesh, OH⁻-form) in H₂O were poured into a column and washed with more distilled water to pH=7, then washing was continued with MeOH in order to replace all the water.

1 g (3.5 mmol) of the white triammonium salt **67** were dissolved in 3-5 ml of MeOH, poured into the column and kept for 15min to allow counter ion exchange, then washed again with MeOH to collect the compound. The solution was evaporated and the oily compound **69** of the free base (600 mg) was kept under N₂ gas to avoid uptake of atmospheric CO₂.

600 mg (3.4 mmol) of **69** were dissolved in 12 ml of dry CH₃CN, the mixture was heated to 85°C, then a solution of 917 mg (5.1 mmol) of thiocarbonyldiimidazole in 5 ml of dry CH₃CN was added. The reaction mixture was kept stirring at 85°C over

night, the reaction was cooled to RT and 300 μl of CH_3I were added. After another night at RT, the solvent was removed and 6 ml of CHCl_3 were added to the crude product. Extraction with water was necessary, in order to remove most of the undesired products to the water phase (the extraction was repeated 3-4 times). The organic phase was dried over MgSO_4 , filtered and evaporated to obtain 70% 768 mg (2.38 mmol, 70%) of product **71**. Which could be recrystallized from $\text{MeOH}/\text{H}_2\text{O}$.

71: $\text{C}_{11}\text{H}_{22}\text{N}_3\text{I}$ (MW 323)

mp: 185°C (lit). 183°C

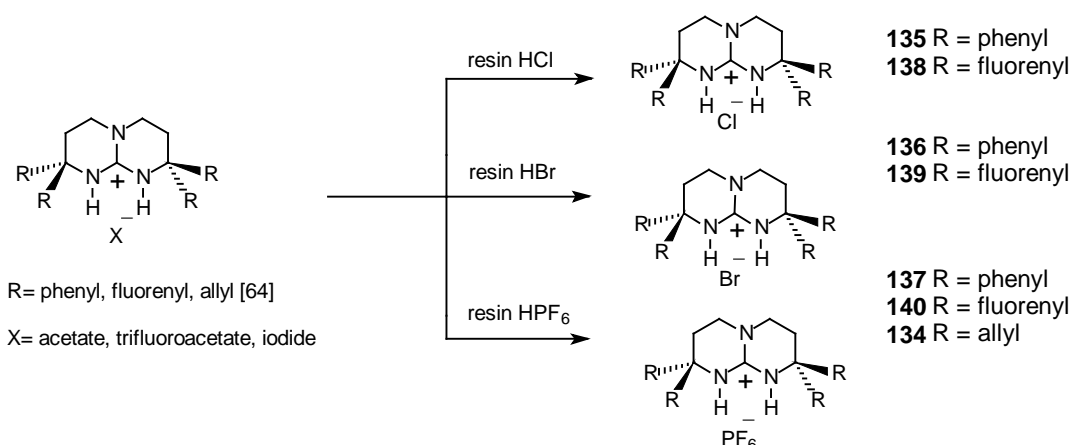
HPLC3 analysis: R_V (**69**) = 3 ml; R_V (**71**) = 11.8 ml.

^{13}C -NMR of (**71**) (90.5 MHz; MeOD): δ = 151.0 (guanidinium carbon) 50.1 ($2 \times \text{C}(\text{CH}_3)_2$), 44.9, 33.9 (aliphatic-carbons), 28.5 ($4 \times \text{CH}_3$).

^1H -NMR of (**71**) (360 MHz; MeOD): δ = 3.37 (t, J = 6.6 Hz, 4H aliphatic), 1.81 (t, J = 6.6 Hz, aliphatic-H), 1.23 (s, $4 \times \text{CH}_3$).

A general method for counter anion exchange for different guanidinium compounds.

To exchange the counter anions of the different guanidinium compounds to the halogen counter anions (scheme 25), we used an anion exchange resin, acryl matrix AG 4X4, 100-200 mesh, free base form.



Scheme 25

3 g of the anion exchange resin in a column were washed with distilled water, then 5-10 ml of an acid (6N HCl, 6N HBr, TFA, acetic acid or hexafluorophosphoric acid which was dissolved in 1:1 water/acetonitrile), were poured slowly into the column till

Table 10. The recrystallization conditions of different guanidinium compounds

compound's number	crystallized from
135	CH ₃ NO ₂ or CH ₃ CN
136	CH ₃ NO ₂ or CH ₃ CN
137	CH ₃ CN/toluene
134	MeOH/H ₂ O
138	MeOH/toluene or CH ₃ CN
139	MeOH/toluene or CH ₃ CN
140	MeOH/toluene or CH ₃ CN

the resin was saturated with the required acid, and was converted to the tertiary ammonium salt. This was confirmed by pH test, of the column efficient. The column then was washed with distilled water to remove all the excess of the acid till pH = 7. The resin was washed with MeOH in order to replace all the water solvent, due to the poor solubility of the guanidinium compounds in water.

100 mg of the guanidinium compound were dissolved in 3-4 ml of MeOH. The solution was poured into through the column till it hardly covered the top of the resin. After 5-10min the resin was washed with more MeOH in order to collect the guanidinium compound with its new counter anion. The solvent was evaporated and the compound was recrystallized as it is shown in table 10

A preparation of Fluoreneguanidinium iodide from Fluorenylguanidinium acetate.

A column of 1.0 g of anion exchange resin AG 4×4, acetate form, was converted into the iodide form by passing 30 ml of a 0.5 M solution of KI in water slowly through it. The column was washed with distilled water until a test with AgNO₃/HNO₃ for soluble iodide in the effluent was negative. Then 30 mg of fluorenylidenguanidinium acetate **48** were dissolved in 1-2 ml of MeOH, the mixture was poured into the column, and kept for 10-20 min to allow counter anion exchange, then washed with more

MeOH to collect the compound. The solvent was evaporated and the fluorenylidenguanidinium iodide was crystallized from MeOH/Toluene.

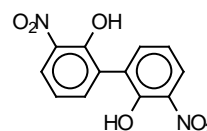
2,2'-dihydroxy 3,3'-dinitro 1,1'-biphenyl **85**

reference: [94]

85: C₁₂H₈N₂O₆ (MW 276.2)

mp: 180°C

HPLC6 analysis: R_v = 8.5 ml



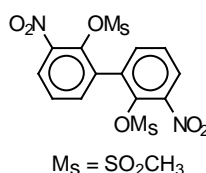
85

MS- ESI: m/z = 275.5 [100%, (M-H)⁻]

¹H-NMR (360 MHz, CDCl₃): δ= 10.98 (s, OH), 8.21 (d, J= 8.2 Hz, 2H), 7.63 (d, J= 7.0 Hz, 2H), 7.10 (t, J= 7.6 Hz, 2H).

¹³C-NMR (90.56 MHz, CDCl₃): δ= 153.0 (C-OH), 139.1 (CH), 134.1 (C-NO₂), 127.3 (quaternary C), 125.4, 119.6 (aromatic carbons).

2,2'-methanesulfonyloxy 3,3'-dinitro 1,1'-biphenyl **86**



86

500 mg (1.81 mmol) of 2,2'-dihydroxy-3,3'-dinitrobiphenyl **85** were dissolved in 40 ml of dry CH₂Cl₂. The yellow solution was stirred at 0°C-5°C under nitrogen, when 630 μl (4.52mmol) of triethyl amine were added and the resulting orange color of the mixture became again yellow after the dropwise addition of 350 μl (4.52 mmol) of mesylchloride. A precipitate of Et₃NHCl appeared immediatly. After 1.5 h stirring at 5°C followed by 15 min at room temperature, the reaction mixture was extracted with aqueous acetic acid followed by another extraction with 5% NaHCO₃. The organic

phase was dried with MgSO_4 and evaporated to obtain a yellow product **86** which was recrystallized from acetonitrile to yield 570 mg (1.31 mmol), 73%.

86: $\text{C}_{14}\text{H}_{12}\text{N}_2\text{O}_{10}\text{S}_2$ (MW 432)

mp: 218°C

HPLC6 analysis: $R_v = 5\text{ml}$

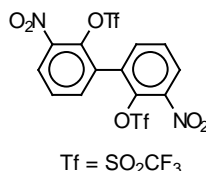
MS-ESI: $m/z = 433.5$ [100% $(\text{M}+\text{H})^+$]

$^1\text{H-NMR}$ (250.13, acetone d_6): $\delta = 8.22$ (d, $J = 7.9$ Hz, 2H), 7.97 (d, $J = 7.3$ Hz, 2H), 7.75 (t, $J = 7.9$ Hz, 2H), 3.07 (s, $2 \times \text{CH}_3$).

$^1\text{H-NMR}$ (250.13, CD_3CN): $\delta = 8.13$ (d, $J = 7.7$ Hz, 2H), 7.86 (d, $J = 7.3$ Hz, 2H), 7.66 (t, $J = 8.1$ Hz, 2H), 2.91 (s, $2 \times \text{CH}_3$).

$^{13}\text{C-NMR}$ (62.90, CD_3CN): $\delta = 145.2$ (C-OMs), 139.5 (C- NO_2), 138.4 (CH), 133.5 (quaternary C), 129.3 (CH), 127.9 (CH), 39.8 ($2 \times \text{CH}_3$).

2,2'-Trifluoromethanesulfonyloxy 3,3'-dinitro 1,1'-biphenyl **97**



97

400 mg (1.44 mmol) of 2,2'-dihydroxy 3,3'-dinitro biphenyl **85** were added to 10 ml dry pyridine at 0°C, the mixture was stirred under nitrogen when 855 μl (5.18 mmol) of (Tf_2O) trifluoromethanesulfonic anhydride were added dropwise. After 3 h at 0°C, the ice bath and nitrogen were removed and the pyridine solvent was evaporated in *vacuo*, the residue was extracted with $\text{CH}_2\text{Cl}_2/\text{H}_2\text{O}$ for 3-4 times. The organic phase was dried with MgSO_4 , filtered and evaporated to obtain a yellow-brown product. Recrystallization from acetonitrile yielded 659 mg (1.22 mmol, 85%).

97: $\text{C}_{14}\text{H}_6\text{F}_6\text{N}_2\text{O}_{10}\text{S}_2$ (MW 540)

mp: 130-132°C

HPLC6 analysis: $R_v = 11.0$ ml

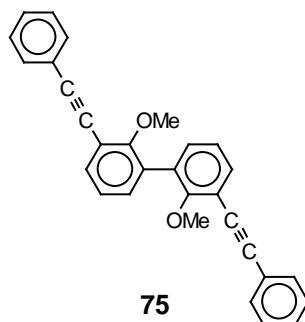
MS-ESI: $m/z = 541.3$ [100% (M+H)⁺]

¹H-NMR (250.13 MHz, CDCl₃): $\delta = 8.25$ (d, $J = 7.3$ Hz, 2H), 7.76 (d, $J = 13.1$ Hz, 2H), 7.77 (t, $J = 11.6$ Hz, 2H).

¹³C-NMR (62.90 MHz, CDCl₃): $\delta = 143.0$ (C-OTf), 138.3 (C-NO₂), 137.3 (CH), 131.3 (quaternary C), 129.4 (CH), 127.8 (CH), 117.9 (d, $J = 320.9$ Hz, 2×CF₃).

¹⁹F-NMR (235.34, CDCl₃) $\delta = 88.4$

2,2'-Dimethoxy-3,3'-bis-phenylethynyl-1,1'-biphenyl 75



A degassed solution of 73.7 mg (0.1 mMol) of [PdCl₂(PPh₃)₂] and 20 mg CuI in 5 ml of dry THF was added to a degassed solution of 1.0 g (2.1 mMol) of 2,2'-Dimethoxy-3,3'-diiodo-1,1'-biphenyl [89] in 18 ml dry THF, 30 ml of dry (i-Pr)₂NH and 1 ml (11.1 mMol) of phenylacetylene at 40°C. The mixture was stirred under N₂ at 40C for 4 h. 20 ml of sat. aqueous NaCl solution and 40 ml of CH₂Cl₂ were added, the phases were separated, and the aqueous phase was extracted with CH₂Cl₂ (30 ml). The combined organic phases were dried (Na₂SO₄) and concentrated. Column chromatography (CC) (SiO₂ 230-400 mesh; hexane/AcOEt 6:1 containing 0.5% Et₃N), followed by recrystallization from hexane yielded 738 mg (1.78 mmol, 85%) of product **75**.

75: C₃₀H₂₂O₂ (MW 414)

mp: 77°C

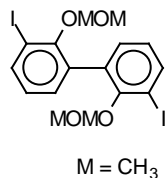
HPLC5 analysis: R_v = 17.0 ml

MS (GC-MS, EI): $m/z = 413.9$ (100%)

¹H-NMR (250.13, CDCl₃): $\delta = 7.55$ -7.16 (m, 16H), 3.79 (s, -OCH₃)

^{13}C -NMR (62.90, CDCl_3): δ = 158.8, 133.2, 131.9, 131.7, 131.5, 128.3, 123.4, 123.4, 123.3, 117.2 (aromatic carbons), 93.7, 86.0 ($-\text{C}\equiv\text{C}-$), 61.1 ($-\text{OCH}_3$).

3,3'-Diiodo-2,2'-bis-methoxymethoxy-1,1'-biphenyl 79



79

1.0 g (25 mMol) of NaH (60% dispersion) were washed with 10 ml of dry THF. To the NaH stirred under nitrogen in 60 ml dry THF was added in portions 1.0 g (2.28 mMol) of 3,3'-diiodo-2,2'-dihydroxy-1,1'-biphenyl **72** [90]. After H_2 evolution stopped, 2.4 ml (30mmol) of chlorodimethylether ($\text{ClCH}_2\text{OCH}_3$) was added to the stirred precipitate, and the resulting mixture was stirred for 3 h. 20 ml of H_2O were added slowly and the mixture was shaken with 30 ml of CH_2Cl_2 . The aqueous layer was extracted with CH_2Cl_2 (2x15 ml), and the combined organic layers were washed with saturated KHCO_3 solution. The organic layer was dried (MgSO_4) and evaporated. Crystallization from petroleum ether yielded 1.17 g (2.22 mmol, 92%) crystals of product **79**.

79: $\text{C}_{16}\text{H}_{16}\text{O}_4\text{I}_2$ (MW 526)

mp:102°C

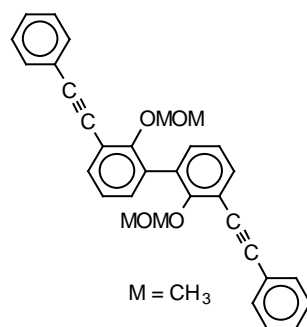
HPLC5 analysis: $R_v = 12.0$ ml

MS (GC-MS, EI): $m/z = 525.8$ (4%, M^+), 449.8 (100%, $\text{M}-\text{C}_3\text{H}_8\text{O}_2^+$)

^1H -NMR (250.13, CDCl_3): δ = 7.82 (d, $J = 7.6$ Hz, 2H), 7.34 (d, $J = 7.3$ Hz, 2H), 6.91 (t, $J = 7.6$ Hz, 2H), 4.79 (s, 2x- OCH_2^-), 3.02 (s, 2x- OCH_3).

^{13}C -NMR (62.90, CDCl_3): δ = 154.6, 139.2, 133.3, 132.1, 125.7 (aromatic carbons), 99.5 (OCH_2^-), 92.8, 57.1 (OCH_3).

2,2'-Bis-methoxymethoxy-3,3'-bis(phenylethynyl)-1,1'-biphenyl 80



80

A degassed solution of 38 mg (0.05 mMol) of [PdCl₂(PPh₃)₂] and 10 mg (0.05 mMol) of CuI in 3 ml of dry THF was added to a degassed solution of 600 mg (1.07 mMol) of 2,2'-bis-methoxymethoxy-3,3'-diiodo-1,1'-biphenyl **79** in 15 ml dry THF, 20 ml of dry (i-Pr)₂NH and 520 μl (4.7 mMol) of phenylacetylene **74** at 40°C. The mixture was stirred under N₂ at 40°C for 6 h. 15 ml of sat. aqueous NaCl solution and 20 ml of CH₂Cl₂ were added, the phases were separated, and the aqueous phase was extracted with CH₂Cl₂ (15 ml). The combined organic phases were dried (Na₂SO₄) and concentrated. Column chromatography (CC) (SiO₂ 230-400 mesh; hexane/AcOEt 6:1 containing 0.5% Et₃N) to the crude product **80**, followed by recrystallization from hexane yielded 487 mg (90%) of pure product **80**.

80: C₃₂H₂₆O₄ (MW 474)

mp: 123°C

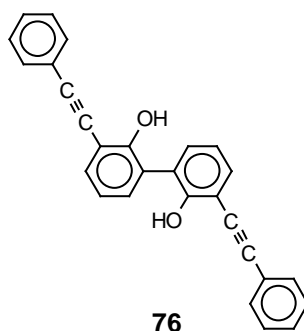
HPLC5 analysis: R_v = 18 ml

MS (GC-MS, EI): *m/z* = 473.9 (38%, M⁺), 398 (100%, M⁺-C₃H₈O₂).

¹H-NMR (250.13, CDCl₃): δ = 7.53 (m, 6H), 7.37 (d, *J* = 7.5 Hz, 2H), 7.35 (m, 8H), 7.18 (t, *J* = 7.5 Hz, 2H), 5.08 (s, -OCH₂-), 3.03 (s, -OCH₃)

¹³C-NMR (62.90, CDCl₃): δ = 156.1, 133.1, 132.8, 132.0, 131.5, 128.4, 123.8, 123.2, 117.7 (aromatic carbons), 99.2 (-OCH₂-), 93.6, 86.0 (-C≡C-), 56.7 (-OCH₃).

2,2'-Dihydroxy-3,3'-bis(-phenylethynyl)-1,1'-biphenyl 76



To 200 mg (0.4 mmol) of **80** in 140 ml THF, 328 μ l of conc. HCl (37%) in 120 ml MeOH were added, and the solution was stirred for 12 h under N₂ at room temp. 200 ml of H₂O and 200 ml of CH₂Cl₂ were added, the aq. phase was extracted with 100 ml of CH₂Cl₂, the combined organic phases were dried (Na₂SO₄), and evaporated to give 80% 125 mg (0.32 mmol) yield of oily product **76**.

76: C₂₈H₁₈O₂ (MW 386)

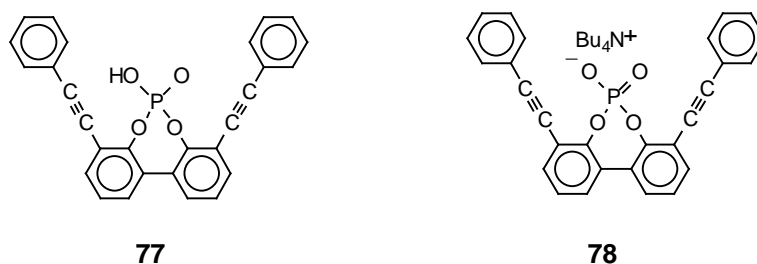
HPLC5 analysis: R_v = 13.0 ml

MS (GC-MS, EI): *m/z* = 386 (100%, M).

¹H-NMR (250.13, CDCl₃): δ = 7.51-7.45 (m, 6H), 7.31-7.26 (m, 8H), 6.97 (t, *J*= 7.32 Hz, 2H), 6.28 (br s, 2H).

¹³C-NMR (62.9 MHz, CDCl₃): δ = 153.5 (-COH, biphenyl), 132.1 (-CH, biphenyl), 131.7 (-CH, biphenyl), 131.5 (aromatic carbon), 128.6 (-CH, biphenyl), 128.3 (Ar), 124.1 (quat. C, biphenyl), 122.4 (-C-C \equiv C, biphenyl), 120.6 (Ar), 110.7 (-C \equiv C-C, Ar), 95.8 (-C \equiv C-), 83.6 (-C \equiv C-).

3,3'-Bis-phenylethynyl-1,1'-biphenyl-2,2'-diylphosphonic acid tetrabutyl ammonium salt 78



To 100 mg (0.24 mMol) of **76** in 35 ml dry CH₂Cl₂, 50 μl (0.54 mMol) of POCl₃ and 105 μl (0.74 mMol) of Et₃N were added at RT under N₂, and the solution was stirred for 5 h. After evaporation in *vacuo*, 30 ml THF/H₂O 1:1 were added, and the mixture was stirred for 12 h at RT. 50 ml of CH₂Cl₂ and 30 ml of H₂O were added, the separated organic phase was washed with H₂O (2x30 ml), dried (Na₂SO₄), and concentrated to give the free acid **77**. Column chromatography (SiO₂; CH₂Cl₂/Et₃N 98:3) to **77**, followed by ion-exchange chromatography (*Dowex 50WX8*, Bu₄N⁺; CH₂Cl₂/CH₃CN 1:1), provided an oily product **78**, 99 mg (60%). The oily product was dried in high *vacuum*, then crystallized from dry CH₂Cl₂/dry ether.

78: C₄₄H₅₂NO₄P (MW 689)

77: C₂₈H₁₇O₄P (MW 448)

mp: (**78**) 88-90°C

HPLC5 analysis: R_v = 9.0 ml

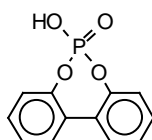
MS (GC-MS, EI): *m/z* = 447.8 (100%)

¹H-NMR of **78** (360 MHz, CDCl₃): δ = 7.60 (m, 4H), 7.51 (d, *J* = 7.3 Hz, 2H), 7.36 (d, *J* = 7.6 Hz, 2H), 7.26 (m, 6H), 7.12 (t, *J* = 7.6 Hz, 2H), 2.9 (m, 8H), 1.3 (m, 8H), 1.13 (m, 8H), 0.7 (t, *J* = 6.7, 12H).

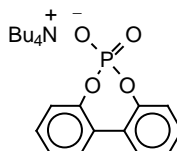
¹³C-NMR of **78** (90.56 MHz, CDCl₃): δ = 151.2 (*J*_{PC} = 9.0 Hz), 132.6, 131.9, 130.3, 129.2, 128.1, 128.0, 123.7, 123.6, 117.7 (*J*_{PC} = 3.8 Hz), 93.3, 86.2, 58.2, 23.7, 19.4, 13.5.

³¹P-NMR (101.25 MHz, CDCl₃): -3.50.

1,1'-Biphenyl -2,2'-diylphosphoric acid tetrabutyl ammonium salt 84



83



84

1.0 g (5.37 mmol) of 2,2'-dihydroxy 1,1'-biphenyl **81** were mixed with 492 μ l (5.37 mmol) of POCl₃ and 125 μ l of DMF. The reaction mixture was heated at 117°C for 5 h then at 135°C for overnight. The mixture was cooled to room temperature and 5 ml of acetic acid were added. An immediate precipitate product appeared but it was collected only after one hour and was recrystallized over night from MeOH/CH₃CN or immediately from CHCl₃/ether to give the clean free acid **83**. The free acid was subjected to cation-exchange chromatography (*Dowex 50WX8*, Bu₄N⁺ form; MeOH), to provide an oily-solid product **84** which was recrystallized from CHCl₃/ether to give a white precipitate (like needles) in 1.83 g (3.76 mmol, 70%).

83: C₁₂H₉PO₄ (MW 248)

mp: **83** 175°C

MS ESI: m/z = 249.1 [100% (M+H)⁺]

HPLC4 analysis: R_v = 5.0 ml

¹H-NMR of **83** (250.13, MeOD): δ = 7.46 (d, J = 7.0 Hz, 2H), 7.33-7.24 (m, 4H), 7.14 (d, J = 7.3 Hz, 2H).

¹³C-NMR of **83** (62.9 MHz, MeOD): δ = 149.6 (d, J = 9.1 Hz, COP), 131.1 (CH), 130.93 (CH), 130.0, 127.4 (d, J = 1.9 Hz, CH), 122.4 (d, J = 4.3 Hz, CH).

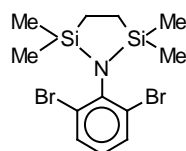
³¹P-NMR of **83** (101.25 MHz, MeOD): 0.32

¹H-NMR of **84** (360.13, CDCl₃): δ= 7.43 (d, *J*= 7.3 Hz, 2H), 7.28-7.20 (m, 4H), 7.15 (t, *J*= 7.3 Hz, 2H), 3.16 (m, 8H), 1.50 (m, 8H), 1.31 (m, 8H), 0.91 (t, *J*= 7.0 Hz, 4CH₃).

¹³C-NMR of **84** (62.9 MHz, MeOD): δ= 151.2 (d, *J*= 9.2 Hz, COP), 130.43 (quaternary carbon), 128.85 (CH), 128.78 (CH), 123.62 (CH), 122.1 (d, *J*= 4.3 Hz, CH), 58.51 (4CH₂), 23.91 (4CH₂), 19.58(4CH₂), 13.60 (4CH₃).

³¹P-NMR of **84** (101.25 MHz, MeOD): -1.04

1-(2,6-Dibromophenyl)-2,2,5,5-tetramethyl-2,5-disila pyrrolidine **104**



104

A solution of 5.0 g (20 mmol) of dibromoaniline **101** in 40 ml dry THF was stirred at 0°C under nitrogen atmosphere. 14 ml (40 mmol) of MeMgCl **102** were added dropwise. The mixture was warmed to room temperature and a solution of 4.3 g (20 mmol) 1,2-bis(chlorodimethylsilyl)ethane (stabase) **103** in 15 ml dry THF was added. The yellow-brown mixture was warmed to 50°C for 2 h, then at 38°C for overnight. The THF was evaporated and the mixture was extracted between water/hexane, the organic phase was concentrated and chromatographed on Silica gel 60 (230-400 mesh) with hexane to yield 51%, 4.0 g (10.2 mmol) of the desired product **104**.

104: C₁₂H₁₉NSi₂Br₂ (MW 393)

mp: 40°C

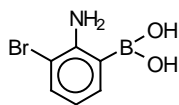
MS (GC-MS, EI): *m/z* =378 (100% M-CH₃)

HPLC5 analysis: R_v = 18 ml

¹H-NMR (250.13, CDCl₃): δ= 7.53 (d, *J*= 7.9 Hz, 2H), 6.74 (t, *J*= 7.9 Hz, 1H), 0.96 (s, 4H, 2SiCH₂), 0.19 (s, 12H, 2Si(CH₃)₂).

¹³C-NMR (62.9 MHz, CDCl₃): δ= 144.3 (C-N-), 132.8 (2×CH), 126.6 (2×CBr), 125.5 (CH), 8.7 (2×CH₂), 1.4 (4×CH₃).

6-Bromo aniline- 2-boronic acid **113**



113

A solution of 1.0 g (3.98 mmol) of 2,6-dibromoaniline **101** in 15 ml of dry THF was stirring at -78°C under N_2 . 7.4 ml of *n*BuLi (1.6 M in hexane, 11.95 mmol) were added. After stirring at this temperature for one hour, this was followed by addition of 1.3 ml trimethyl borate **112**, and stirring was continued at -78°C for another hour, then at room temperature for 2 hours, 5 ml of 3N HCl were poured into the reaction mixture. 1.5 hours later the mixture was extracted with chloroform. Side products accompanied the desired one in the extract. The crude product was dissolved in a minimum amount of MeOH and separated using a preparative reverse phase column (nucleosil C-8, $30\mu\text{m}$). The product was eluted with 42% MeOH/0.1% TFA at 254 nm, 4 ml/min to give 515 mg (2.38 mmol, 60%) of **113**.

113: $\text{C}_6\text{H}_7\text{BBrNO}_2$ (MW 215.7)

mp: 110°C

MS ESI: 215.1 [24% $(\text{M}+\text{H})^+$, $(\text{C}_6\text{H}_7^{10}\text{B}^{79}\text{BrNO}_2+\text{H})^+$], 216.1 (96% $[(\text{M}+\text{H})^+$, $(\text{C}_6\text{H}_7^{11}\text{B}^{79}\text{BrNO}_2+\text{H})^+$], 217 [32% $(\text{M}+\text{H})^+$, $(\text{C}_6\text{H}_7^{10}\text{B}^{81}\text{BrNO}_2+\text{H})^+$], 218.0 [92% $(\text{M}+\text{H})^+$, $(\text{C}_6\text{H}_7^{11}\text{B}^{81}\text{BrNO}_2+\text{H})^+$].

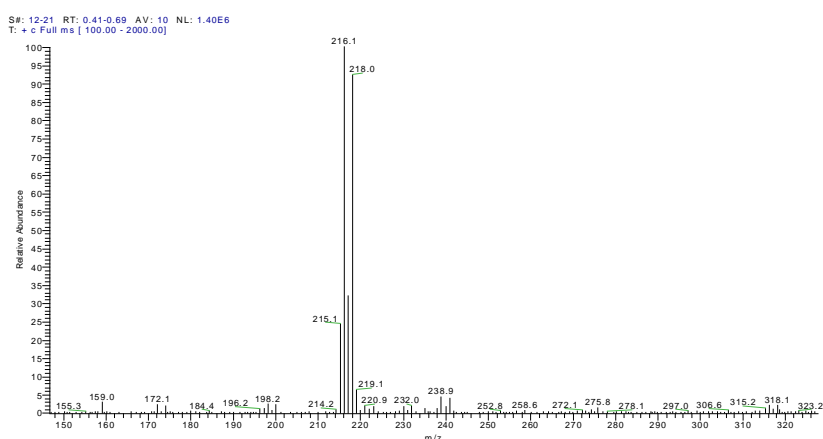


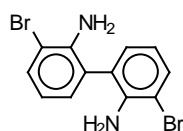
Figure 19. ESI-MS of **113**

HPLC5 analysis: $R_v = 6.0$ ml

$^1\text{H-NMR}$ (360 MHz, MeOD): δ = 7.79 (d, J = 7.0 Hz, 1H), 7.70 (d, J = 7.7 Hz, 1H), 7.14 (t, J = 7.5 Hz, 1H).

$^{13}\text{C-NMR}$ (90.56 MHz, MeOD): δ = 162.2 (d, J = 35.7 Hz, C-B(OH)₂), 140.2 (C-NH₂), 136.8 (CH), 136.4 (CH), 127.5 (CH), 116.6 (C-Br).

3,3'-Dibromo-2,2'-diamino-1,1'-biphenyl **106**



106

A solution of 800 mg (3.7 mmol) of 6-bromo aniline 2- boronic acid **113** in 5-10 ml EtOH, 14 ml 2M Na₂CO₃ and 428 mg (10 mol%) (PPh₃)₄Pd was added to 2.78 g (11.0 mmol) of 2,6-dibromoaniline **101** in 70 ml benzene. After the resulting mixture was purged with nitrogen, it was gently refluxed for 24 h with stirring under nitrogen. After cooling, the organic layer was separated, and the aqueous solution was extracted with benzene. The combined organic layers were dried with MgSO₄ and evaporated, and the residue was chromatographed on preparative reverse phase column (nucleosil C-8, 30 μm) with 66% MeOH / 0.1% TFA eluent, 4ml/min at 254 nm) to obtain the product **106** which was well recrystallized from MeOH in 835 mg (2.44 mmol, 66%).

106: C₁₂H₁₀N₂Br₂ (MW 342)

mp: 105°C

MS ESI: 341 [41% (M+H)⁺ (C₁₂H₁₀⁷⁹Br⁷⁹BrN₂ +H)⁺], 343 [80% (M+H)⁺ (C₁₂H₁₀⁷⁹Br⁸¹BrN₂ +H)⁺], 345 [41% (M+H)⁺ (C₁₂H₁₀⁸¹Br⁸¹BrN₂ +H)⁺].

HPLC5 analysis: R_v = 8 ml

$^1\text{H-NMR}$ (360 MHz, MeOD): δ = 7.43 (d, J = 7.6 Hz, 2H), 7.0 (d, J = 7.0 Hz, 2H), 6.67 (t, J = 7.5 Hz, 2H).

$^{13}\text{C-NMR}$ (90.56 MHz, MeOD): δ = 143.7 (C-NH₂), 133.5 (CH), 131.2 (CH), 126.6 (quaternary), 119.9 (CH), 110.7 (C-Br).

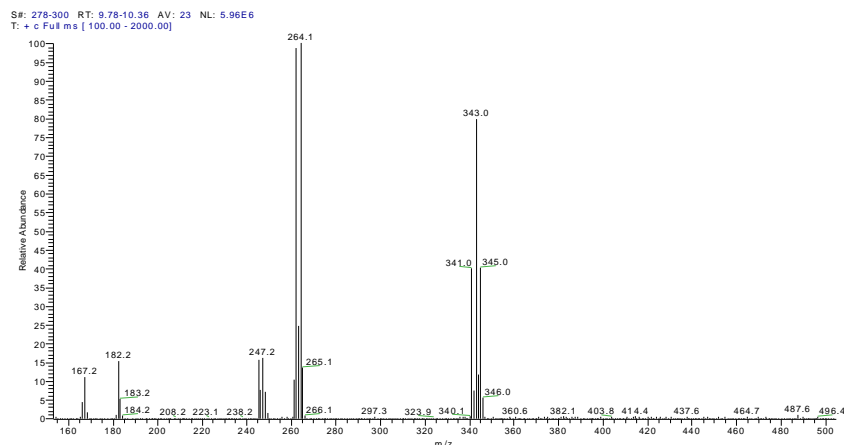
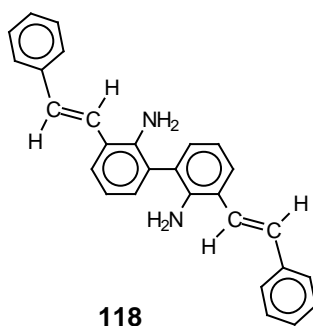


Figure 20. ESI-MS of **106**

3,3'-Di- β -styryl-2,2'-diamino 1,1'-biphenyl 118



600 mg (1.75 mmol) of 3,3'-dibromo-2,2'-diamino-1,1'-biphenyl **106** and 12 mol% (0.21 mmol, 243 mg) of Pd(PPh₃)₄ were dissolved in 15 ml benzene. A solution of 3 equiv (5.52 mmol, 777 mg) of trans-phenylvinyl boronic acid **117** in 10 ml ethanol and 6 equiv. of 7 ml 2M Na₂CO₃ solution were added to the reaction mixture. The reaction mixture was flushed with nitrogen, then refluxed for 24 h at 75°C. The desired product precipitated from the mixture while refluxing. The product was collected, washed with MeOH several times, then dissolved in CHCl₃ and extracted with water. The organic phase was dried over Na₂SO₄, filtered and evaporated to yield 680 mg (1.75 mmol, 70%) of product.

118: C₂₈H₂₄N₂ (MW 388.5)

mp: 220°C-223°C

MS ESI: $m/z = 389$ (100% (M+H)⁺).

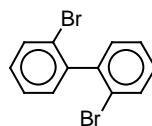
HPLC5 analysis: Rv = 10.0 ml

$^1\text{H-NMR}$ (250.13 MHz, CDCl_3): δ = 7.53-6.85 (m, 20H of aromatic and vinyl groups), 3.86 (s, 4H, $2\times\text{NH}_2$).

$^{13}\text{C-NMR}$ (62.9 MHz, CDCl_3): δ = 142.0, 137.6, 131.0, 130.4, 128.7, 127.7, 126.5, 125.0, 124.5, 124.3, 119.0.

2,2'-Dibromo-1,1'-biphenyl 126

Reference [100]



126: $\text{C}_{12}\text{H}_8\text{Br}_2$ (MW 312)

126

mp: 73°C

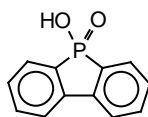
MS (GC-MS, EI): m/z = 312 [57% $\text{C}_{12}\text{H}_8^{79}\text{Br}^{81}\text{Br}$], 231[74% ($\text{C}_{12}\text{H}_8^{79}\text{Br}$) $^-$], 233 [71% ($\text{C}_{12}\text{H}_8^{81}\text{Br}$) $^-$], 152 [100% ($\text{M}-2\text{Br}$) $^{2-}$].

HPLC3 analysis: Rv = 14 ml

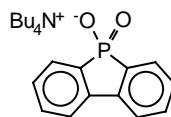
$^1\text{H-NMR}$ (360 MHz, CDCl_3): δ = 7.65 (d, J = 7.7 Hz, 2H), 7.38-7.34 (m, 2H), 7.26-7.22 (m, 4H).

$^{13}\text{C-NMR}$ (62.9 MHz, CDCl_3): δ = 142.0 (C-Br), 132.5 (CH), 130.9 (CH), 129.3 (CH), 127.1 (CH), 123.5 (quaternary C).

1,1'-biphenyl- 2,2'-phosphinic acid tetrabutyl ammonium salt 128



127



128

A solution of 1.0 g (3.2 mmol) of the dibromide **126** in 60 ml of dry THF was cooled to -78°C under nitrogen. 4 ml (6.4mmol) of n-BuLi (1.6 M in hexane) were added with cooling, after 3 h at -78°C, followed by 279 μl (3.2 mmol) of phosphorus

trichloride. After 2.5 h more, still at -78°C , 3 ml of water were added dropwise (which yielded an inhomogenous mixture for 2-3 h only) and the nitrogen cover and cooling were discontinued. Next day the clear pale yellow solution was evaporated and the residue was suspended in 45 ml acetone and warmed to 40°C , the mixture was treated dropwise during 10 min with 8 ml (30%) hydrogen peroxide then boiled gently (reflux) for 4 h, with the addition of more 4 ml H_2O_2 after 1 h. 70 ml of water were added and the reaction mixture was extracted with CHCl_3 , most of the undesired products remain in the organic phase, the aqueous phase was evaporated and the free base product **127** was recrystallized by $\text{MeOH}/\text{CHCl}_3$ to yield 483.8 mg (2.24 mmol) around 70% product. The phosphinic acid **127** was converted to the TBA-phosphinate salt **128** through ion-exchange chromatography (*Dowex 50WX8*, Bu_4N^+ ; $\text{MeOH}/\text{CH}_3\text{CN}$ 1:1) The oily salt **128** was crystallized by MeOH/water to obtain 872 mg (1.9 mmol, 85%) of a pure product **128**.

127: $\text{C}_{12}\text{H}_9\text{PO}_2$ (MW 216)

mp (**127**): 210°C

MS ESI: $m/z = 215.3$ (100% $(\text{M}-\text{H})^-$).

HPLC4 analysis: $R_v = 5$ ml

^1H -NMR of **127** (250.13 MHz, MeOD): $\delta = 7.67$ (m, 2H), 7.50 (t, $J = 8.2$ Hz, 2H), 7.39 (t, $J = 7.3$ Hz, 2H), 7.23 (m, 2H).

^{13}C -NMR of **127** (62.9 MHz, MeOD): $\delta = 141.2$ (d, $J = 28.1$ Hz, quaternary C), 134.4 (d, $J = 1.9$ Hz, CH), 131.7 (d, $J = 137.3$ Hz, CP), 130.5 (d, $J = 11.9$ Hz, CH), 128.7 (d, $J = 8.6$ Hz, CH), 122.3 (d, $J = 11.9$ Hz, CH).

^{31}P -NMR of **127** (101.25 MHz, MeOD): 37.47

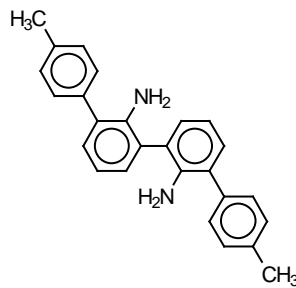
^1H -NMR of **128** (250.13 MHz, MeOD): $\delta = 7.60$ (d, $J = 7.5$ Hz, 2H), 7.46 (t, $J = 7.5$, 2H), 7.24-7.21 (m, 2H), 7.14 (d, $J = 4.9$ Hz, 2H), 2.95 (m, 8H), 1.38 (m, 8H), 1.19-1.11 (m, 8H), 0.77 (t, $J = 71$ Hz, 2H).

^{13}C -NMR of **128** (62.9 MHz, MeOD): $\delta = 140.3$ (d, $J = 25.27$ Hz, quaternary C), 137.9 (d, $J = 132.6$ Hz, CP), 131.8 (d, $J = 1.9$ Hz, CH), 129.4 (d, $J = 10.5$ Hz, CH), 127.9 (d,

$J = 8.6$, CH), 121.4 (d, $J = 11.0$ Hz, CH), 59.3 (d, $J = 2.5$ Hz, $4 \times \text{CH}_2$), 24.65 ($4 \times \text{CH}_2$), 20.60 ($4 \times \text{CH}_2$), 13.95 ($4 \times \text{CH}_3$).

^{31}P -NMR of **128** (101.25 MHz, MeOD): 29.9

4,4''-Dimethyl-[1,3',1',1'',3'',1''']quaterphenyl-2,2''-diamine **124**



300 mg (0.87 mmol) of 3,3'-dibromo-2,2'-diamino-1,1'-biphenyl **106** and 12 mol% 121 mg of $\text{Pd}(\text{PPh}_3)_4$ were dissolved in 15 ml benzene. A solution of 600 mg (4.41 mmol) of p-tolueneboronic acid **117** in 10 ml ethanol and 2 ml 2N Na_2CO_3 solution were added to the reaction mixture. The mixture was flushed with nitrogen, then heated gently till reflux at 85°C for 2 h. Extraction between benzene and water phase, drying and evaporating the organic phase provided the crude product **124**. The product was collected, washed with MeOH several times, then dissolved in CHCl_3 and extracted with water. The organic phase was dried over Na_2SO_4 , filtered and evaporated. The product was recrystallized from CHCl_3 /ether to yield 205 mg (0.56 mmol, 65%) product **124**.

124: $\text{C}_{26}\text{H}_{24}\text{N}_2$ (MW 364.48)

mp: 122°C

MS ESI: $m/z = 365.4$ (100% $(\text{M}+\text{H})^+$).

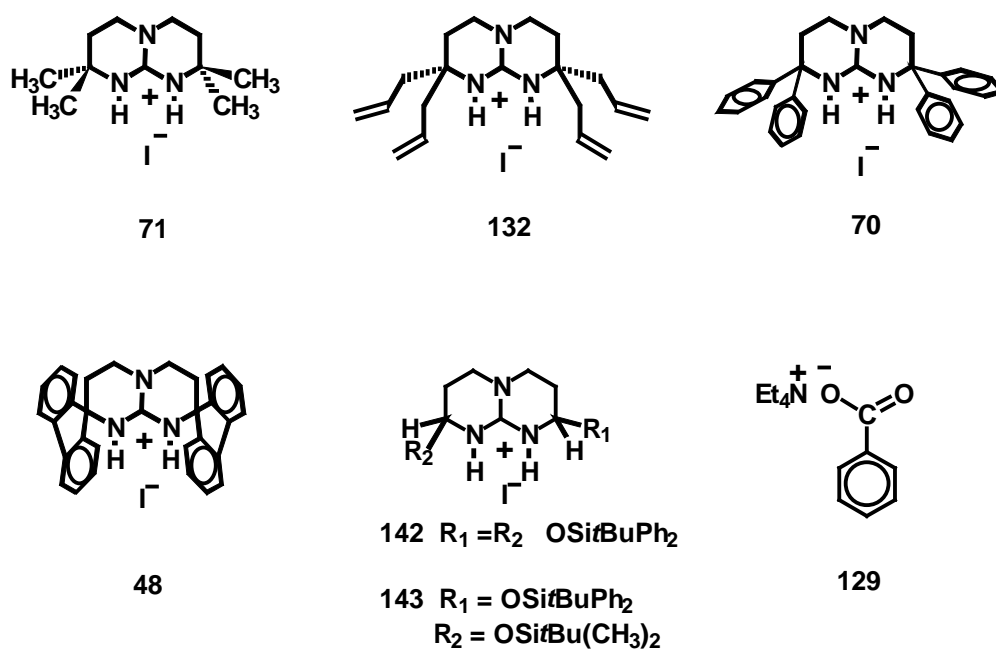
HPLC5 analysis: $R_v = 12.0$ ml

^1H -NMR (250.13 MHz, CDCl_3): $\delta = 7.40$ -7.37 (m, 4H aromatic), 7.26-7.23 (m, 4H aromatic), 7.15-7.13 (m, 4H aromatic), 6.87 (t, $J = 7.3$ Hz, 2H aromatic), 3.87 (s, 4H $2 \times \text{NH}_2$), 2.39 (s, 6H $2 \times \text{CH}_3$).

^{13}C -NMR (62.9 MHz, CDCl_3): $\delta = 141.5$, 136.9, 136.7, 130.2, 130.0, 129.5, 129.1, 128.0, 125.0, 118.3 (24C aromatic), 21.1 ($2 \times \text{CH}_3$).

6. Summary

In the present study, we have investigated the association behavior of a series of guanidinium host derivatives (**48**, **70**, **71**, **132**, **141**, **142**), which differ in their steric properties, to tetraethylammonium benzoate (**129**), tetrabutylammonium phosphates (**78**, **84**) and to tetrabutylammonium phosphinate (**128**) guests in the non-hydrogen bonding and the highly dielectric solvent acetonitrile at 30°C. The lining of the binding site of the guanidinium hosts was modified synthetically to introduce substituents with different hydrophobicity properties in order to study their effect on complexation with the same guest anion. In comparison to anion **84**, the guest anion **78** has two extended substituents adjacent to the binding site, that increase the binding directionality to the guanidinium hosts and may lead to tighter complexes, as the two arms can wrap around the host by projecting above and beneath the main plain of the host and thus to can profit from additional enthalpic interaction securing an optimal orientation.



The guanidinium hosts **48**, **70** and the guest anion **78**, were newly prepared in this study whereas the other guanidinium hosts were previously prepared in our lab. The phosphate **84** and the phosphinate **128** were prepared with some modifications to literature procedures. The interaction mode between the guanidinium hosts and the different oxoanions follows 1:1 stoichiometry with a planar cation-anion arrangement, assisted by two parallel hydrogen bonds. The modifications in the guanidinium hosts

and the introduced substituents in the phosphate anion guest **78** were carried out without harming the preferential binding mode.

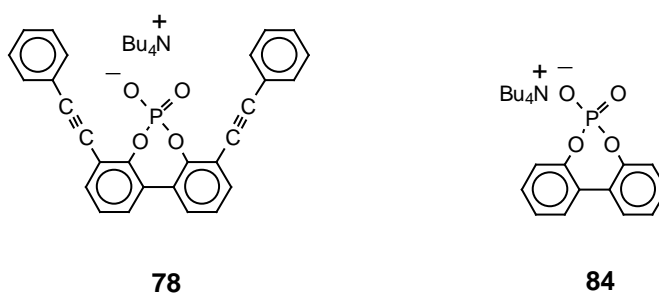
Isothermal titration calorimetry (ITC) was utilized to study the association properties of the host-guest complexation. This technique provides a measure of association strength, stoichiometry of binding, as well as thermodynamic parameters of association from a single experiment. The factorization into the energetic components allowed the deduction of the energetic signature of the complexation, i.e., whether it is an enthalpically or entropically driven process. This outcome is determined by the host and guest character and the environment (*i.e.*, solvent molecules).

The iodide counter anion of the guanidinium hosts **132**, **48**, and **70** was replaced by different counter anions (Cl^- , Br^- , and PF_6^-) in order to evaluate its influence on complexation with the benzoate anion **129**. The calorimetric determination of the host-guest binding in acetonitrile revealed a surprisingly strong dependence on the counter anion. In general, switching the counter anion from chloride to hexafluorophosphate shifts the experimental host-guest affinity to higher values and to a stronger enthalpic response due to the shift from the more stable hydrogen bonding Cl^- to the larger and less hydrogen-bonding PF_6^- in the exchange for benzoate. A positive entropy contribution indicates the release of solvent molecules and counter anions, engaged in the solvation of the binding site, to the bulk.

The trend analysis of the complexation of different guanidinium iodide hosts (**141**, **142**, **132**, **70** and **48**) with TEA-benzoate **129** unfolded the decisive role of solvation. The less positive ΔS° values seen in hosts **70** and **48** with the aromatic substituents indicate the release of fewer solvent molecules on benzoate binding than in the other guanidinium hosts, because these substituents are less solvated than the others. Even though the fluorenyl compound **48** and the tetraphenyl compound **70** showed identical solvation changes ($\Delta S^\circ = +6.5$ and $+6.0 \text{ cal K}^{-1}\text{M}^{-1}$, respectively) and thereby enhancement of the coulombic attraction for the anionic guest, however, the exothermicity enhancement was more pronounced for the fluorenyl compound **48** (-6.03 kcal/mol). This result is attributed to the presumed higher rigidity of **48** which opposes the reorientation of the solvent dipoles to cope with the change of the electrostatic field on complex formation.

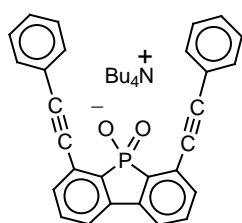
The complexation of the guanidinium iodide compounds **71**, **132**, **70**, and **48** with the two arms substituted phosphate **78** showed a clear trend of increasing host-guest affinity with host rigidity, yielding the highest K_{ass} for the fluorene-guanidinium host **48** ($2.3 \times 10^4 \text{ M}^{-1}$) but the strongest enthalpy response was obtained for the tetraphenyl host **70** (-5.77 kcal/mol). The entropy contribution for host **70** was the lowest in this series ($-0.8 \text{ cal K}^{-1} \text{ M}^{-1}$) indicating the release of fewer solvent molecules and stronger structural definition toward the guest **78**.

The conclusion that the anion **78** contributed to the enhancement in binding directionality to the aforementioned hosts was supported by a comparable trend analysis of the same guanidinium hosts with phosphate **84** that lacks the two side arms. This trend actually showed that there was no significant change in the association constants but a clear decrease in the binding enthalpy of about 1-1.5 kcal/mol. (e.g., -5.19 kcal/mol for the tetraphenyl **70**) and an increase in the entropy component in the range of 2-4 $\text{cal K}^{-1} \text{ M}^{-1}$ (e.g., +1.3 for **70**) due to the release of more solvent molecules than in the previous trend. Therefore, the two arm substituents followed the assumption that this structure would deliberately form tighter complexes and stronger binding enthalpy than the parent phosphate **84**. Hence, there was a clear benefit of the structural lay-out in anion **78**. This benefit would have never been realized if the analysis were restricted to only the association constant and the free energy of association, because the latter did not significantly change in most of the trend analyses.

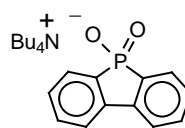


An attempt to improve the structural definition by preparing and using phosphinate anion guest **92** was planned. The advantage of **92** over the anion **78** is in the smaller opening angle between the two substituents that would diminish the abundance of solvent molecules in the vicinity of the binding site and form tighter complexes with

the same trend of the guanidinium hosts. Unfortunately, the anion **92** is still in preparation but the complexation with the parent anion **128** that also lacks the two side arms already showed a surprising result with tetraphenyl host **70**. Host-guest binding revealed the strongest enthalpy value ($\Delta H^\circ = -10$ kcal/mole) and the lowest entropy contribution ($\Delta S^\circ = -15.3$ cal K⁻¹ M⁻¹) among all titration experiments that were carried out in this study. Therefore, we expect even better complexation energetics if the anion **92** is used.



92



128

As a conclusion, the dissection of the free energy ΔG° into its enthalpy ΔH° and entropy ΔS° components was essential for understanding the correlation between structure and thermodynamics of complexation whereas relying exclusively on the association constant and the free energy can easily hamper the interpretation of the binding properties of a given host-guest set.

6. References

- [1] J.W. Steed, J.L. Atwood, *Supramolecular Chemistry*, **2000**, John Wiley & Sons Ltd, Chichester, England.
- [2] J.M. Lehn, *Supramolecular Chemistry Concepts and Perspectives*, **1995**.
- [3] H.-J. Schneider, A. Yatsimirsky, *Principles and Methods in Supramolecular Chemistry*, **2000**, John Wiley & Sons Ltd, Chichester, England.
- [4] K. Müller-Dethlefs, P. Hobza, Noncovalent interactions: A challenge for experiment and theory, *Chem. Rev.* **2000**, *100*, 143-167.
- [5] P. Atkins, J. de Paula, *Atkins' Physical Chemistry*, seventh edition **2002**, Oxford University Press Inc, New York.
- [6] M.A. Hossain, H.J. Schneider, *Chem. Eur. J.* **1999**, *5*, 1284-1290.
- [7] T. Liljefors, P.O. Norrby, *J. Am. Chem. Soc.* **1997**, *119*, 1052-1058.
- [8] G.S. Manning, *Rev. Biophys.* **1975**, *14*, 2137.
- [9] E. Fischer, *Chem. Ber.* **1894**, *27*, 2985-2993.
- [10] T. Steiner, *Angew. Chem.* **2002**, *114*, 50-80.
- [11] B.T. Holland, L. Abrams, A. Stein, *J. Am. Chem. Soc.* **1999**, *121*, 4308-4309.
- [12] M. Schwartz, G. Miehe, A. Zerr, E. Krohe, B.T. Poe, H. Fuess, R. Riedel, *Adv. Mater.* **2000**, *12*, 883-887.
- [13] G.A. Jeffrey, *An introduction to hydrogen bonding*, **1997**.
- [14] T. Sekine, H. He, T. Kobayashi, M.Z. Hang, F. Xu, *Appl. Phys. Lett.* **2000**, *76*, 3706-3708.
- [15] T. Steiner, *Chem. Commun.* **1997**, 727-734.
- [16] T. Steiner, R. Desiraju, *Chem. Commun.* **1998**, 891-892.
- [17] L. Stephan De Wall, E.S. Meadows, L.J. Barbour, G.W. Gokel, *Chem. Commun.* **1999**, 1553-1554.
- [18] V. Böhmer, A. Dalla-Cort, L. Mandolini, *J. Org. Chem.* **2001**, *66*, 1900-1902.
- [19] M.J. Rashkin, M.L. Waters, *J. Am. Chem. Soc.* **2002**, *124*, 1860-1861.
- [20] J.C. Ma, D.A. Dougherty, *Chem. Rev.* **1997**, *97*, 1303-1324.
- [21] E. Grunwald, C. Steel, *J. Am. Chem. Soc.* **1995**, *117*, 5687-5692.
- [22] O. Exner, *Chem. Commun.* **2000**, 1655-1656.
- [23] M. Berger, F.P. Schmidtchen, *J. Am. Chem. Soc.* **1999**, *121*, 9986-9993.
- [24] M. Berger, F.P. Schmidtchen, *Angew. Chem, Int. Ed.* **1998**, *37*, 2694-2696.

- [25] a) I. Wadsö, *Chem. Soc. Rev.* **1997**, 79-86; b) J.E. Ladburg, B.Z. Chowdhry, *Chem. Biol.* **1996**, 3, 791-801.
- [26] MCS-ITC Handbook, MicroCal Ltd, USA.
- [27] a) I. Jelesarov, H.R. Bosshard, *J. Mol. Recognit.* **1999**, 12, 3-18; b) A. Cooper, *Curr. Opin. Chem. Biol.* **1999**, 3, 557-563.
- [28] a) M. Stödeman, I. Wadsö, *Pure & Appl. Chem.* **1995**, 67, 1059-1068; b) M.J. Blandamer, P.M. Cullis, J.B.F.N. Engberts, *Pure & Appl. Chem.* **1996**, 68, 1577-1582; c) M.A. White in *Comprehensive Supramolecular Chemistry*, J.L. Atwood, J.E.D. Davies, D.D. MacNicol, F. Vögtle (Hrsg), Pergamon, Elsevier, Oxford, **1996**, p.179-224.
- [29] J.M. Lehn, *Angew. Chem.* **1988**, 100, 91.
- [30] F.P. Schmidtchen, *Chem. Rev.* **1997**, 97, 1609-1646.
- [31] A.I. Boldyrev, M. Gutowski, J. Simons, *Acc. Chem. Res.* **1996**, 29, 497
- [32] P.W. Schultz, G.E. Leroi, A.I. Popov, *J. Am. Chem. Soc.* **1996**, 118, 10617-10625.
- [33] Y. Marcus, *Ion Solvation*, John Wiley, Chichester, **1985**, pp. 45ff.
- [34] R.S. Alexander, Z.F. Kanyo, L.E. Chirlian, D.W. Christianson, *J. Am. Chem. Soc.* **1990**, 112, 933-937.
- [35] G.R.J. Thatcher, D.R. Cameron, R. Nagelkerke, J. Schmitke, *J. Chem. Soc. Chem. Commun.* **1992**, 386.
- [36] K.T. Chapman, W.C. Still, *J. Am. Chem. Soc.* **1989**, 111, 3075-3077.
- [37] I. Labadi, E. Jenei, R. Lahti, H. Lonnberg, *Acta Chem. Scand.* **1991**, 45, 1055.
- [38] A. Bencini, A. Bianchi, M.I. Burguete, P. Dapporto, A. Domenech, E. Garcia-España, S.V. Luis, P. Paoli and J.A. Ramírez, *J. Chem. Soc., Perkin Trans. 2*, **1994**, 569-577.
- [39] J.M. Lehn, E. Sonveaux, A.K. Willard, *J. Am. Chem. Soc.* **1978**, 100, 4914-4916.
- [40] B. Dietrich, J. Guilhem, J.M Lehn, C. Pascard, E. Sonveaux, *Helv. Chim. Acta.* **1984**, 67, 91-104.
- [41] M.W. Hosseini, J.M. Lehn, *Helv. Chim. Acta.* **1988**, 71, 749-756.
- [42] B. Dietrich, B. Dilworth, J.M. Lehn, J.-P. Souchez, M. Cesario, J. Guilhem, C. Pascard, *Helv. Chim. Acta.* **1996**, 79, 569-587.

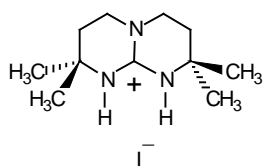
- [43] P.A. Gale, J.L. Sessler, V. Kral, V. Lynch, *J. Am. Chem. Soc.* **1996**, *118*, 5140-5141.
- [44] F.P. Schmidtchen, *Org. Lett.* **2002**, *4*, 431-434.
- [45] A. Bencini, A. Bianchi, P. Paoletti, P. Paoli, *Pure Appl. Chem.* **1993**, *65*, 381.
- [46] D. Rudkevich, W.R.P. Stauthamer, W. Verboom, J.F.J. Engbersen, S. Harkema, D.N. Reinhoudt, *J. Am. Chem. Soc.* **1992**, *114*, 9671-9673.
- [47] D.M. Rudkevich, W. Verboom, Z. Brzozka, M.J. Palys, W.P.R. Stauthamer, G.J. van Hummel, S.M. Franken, S. Herkema, J.F.J. Engbersen, D.N. Reinhoudt, *J. Am. Chem. Soc.* **1994**, *116*, 4341-4351.
- [48] M.E. Jung, H. Xia, *Tetrahedron Lett.* **1988**, *29*, 297.
- [49] P.D. Beer, Z. Chen, A.J. Goulden, A. Grieve, D. Heseck, F. Szemes, T.J. Wear, *Chem. Soc., Chem. Commun.* **1994**, 1269.
- [50] P.D. Beer, *Chem. Soc., Chem. Commun.* **1996**, 689.
- [51] P.D. Beer, S.W. Dent, T.J.J. Wear, *Chem. Soc., Dalton Trans.* **1996**, 2341.
- [52] H. Ishida, M. Suga, K. Donowaki, K. Ohkubo, *J. Org. Chem.* **1995**, *60*, 5374-5375.
- [53] A. Gleich, F.P. Schmidtchen, P. Mikulcic, G. Mueller, *J. Chem. Soc., Chem. Commun.* **1990**, 55-57.
- [54] G. Mueller, J. Riede, F.P. Schmidtchen, *Angew. Chem.* **1988**, *100*, 1574.
- [55] Y. Kashman, J. Hirsh, O.J. McConnell, I. Ohtani, T. Kusumi, H. Kakisawa, *J. Am. Chem. Soc.* **1989**, *111*, 8925.
- [56] A. Yokoo, *J. Chem. Soc. Japan*, **1960**, *71*, 590.
- [57] E.J. Schantz, J.D. Mold, D.W. Stanger, W. Shavel, F.J. Riel, J.P. Bowden, J.M. Lynch, R.S. Wyler, B. Riegel, H. Sommer, *J. Am. Chem. Soc.* **1957**, *79*, 5230.
- [58] B. Dietrich, T.M. Fyles, J.M. Lehn, L.G. Pease, D.L. Fyles, *J. Chem. Soc. Chem. Commun.* **1978**, 934.
- [59] B. Dietrich, D.L. Fyles, T.M. Fyles, J.M. Lehn, *Helv. Chim. Acta.* **1979**, *62*, 2763.
- [60] R.P. Dixon, S.J. Geib, A.D. Hamilton, *J. Am. Chem. Soc.* **1992**, *114*, 365.
- [61] D.J. Weber, A.K. Meeker, A.S. Mildvan, *Biochemistry*, **1990**, *29*, 8632.
- [62] K. Ariga, E.V. Anslyn, *J. Org. Chem.* **1992**, *57*, 417.
- [63] J. Smith, K. Ariga, E.V. Anslyn, *J. Am. Chem. Soc.* **1993**, *115*, 362.

- [64] F.P. Schmidtchen, *Chem. Ber.* **1980**, *113*, 2175-2182.
- [65] C.L. Perrin, D.B. Young, *J. Am. Chem. Soc.* **2001**, *123*, 4446-4450.
- [66] A. Echavarren, A. Galan, J. de Mendoza, A. Salmeron, J.M. Lehn, *Helv. Chim. Acta* **1988**, *71*, 685.
- [67] E.J. Corey, M. Ohtani, *Tetrahedron Lett.* **1989**, *30*, 5227.
- [68] A. Echavarren, A. Galan, J.M. Lehn, J. de Mendoza, *J. Am. Chem. Soc.* **1989**, *111*, 4994.
- [69] J. Rebek Jr., *J. Chemtracts: Org. Chem.* **1990**, *3*, 240.
- [70] A. Galan, D. Andreu, A.M. Echavarren, P. Prados, J. de Mendoza, *J. Am. Chem. Soc.* **1992**, *114*, 1511.
- [71] A. Metzger, K. Gloe, H. Stephan, F.P. Schmidtchen, *J. Org. Chem.* **1996**, *61*, 2051.
- [72] J.O. Magrans, A.R. Ortiz, M.A. Molins, P.H.P. Lebouille, J. Sanchez-Quesada, P. Prados, M. Pons, F. Gago, J. de Mendoza, *Angew. Chem.* **1996**, *108*, 1816.
- [73] G. Deslongchamps, A. Galan, J. de Mendoza, J. Rebek Jr., *Angew. Chem., Int. Ed. Engl.* **1992**, *31*, 61.
- [74] Y. Kato, M.M. Conn, J. Rebek Jr., *J. Am. Chem. Soc.* **1994**, *116*, 3279.
- [75] A. Galan, J. de Mendoza, C. Toiron, M. Bruix, G. Deslongchamps, J. Rebek Jr., *J. Am. Chem. Soc.* **1991**, *113*, 9424.
- [76] C. Andreu, A. Galan, K. Kobiro, J. de Mendoza, T.K. Park, J. Rebek Jr., A. Salmeron, N. Usman, *J. Am. Chem. Soc.* **1994**, *116*, 5501.
- [77] F.P. Schmidtchen, *Tetrahedron Lett.* **1989**, *30*, 4493.
- [78] P. Schiessl, F.P. Schmidtchen, *J. Org. Chem.* **1994**, *59*, 509.
- [79] H. Stephan, K. Gloe, P. Schiessl, F.P. Schmidtchen, *Supramol. Chem.* **1995**, *5*, 273-280.
- [80] P. Schiessl, F.P. Schmidtchen, *Tetrahedron Lett.* **1993**, *34*, 2449.
- [81] W. Peschke, F.P. Schmidtchen, *Tetrahedron Lett.* **1995**, *36*, 5155.
- [82] K. Vladimir, F.P. Schmidtchen, K. Lang, M. Berger, *Org. Lett.* **2002**, *1*, 51-54.
- [83] P. Molina, M. Alajarin, A. Vidal, *Tetrahedron* **1995**, *51*, 5351.
- [84] J.L. Chicharro, P. Prados, J. de Mendoza, *J. Chem. Soc., Chem. Commun.* **1994**, 1193.
- [85] P. Molina, M. Alajarin, A. Vidal, *J. Org. Chem.* **1993**, *58*, 1687.

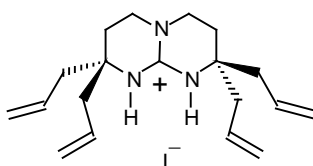
- [86] R.S. Hutchins, P. Molina, M. Alajarin, A. Vidal, L.G. Bachas, *Anal. Chem.* **1994**, *66*, 3188.
- [87] J.O.M. Bockres, A.K.N. Reddy, *Modern Electrochemistry*, **1970**, Plenum, New York.
- [88] J.H. Forsberg, V.T. Spaziano, T.M. Balasubramanian, G.K. Liu, S.A. Kinsley, C.A. Duckworth, J.J. Poteruca, P.S. Brown, J.L. Miller, *J. Org. Chem.*, **1987**, *52*, 1017-1021.
- [89] D.J. Cram, M. de Grandpre, C.B. Knobler, K.N. Trueblood, *J. Am. Chem. Soc.* **1984**, *106*, 3286-3292.
- [90] R.C. Helgeson, B.P. Czech, E. Chapoteau, C.R. Gebauer, A. Kumar, D.J. Cram, *J. Am. Chem. Soc.* **1989**, *111*, 6339-6350.
- [91] S.S. Peacock, D.M. Walba, F.C.A. Gaeta, R.C. Helgeson, D.J. Cram, *J. Am. Chem. Soc.* **1980**, *102*, 2043.
- [92] A. Bähr, A.S. Droz, M. Püntener, U. Neidlein, S. Anderson, P. Seiler, F. Diederich, *Helv. Chem. Acta*, **1998**, *81*, 1929-1930.
- [93] Svara Juergen, Ger. Offen, patent "an easy preparation of pure diaryl phosphate", **1991** (Hoechst A.-G; Fed. Rep. Ger.). Ger. Offen. (1991), Patent Code: GWXXbX. Priority Application Information: DE 1989-3940765 19891209.
- [94] O. Diels, A. Biebergeil, *Ber. dt. chem. Gesellschaft.* **1902**, *35*, 302-313.
- [95] I. Leupold, H. Musso, *Liebigs Ann. Chem.* **1971**, *746*, 134-148.
- [96] H. Hoffmann, L. Horner, H. Wippel, D. Michael, *Chem. Ber.*, **1962**, 523-527.
- [97] a) Schmid, *Organometallics*, **2001**, volume 20, number 11, 2321; b) Y. Miura, H. Oka, M. Morita, *Macromolecules*, **1998**, *31*, 2041-2046.
- [98] S.F. Gait, M.E. Peek, C.W. Rees, R.C. Storr, *J. Chem. Soc. Perkin I*, **1974**, 1248-1260.
- [99] a) J. Cornforth, A.D. Roberston, *J. Chem. Soc. Perkin Trans. I*, **1987**, 867-870; b) J. Cornforth, L.M. Huguenin, J.R.H. Wilson, *J. Chem. Soc. Perkin Trans. I*, **1987**, 871-875; c) J. Cornforth, *J. Chem. Soc. Perkin Trans. I*, **1996**, 2889-2893.
- [100] H. Gelman, B.J. Gaj, *J. Org. Chem.*, **1957**, *22*, 447-449.

- [101] G. Müller, J. Riede, F.P. Schmidtchen, *Angew. Chem.* **1988**, *100*, 1574–1575; *Angew. Chem. Int. Ed. Engl.* **1988**, *27*, 1516–1518.
- [102] D.M. Kneeland, K. Ariga, V.M. Lynch, C.Y. Huang, E.V. Anslyn, *J. Am. Chem. Soc.* **1993**, *115*, 10042–10055.
- [103] V. Boehmer, A. Dalla-Cort, L. Mandolini, *J. Org. Chem.* **2001**, *66*, 1900–1902.
- [104] M. Haj-Zaroubi, N.W. Mitzel, F.P. Schmidtchen, *Angew. Chem. Int. Ed.* **2002**, *41*, 104–107.
- [105] The original description refers to a scenario where only two interacting entities perform “rigid-body docking”. Much later the complementarity of functional groups and their preorganization were included aiding substantially in the comprehension of the molecular events especially in solvents of low polarity. Recognition processes in more polar solvents in particular in water so far largely eluded rationalization. To avoid confusion the metaphor is used here in its original sense.
- [106] a) J.D. Dunitz, *Chem. Biol.* **1995**, *2*, 709–712; b) E. Grunwald, C. Steel, *J. Am. Chem. Soc.* **1995**, *117*, 5687–5692; c) D.H. Williams, M.S. Westwell, *Chem. Soc. Rev.* **1998**, *27*, 57–63.
- [107] J. Barthel, M. Kleebauer, *J. Solution Chem.* **1991**, *20*, 977–993.
- [108] B. Linton, A.D. Hamilton, *Tetrahedron*, **1999**, *155*, 6027–6038.
- [109] a) A. Gleich, F.P. Schmidtchen, *Chem. Ber.* **1990**, *123*, 907–915; b) F.P. Schmidtchen, H. Oswald, A. Schummer, *liebig's Ann. Chem.* **1991**, 539–543; c) M. Berger, F.P. Schmidtchen, *J. Am. Chem. Soc.* **1999**, *121*, 9986–9993.
- [110] S. Boudon, G. Wipff, *Studies in Physical and Theoretical Chemistry*, **1990**, *71*, 203–209.
- [111] R.S. Alexander, Z.F. Kanyo, L.E. Chirlian, D.W. Christianson, *J. Am. Chem. Soc.* **1999**, *121*, 933–937.
- [112] T.H. Schrader, *Tetrahedron Lett.* **1998**, *39*, 517–520.
- [113] B.P. Orner, X. Salvatella, J.S. Quesada, J. de Mendoza, E. Giralt, A.D. Hamilton, *Angew. Chem. Int. Ed.* **2002**, *41*, 117–119.
- [114] the compound was synthesized in the lab of Prof. F.P. Schmidtchen.

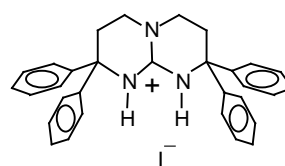
List of compounds



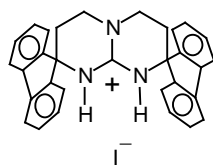
71



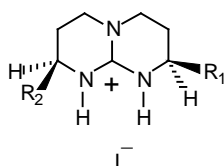
132



70

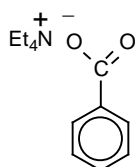


48

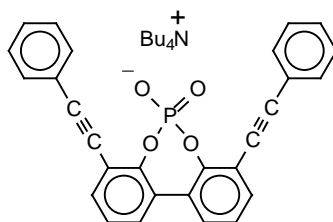


142 $R_1 = R_2 = \text{OSi}t\text{BuPh}_2$

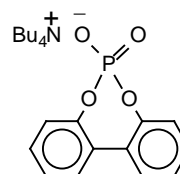
143 $R_1 = \text{OSi}t\text{BuPh}_2$
 $R_2 = \text{OSi}t\text{Bu}(\text{CH}_3)_2$



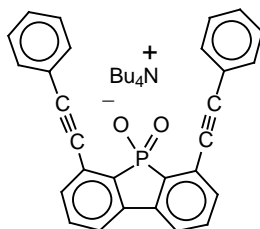
129



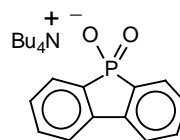
78



84



92



128